Identification of a protein kinase substrate in *Sulfolobus solfataricus* P2

Ruth Ann Redbird

Dissertation submitted to the faculty of the Virginia Polytechnic Institute and State University in partial fulfillment of the requirements for the degree of

Doctor of Philosophy
In
Biochemistry

Peter J. Kennelly, Chair
Richard Helm
James Mahaney
Renee Prater

April 1, 2010
Blacksburg, VA

Keywords: protein kinase, phosphorylation, *Archaea*, ATP Synthase

Identification of a protein kinase substrate in *Sulfolobus solfataricus* P2

Ruth Ann Redbird

Abstract

Living organisms rely on many different mechanisms to adapt to changes within their environment. Protein phosphorylation and dephosphorylation events are one such way cells can communicate to generate a response to environmental changes. In the Kennelly laboratory we hope to gain insight on phosphorylation events in the domain *Archaea* through the study of the acidothermophilic organism *Sulfolobus solfataricus.* Such findings may provide answers into evolutionary relationships and facilitate an understanding of phosphate transfer via proteins in more elaborate systems where pathway disturbances can lead to disease processes.

A λ-phage expression library was generated from *S. solfataricus* genomic DNA. The immobilized expression products were probed with a purified protein kinase, SsoPK4, and radiolabeled ATP to identify potential native substrates. A protein fragment of the ORF *sso0563,* the catalytic A-type ATPase subunit A (AtpA), was phosphorylated by SsoPK4. Full length and truncated forms of AtpA were overexpressed in *E. coli*. Additional subunits of the ATPase were also overexpressed and ATPase activity reconstituted *in vitro*. Phosphoamino acid analysis and MS identified the phosphorylation sites on AtpA. Several variants of AtpA were derived via site-directed mutagenesis and assayed for ATPase activity. Chemical cross-linking was employed to determine possible ATPase subunit interactions; tryptic digests of AtpA and its mutant

variants were performed to examine protein folding. The phosphorylated-mimic variant of AtpA, T98D, resulted in an inactive ATPase complex as determined by ATPase activity assays and native-PAGE indicating potential phosphoregulation by SsoPK4 on enzyme activity. Ultimately, any findings would need verification with *in vivo* studies.

Acknowledgements

Let me start by thanking my advisor and mentor, Dr. Peter J. Kennelly, for giving me the chance to work in the lab first as a technician and then as a graduate student. "Dr. K" always found time for questions, input, and advice on all matters both professional and personal even after his life became hectic with department chair duties. Thanks for teaching me to "think like a scientist" and to become a better person all around. You have made a great impact on my life and it will not go unnoticed or underappreciated!

Another round of thanks goes out to the people who have passed through the lab in my time at VT: graduate students Archana Mukhopadhyay, January Haile and Brian Jordan, undergraduates Andrew Chute and my advisees Laura Pompano and Joe Arthur. To Ben Potters and grad student Hanan Dahche, many thanks for "Salad Fingers", Conan clips and random photo shoots with blue liquid – that *must* be science at work. You two made the last years a lot of fun.

Special acknowledgement goes to Dustin Hite for teaching me the basics during my year as a technician. All of those late hours playing around with membranes and plates have paid off. And a rousing round of applause goes to Dr. Keith Ray for being so patient with all of my questions and for all of his assistance with general biochemistry and MS expertise on my project.

To my dissertation committee: Drs. Rich Helm, James Mahaney, and Renee Prater. You three were extremely helpful and offered great advice and encouragement. I appreciate all of the time taken for meetings, presentations, critiques, etc. Thank you.

I want to thank the friends I've made during my time in Blacksburg: Yvette Edmonds – who knew we would find our personality twin and life-long friend in the biochemistry department? The Star City Roller Girls (Roanoke, VA) – thanks for keeping me active, sane, and supplied with lasting friendships. You are a perfectly dysfunctional family for me and I wouldn't have it any other way. And a special shout-out goes to my "derby wife" Cyndi Withrow: Thanks for being my friend, Martial Brady!

The Kroenleins: I am so glad to call you family *and* friends; you have always been there to cheer me on and I thank you all!

The Redbirds: Charlotte, Darrin and Ryan Redbird – my mom and little brothers, you have always been there whenever I call to hear my ups, downs, and everything in between. Thanks for making me who I am today and for reminding of where I come from, who I am now, and what I have yet to accomplish. I love you all very much!

And finally to Karl Kroenlein, my best friend and husband: You have tolerated my love of roller derby, monkeys, cookies, Buffy, and Martha Stewart all while providing a shoulder for leaning and an ear for listening. I love the little four-legged family we have started and soon we can start adding the two-legged variety. You guessed correctly—birds. I support you always, you support me always, and that's the way it should be. *I love you the most*!

Table of Contents

Chapter VI:

List of Figures

List of Tables

List of Abbreviations

Amp	ampicillin
ATP	adenosine triphosphate
BCIP	5-Bromo-4-Chloro-Indolyl-Phosphatase
BSA	bovine serum albumin
cAMP	cyclic adenosine monophosphate
$CaCl_2$	calcium chloride
Cam	chloramphenicol
CAPS	3-(cyclohenylamion)-1-propane sulfonic acid
cpm	counts per minute
dATP	deoxyadenosine triphosphate
dCTP	deoxycytidine triphosphate
dGTP	deoxyguanosine triphosphate
dTTP	deoxythymidine triphosphate
DNA	deoxyribonucleic acid
dNTP	deoxynucleoside triphosphate
DTT	dithiothreitol
EDC	1-ethyl-3-(dimethylaminopropyl)
EDTA	ethylenediaminetetraacetic acid
EGTA	ethylene glycol tetraacetic acid
ePK	eukaryotic protein kinase
EtBr	ethidium bromide
H_2SO_4	sulfuric acid
HCl	hydrochloric acid
HPLC	high-performance liquid chromatography
IMAC	immobilized metal affinity chromatography
IPTG	isopropylthio-β-D-galactoside
K_2HPO_4	potassium phosphate, monobasic
Kan	kanamycin
Kb	kilobase
KRB	kinase reaction buffer
LB	Luria-Bertani media
LSF	liquid scintillation fluid
MES	2-(N-morpholino)ethanesulfonic acid
$MgCl_2$	magnesium chloride
$MgSO_4$	magnesium sulfalte
Mn^{2+}	manganese (divalent cation)
$MnCl_2$	manganese chloride
MOPS	3-(N-morpholino)propanesulfonic acid
MS	mass spectrometry
M_r	relative molecular mass
NaCl	sodium chloride
$NaPP_i$	sodium pyrophosphate
NBT	nitro blue tetrazolium

ORF	open reading frame
PAA	phosphoamino acid analysis
PAGE	polyacrylamide gel electrophoresis
PCR	polymerase chain reaction
Pfu	plaque forming unit
P_i	inorganic phosphate
PTM	posttranslational modification
PVDF	polyvinylidene fluoride
RNA	ribonucleic acid
RWB	reaction wash buffer
S.O.C.	Super Optimal broth with Catabolite repression media
SAP	shrimp alkaline phosphatase
SDS	sodium dodecyl sulfate
TAE	Tris-acetate/EDTA
TBS	Tris-buffered saline
TCA	trichloroacetic acid
Tet	tetracycline
TFA	trifluoroacetic acid
TLC	thin-layer chromatography
TWB	Triton wash buffer
µCi	microcurie

Chapter I: Introduction

Protein Phosphorylation Events in Living Systems

Living organisms rely on many different mechanisms to adapt to changes within their environment. Such changes need to be enacted and targeted rapidly and effectively in response to a myriad of stimuli and most often involve multiple enzymes or even multiple physiological pathways. Protein phosphorylation and protein dephosphorylation events are ubiquitous and a versatile means by which cells generate rapid, reversible responses to environmental changes (Roach 1991; Hunter 1995; Kennelly 1999).

Phosphate-containing molecules (e.g. ATP, DNA, RNA) are abundant within organisms. The Kennelly lab strives to delineate the regulatory and mechanistic properties of two families of enzymes—protein kinases and protein phosphatases—that utilize the readily available phosphate. A traditional description of protein kinase activity involves enzymes catalyzing the transfer of a γ-phosphate (from a nucleoside triphosphate) to the side chain nucleophile of an amino acid residue(s) of a target protein—the protein kinase substrate. The covalent addition of inorganic phosphate frequently induces structural changes within the substrate protein as a consequence due to the large negatively charged, electrostatic field generated by the ionized form of the phosphate at physiological pH (Westheimer 1987; Kennelly 2003). It is these perturbations of protein structure that produce changes in enzymatic activity or other functions, thus actuating responses to environmental stimuli. The protein kinase counterparts, protein phosphatases, remove the phosphate group from the substrate

protein thereby making the phosphorylation process reversible, which in turn provides further means of cellular regulation.

Phosphorylative events involving protein kinases and protein phosphatases have been discovered within the *Eukarya*, *Bacteria* and *Archaea*. In eukaryotic cells protein kinases and protein phosphatases constitute the most prevalent classes of signal transduction elements (Manning, Whyte et al. 2002). Protein phosphorylation plays a role in myriad essential cellular processes within humans including the regulation of the cell cycle, cellular differentiation, and apoptosis (Hunter 1995; Carnero 2002; Manning, Whyte et al. 2002; Hanks 2003; Basu and Sivaprasad 2007; Raman, Chen et al. 2007). Disruptions of these regulatory mechanisms can result in or contribute to pathologies such as cancer (Raman, Chen et al. 2007; Ashman and Villar 2009), Alzheimer's disease (Wang, Grundke-Iqbal et al. 2007), and diabetes (Bridges 2005; Raman, Chen et al. 2007; Wang, Grundke-Iqbal et al. 2007). Therefore, a better understanding of protein kinase and protein phosphatase action could lead to the development of therapeutic drugs to target aberrant phosphorylative mechanisms (Carnero 2002; Cohen 2002; Levitzki 2003; Bridges 2005; Turk 2008; Ashman and Villar 2009).

Protein Kinases

The ability of protein kinases to regulate cellular processes has been studied since the mid-20th century following the realization that glycogen phosphorylase *b* could be converted to glycogen phosphorylase *a* in the presence of ATP and a divalent metal cation (Fischer and Krebs 1955). By the late 1960s it was determined that protein phosphorylation was not unique to glycogen metabolism; instead, protein phosphorylation by protein kinases, such as the cAMP-dependent protein kinase, a.k.a.

protein kinase A (PKA), appeared to constitute a widespread means of signal transduction (Walsh, Perkins et al. 1968). For a time, it was believed that eukaryotic protein kinases only phosphorylated serine and threonine residues on their protein substrates. Then, in 1979 the discovery of phosphotyrosine residues on polyoma T antigen, a viral oncoprotein, led to identification of another family of protein kinases, the protein-tyrosine kinases (Eckhart, Hutchinson et al. 1979). Sequence analysis revealed that the protein-serine/threonine protein kinases and protein-tyrosine kinases comprise two superfamilies of a single protein kinase superfamily: the eukaryotic protein kinases or ePKs.

Traditionally, posttranslational modification (PTM) of proteins by ePKs was thought to be unique to the more "complex" eukaryotic cellular functions (Hanks, Quinn et al. 1988; Hanks and Hunter 1995; Shi, Potts et al. 1998). However, protein phosphorylation events were eventually discovered within all three domains of life. Evidence of protein kinase activity in prokaryotes was not observed until 1969, when Kuo and Greengard first reported the activity of a cyclic-AMP dependant protein kinase in *Escherichia coli* (Kuo and Greengard 1969). Although the *E. coli*-isolated protein kinase utilized ATP to phosphorylate, the protein substrate was exogenous to the bacterium: histone from calf thymus. Verification of the presence of bacterial protein kinase activity *in vivo* was not documented until the late 1970s when several groups simultaneously published reports of covalently modified phosphoresidues on proteins in *E. coli* and *Salmonella typhimurium* (Wang and Koshland 1978; Garnak and Reeves 1979). The *in vivo* phosphorylation of bacterial proteins, such as isocitrate dehydrogenase in *E. coli*, was concluded to be the result of prokaryotic protein kinase activity.

Prokaryotic protein kinases were initially observed to phosphorylate their substrates primarily on histidine or aspartate residues, thus utilizing different catalytic mechanisms than the traditional ATP-dependent kinases. For several years the pervading assumption was that prokaryotic protein kinases and ePKs evolved from separate ancestors following the divergence of prokaryotic and eukaryotic organisms (Hanks, Quinn et al. 1988; Kennelly and Potts 1996; Cozzone 1998; Leonard, Aravind et al. 1998; Shi, Potts et al. 1998). Subsequently, however, several groups of researchers published reports on the presence of "eukaryotic-like" protein kinases in bacteria (Zhang, Munoz-Dorado et al. 1992) and archaea (Skorko 1984; Smith and King 1995). Moreover, histidine kinase-like enzymes, once thought to be exclusive to bacteria, have been discovered within rat mitochondria (Popov, Zhao et al. 1992), *Arabidopsis thaliana* (Chang, Kwok et al. 1993), and yeast (Ota and Varshavsky 1993; Maeda, Wurgler-Murphy et al. 1994). Such findings challenged the historic assumption of ePKs evolving to meet the cell-signaling demands of "higher" organisms (Kennelly and Potts 1996).

The Eukaryotic Protein Kinases or "ePKs"

A review by Hanks and Hunter characterizes the eukaryotic protein kinase superfamily as having a 250-300 amino acid catalytic core domain containing the 12 subdomains outlined in Table 1-1 (Hanks and Hunter 1995). These subdomain sequences perform three main catalytic roles:

1) Bind and orient a phosphate donor (e.g. ATP) into a complex with a divalent cation such as Mn^{2+};

2) Bind and orient the peptide/protein substrate relative to the phosphate donor;
3) Transfer the γ-phosphate from the phosphate donor to an acceptor hydroxyl residue of serine, threonine, or tyrosine on the protein substrate.

In humans, the ePKs represent one of the largest protein families, constituting the products of approximately 1.7% of all human genes, as well as the overwhelming majority of all protein kinases (Kostich, English et al. 2002; Manning, Whyte et al. 2002). Following completion of the human genome sequencing project, 518 protein kinases were identified and of these, 478 were determined to be typical ePKs (Manning, Whyte et al. 2002).

The human ePKs can be divided into seven major groups of enzymes each containing all 12 of the conserved ePK subdomains and one "other" group containing unclassifiable, atypical eukaryotic protein kinases (aPKs) (Hanks 2003). The cyclic-nucleotide and calcium-phospholipid-dependant kinase (or AGC) group, for example, contains 61 typical ePKs further sub-classified into subfamilies such as the protein kinases A and C (PKA, PKC) found in many phosphorylative cell-signaling pathways.

Both protein-serine/threonine kinases and protein-tyrosine kinases exist within the ePK superfamily. Whether a protein kinase will phosphorylate its protein substrate on serine/threonine or tyrosine residues can be predicted from the sequence of the catalytic loop subdomain VIb (Table 1-1). Protein-serine/threonine kinases commonly contain the sequence Asp-Xaa-Lys-Xaa-Xaa-Asn with the basic amino acid lysine being conserved. Tyrosine protein kinases usually have, in lieu of lysine, an arginine residue

Subdomain	Consensus	Function
I	ogxG$_{52}$xogxv	Nucleotide Binding
II	oaoK$_{72}$xo	Nucleotide Binding
III	E$_{91}$xxoo	Nucleotide Binding
IV	h$_{100}$xxooxoxxxo	Structural
V	oooo*oo$_{123}$	Structural
VIa	+oxooh$_{158}$	Structural
VIb	oohrD$_{166}$ok+xNooo	Phosphotransfer Catalysis
VII	oko+D$_{184}$fgo+	Metal-Ion Cofactor Interaction
VIII	+pE$_{208}$oo	Protein Substrate Binding
IX	D$_{220}$oo+ogooo	Salt Bridge Formation
X	ooxxo$_{250}$	Structural
XI	R$_{280}$x+	Salt Bridge Formation

Table 1-1. ePK superfamily sub-domains. Consensus numbering based on mouse cAMP protein kinase Cα. Uppercase letters: universally conserved residues; lowercase letters: highly conserved; 'o': non-polar residues; *: polar residues; 'x': any amino acid; +: small residues with near neutral polarity. Highlighted regions represent the most critical subdomains. Adapted from "The eukaryotic protein kinase superfamily: kinase (catalytic) domain structure and classification" (Hanks and Hunter 1995).

two or four amino acids downstream from the essential aspartic acid residue: Asp-Xaa-Arg-Xaa-Xaa-Asn or Asp-Xaa-Xaa-Xaa-Arg-Asn.

The Importance of Archaea

The archaeal/eukaryotic connection

Over thirty years ago, Carl Woese proposed a controversial rearrangement of a classical taxonomic institution—the prokaryote and eukaryote dichotomy—based on comparative sequence analyses of 16s ribosomal RNA obtained from bacteria, eukaryotes and methanogens (Woese and Fox 1977). The new phylogenetic tree would consist of three main branches, or "urkingdoms", denoted *Eubacteria*, *Eucarya* and the *Archaeabacteria*. It was also recognized that the three urkingdoms might not have evolved in parallel from a single ancestor, as depicted in the universal phylogenetic tree (Figure 1-1). Eventually, *Archaeabacteria* and *Eubacteria* were given their own taxonomic status as the *Archaea* and *Bacteria* thus delineating the three domains of life (Woese, Kandler et al. 1990). Although bacteria and archaea shared similar gross morphology, such as the lack of nuclear membrane and small cell size, results gleaned from the rRNA sequences suggested that the *Archaeabacteria* and *Eucarya* were more closely related than in the previous phenotypic grouping which placed the methanogenic archaeons within the *Bacteria* (Woese and Fox 1977; Whitman 2009).

The *Archaea* make for strange relatives to eukaryotes. Archaeal microorganisms are found in some of the harshest, most unusual environments on earth. They can thrive in high salt concentrations, at temperatures at or above 100°C, and can withstand extreme pH levels. The archaea can be subdivided into two distinct lineages: the *Euryarcheota* and *Chrenarchota* (Woese, Kandler et al. 1990). The *Euryarcheota* are a

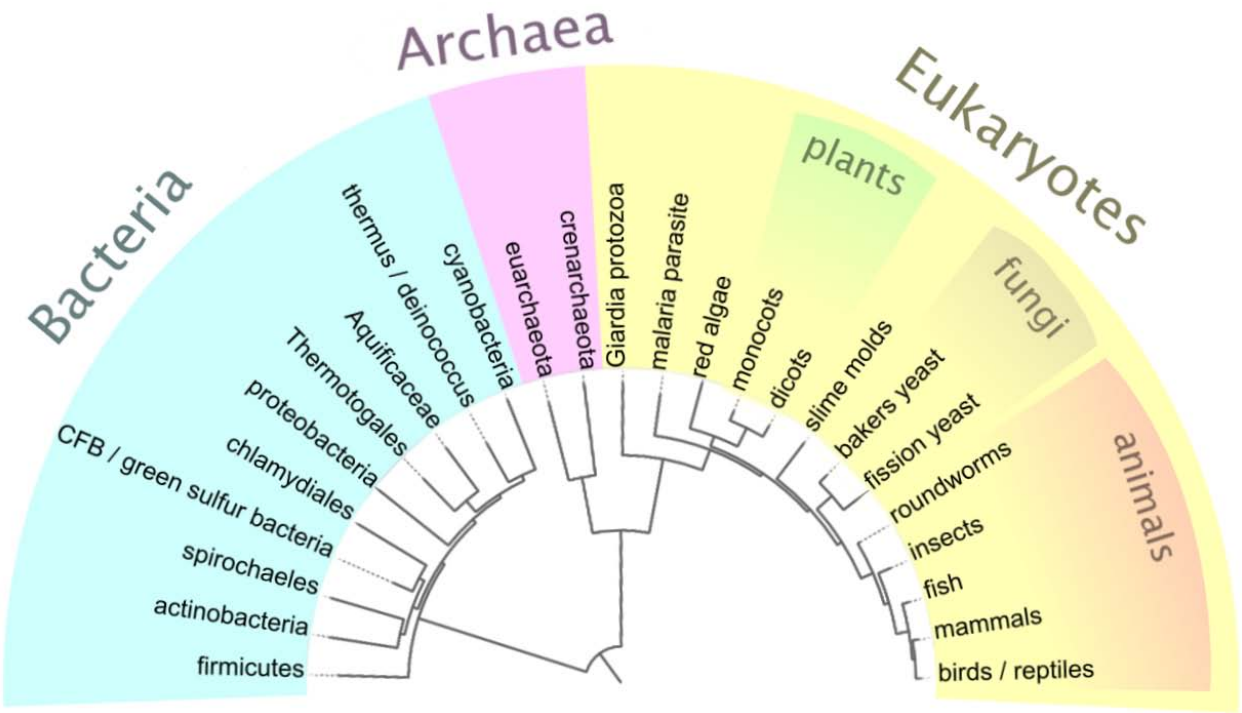

Figure 1-1. Universal tree of life. The Woese phylogenetic tree depicting the three domains of life places the *Archaea* and *Eucarya* on the same branch, apart from *Bacteria*. Figure designed by Madeline Price Ball using information obtained from the "Interactive Tree of Life" (Ciccarelli, Doerks et al. 2006).

diverse group comprised of the halophilic or salt-loving organisms, methanogens, and several extreme acidophiles. The *Chrenarcheota* consist mainly of hyperthermophilic organisms (Lewalter and Müller 2006). Since all three domains of life, including both lineages of *Archaea* contain hyperthermophiles, it has been proposed that the *Chrenarcheota* represent the most ancient forms of life (Woese, Kandler et al. 1990).

Posttranslational modifications (PTMs) in *Archaea*

As evidenced in eukaryotic organisms, within the *Archaea* some PTMs such as glycosylation and methylation have been implicated in the regulation of DNA replication, signal transduction, cell cycle regulation and protein translation (Eichler and Adams 2005). However, with respect to protein phosphorylation in *Archaea,* very little information is available on the identities of proteins that are targeted, the enzymes responsible for phosphorylation-dephosphorylation, or the response(s) generated by this reversible process (Leonard, Aravind et al. 1998; Kennelly 2003; Eichler and Adams 2005; Kennelly 2007).

With the advent of whole genome sequencing in the 1990s, the presence of many homologous gene sequences were identified between *Archaea*, such as the thermoacidophilic *Sulfolobus solfataricus* P2, and *Eucarya.* An interesting find was the presence of ePK-like kinases (ELKs) in many prokaryotic organisms, including archaeal species (Kannan, Taylor et al. 2007). The traditional ePKs and the ELKs contain similar catalytic domains and a conserved protein kinase-like fold (PKL) but typically share low sequence homology, less than 20%, to the ePKs or even between other ELK members (Figure 1-2). Similarly, members of the *Archaea* were discovered to contain PTMs once thought to be strictly eukaryotic in nature (Eichler and Adams 2005). Perhaps archaea

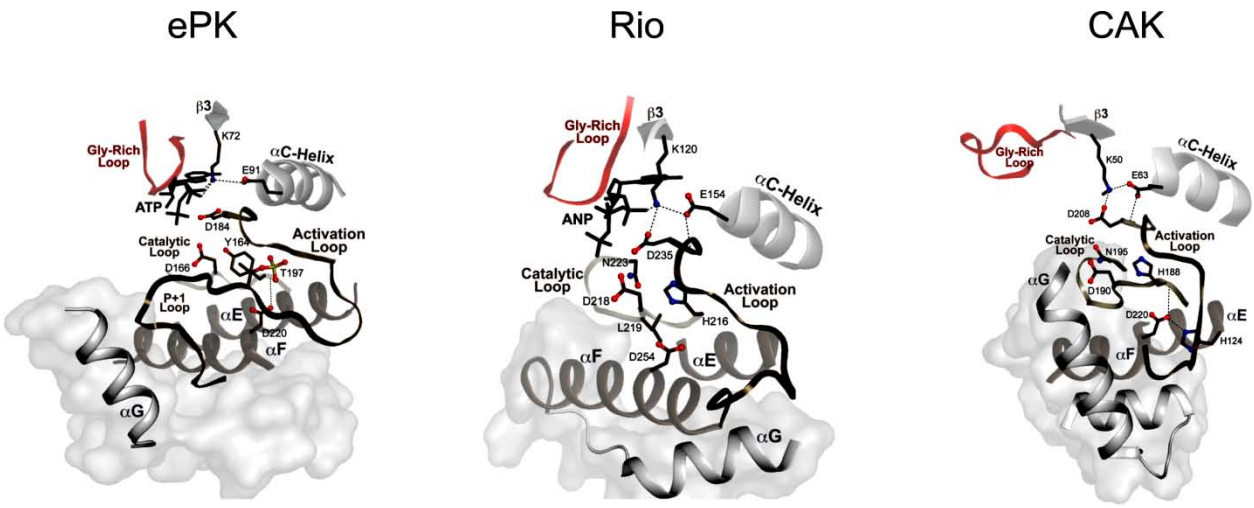

Figure 1-2. The conserved core and variable regions of three PKL family members. The ePK family is represented by PKA, Rio of the Euryarchaeota *Archaeoglobus fulgidis*, and CAK (choline and aminoglycoside kinases) from *Enterococcus*. The conserved regions are shown as ribbon structures and the variable regions by space-filling models. This figure was taken directly from "Structural and Functional Diversity of the Microbial Kinome" (Kannan, Taylor et al. 2007).

are the progenitors of signal transduction elements in eukaryotes (Pertseva and Shpakov 2009). If so, further studies of archaeal organisms offer the potential to simplify the elucidation of eukaryotic signal transduction processes by taking advantage of the former's smaller genomes (Olsen 1997).

An Archaeal Model System for Protein Phosphorylation

The chrenarcheon *Sulfolobus solfataricus*

A member of the chenarchaeal branch, *Sulfolobus solfataricus* prefers an optimal growth temperature of 80° C and a pH of 2-4, rightfully earning its classification as a thermoacidophile. One might not expect to find PTM mechanisms—once thought to be exclusive to eukaryotes and bacteria—within an organism living under such extreme conditions (Eichler and Adams 2005). However, in 1997 phosphotyrosine residues were detected on proteins isolated from cultures of three different archaeal organisms, including *S. solfataricus* (Smith, Kennelly et al. 1997). With the aid of the published genome sequence (She, Singh et al. 2001), homology searches for protein kinases within *S. solfataricus* P2 eventually led to the discovery of eleven open reading frames (ORFs) encoding putative eukaryotic-like protein kinases.

The use of *S. solfataricus* as a model system for the study of protein phosphorylation events lends itself as an attractive option for several reasons. As previously mentioned, its genome has been sequenced so searches and comparisons of ORFs are readily implemented. Also, the entire genome encodes less than 3000 ORFs and eleven putative eukaryotic-like protein kinases—a manageable number for biochemical characterization of protein kinase activity—compared to the approximately 20,000 genes and 500 ePKs identified in the human genome. Lastly, the evolutionary

relationships between the three domains can be elucidated through studies of the little understood *Archaea*. Of particular interest are sequence homologies between *Eucarya* and *Archaea* as evidenced on their placement within contemporary phylogenetic trees (Figure 1-1).

SsoPK4: a serine/threonine protein kinase

Two potential serine/threonine protein kinases, the products of ORFs *sso2387* and *sso0469*, in *S. solfataricus* were shown to exhibit phosphotransfer activity *in vitro* (Lower and Kennelly 2003; Lower, Potters et al. 2004). Another of the potential protein kinases discovered through homology searches of the *S. solfataricus* P2 genome was the ORF *sso3182*. The deduced product of this ORF contained a sequence Asp_{476}-Val-Lys-Pro-Gln-Asn_{481} fitting the consensus for subdomain VIb for catalysis of phosphotransfer in eukaryotic protein-serine/threonine kinases (Figure 1-3).

The portion of ORF *sso3182* encoding the deduced cytoplasmic domain of its protein product, SsoPK4, was cloned and the potential protein kinase expressed as a recombinant fusion protein in *E. coli* (Ray, W.K., unpublished). As shown in Figures 1-4 and 1-5, recombinantly-expressed SsoPK4 phosphorylates exogenous protein substrates *in vitro,* such as modified histone H2A, on serine and threonine residues. SsoPK4 has also been observed to phosphorylate recombinantly-expressed archaeal translation factors (Ray, W.K., unpublished).

Recombinant overexpression and resulting enzyme characterization establishes the general catalytic identity of a protein such as SsoPK4. However, a more formidable challenge lies in dissecting the pieces of the regulatory network(s) in which it participates. What is the native protein kinase substrate(s) for SsoPK4? What cellular

Figure 1-3. Alignment of serine/threonine protein kinase catalytic regions. 1JNK1: c-Jun N-terminal kinase, *Homo sapiens*; SsoPK4, *S. solfataricus*; MDPK, myotonic dystrophy protein kinase, *H. sapiens*; PkaD, developmentally-regulated protein kinase 1, *D. Dictyostelium discoideum*. Underlined region is subdomain VIb. Boxed regions correspond to universally conserved residues in subdomains VIb, VII, VIII, respectively. ":" represents highly conserved residues.

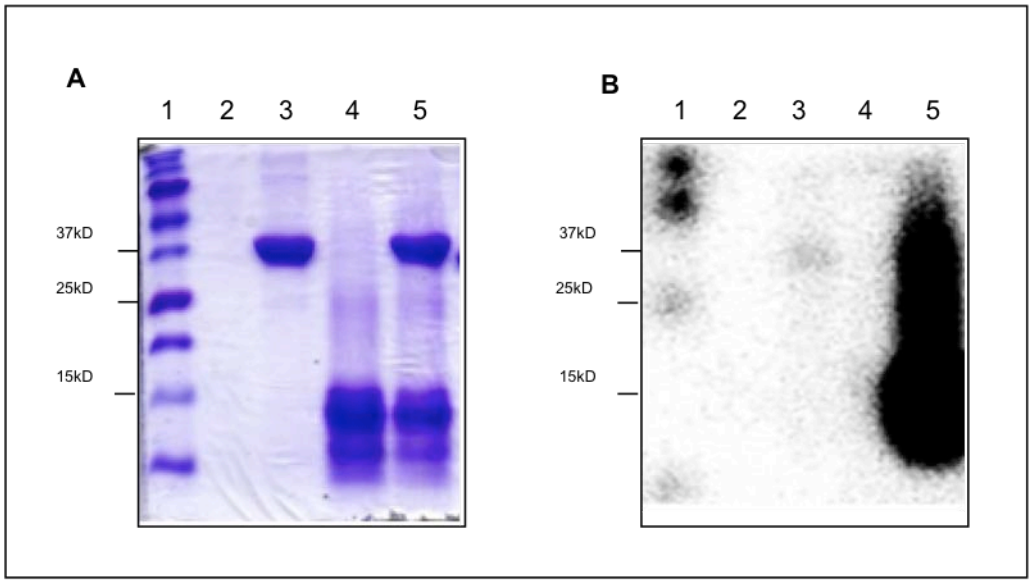

Figure 1-4. SsoPK4 phosphorylates histone protein H2A. Histone H2A was incubated with SsoPK4 and [γ-^{32}P]-ATP and the protein mixture analyzed by SDS-PAGE. Shown are the Coomassie-stained gel (A) and its corresponding autoradiogram (B). Lane 1: Molecular weight ladder; Lane 2: empty; Lane 3: SsoPK4; Lane 4: H2A; Lane 5: SsoPK4 and H2A.

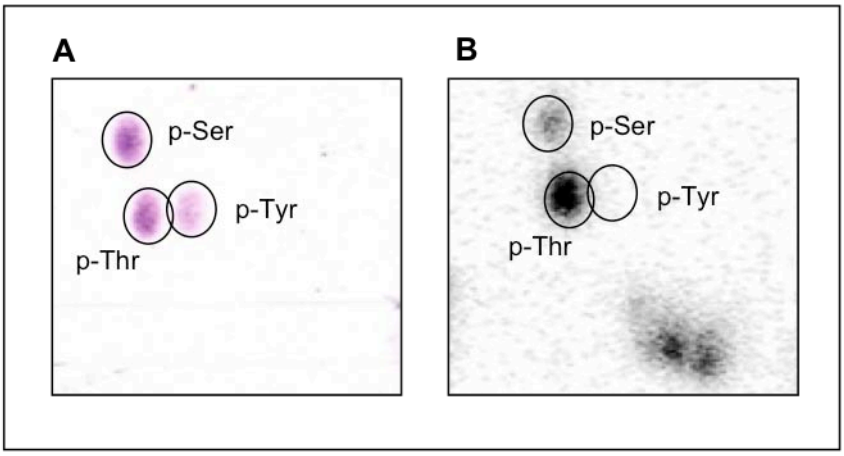

Figure 1-5. SsoPK4 phosphorylates H2A on serine and threonine residues. SsoPK4-phosphorylated histone H2A from Figure 2 was hydrolyzed with HCl. The resulting mixture was then resolved into its component amino acids by 2D electrophoresis. Shown are (A) the ninhydrin-treated residues of phosphoamino acid analysis standards as well as (B) the corresponding autoradiogram of the resolved animo acids.

functions are regulated by SsoPK4-mediated phosphorylation within *S. solfataricus?* Could the activities of protein kinase phosphorylation by SsoPK4 shed some light on phosphorylation mechanisms in more complex organisms?

The Protein Kinase-Protein Substrate Problem

Determining that SsoPK4 has protein kinase activity is only one piece of a much larger puzzle. The most pressing challenge in tracing protein kinase biochemistry lies in the identification of physiologically relevant protein substrates (Berwick and Tavare 2004; Johnson and Hunter 2005; Sopko and Andrews 2008). There are two fundamental questions that must be answered in order to better understand protein phosphorylation signaling: 1) what substrates and residue(s) are phosphorylated, and 2) which protein kinase(s) is responsible for phosphotransfer to these residues (Johnson and Hunter 2005)? Unlike the protein kinases and protein phosphatases, which contain large conserved catalytic domains, the diversity of the phosphoprotein targets of these enzymes renders their identification by simple sequence mining problematic.

Several *in vitro* and *in vivo* strategies have been devised for identifying protein kinase substrates. One *in vitro* technique involves assaying the expression products of ORFs located near the protein kinase gene sequence or, in the case of archaeal and bacterial protein kinases, within the same operon. This approach follows the assumption that, as functionally linked proteins, expression of protein kinases and their substrates may be closely coordinated. However this method fails to consider that many protein kinases are promiscuous in nature; they can phosphorylate multiple substrates, with each substrate potentially having their own physiological pathway.

High-throughput methods such as microarray analysis (Feilner, Hultschig et al. 2005) and identification using mass-spectrometry techniques (Huang, Tsai et al. 2007) offer the virtues of being unbiased and direct. However, these methods can be confounded by the low abundance of a phosphoprotein and/or the anionic nature of many phosphopeptides. Nor do they provide information, in and of themselves, as to the protein kinases responsible for catalyzing these PTMs. Antibodies to specific phosphoamino acids or phosphorylated motifs (Yaffe and Elia 2001; Zhang, Zha et al. 2002) are severely limited by the lack of reliable and sensitive antibodies against phosphoserine and phosphothreonine.

In 1997 Fukunaga and Hunter developed an *in vitro* method for detecting protein kinase substrates through screens of an immobilized phage display expression library of HeLa cell cDNA inserts with purified ERK1 (extra-cellular signal-related kinase 1), MAP (mitogen-activated protein) kinase, and [γ-^{32}P]-ATP (Fukunaga 1997). The result of their efforts was the identification of 120 cDNA clones whose recombinant products tested positive for phosphorylation by ERK1 as detected using radiolabeled ATP. This approach offered the advantages of being unbiased and directly implicating a specific protein kinase. However, more than half of these clones consisted of false-positive artifacts produced as the result of out-of-frame ligations of the cDNA insert within the phage. Of the remainder, seven of the clones identified encoded known structural proteins, two of which have previously been identified as ERK substrates (Blenis 1993; Davis 1993), lending support to the method as a plausible means of identifying physiological substrates. In the end, two novel ERK substrates were discovered, of which MNK1 (mitogen-activated protein kinase-interacting kinase 1) was thoroughly examined *in vitro* as a substrate for ERK.

Although some drawbacks exist such as those encountered using high-throughput methods previously described, the immobilized phage display screening method as a tool to identify protein kinase substrates is attractive to us for several reasons:

1) A phage display expression library can be created directly from genomic *S. solfataricus* DNA, which is virtually devoid of introns,
2) A serine/threonine protein kinase of interest, SsoPK4, was available, readily purified, and exhibited *in vitro* kinase activity toward exogenous protein substrates,
3) Phosphorylated expression products--including those with low-level expression *in vivo*--can be identified through searching the known *S. solfataricus* genome sequence,
4) The same genomic library can be screened with other protein kinases of interest from *S. solfataricus.*

One caveat remains: Such *in vitro* results are "generally considered a necessary but not sufficient" means of identifying a *bona fide* protein substrate (Sopko and Andrews 2008). Therefore any potential substrates identified through expression library screens will ultimately need to be examined *in vivo*.

My research objective involved identifying potential protein kinase substrates by screening a phage display library—created from *S. solfataricus* genomic DNA—with the purified recombinant protein kinase SsoPk4. We hypothesized that phosphorylated *S. solfataricus* peptide fragments discovered through the screening process would be phosphorylated by SsoPK4 on the identified recombinant protein *in vitro*. The specific aims of my research project are delineated on the following page.

Specific Aim 1: ***Identify and overexpress potential SsoPK4 protein substrates through utilization of a genomic phage display expression library and protein kinase activity assays.***

Purified kinase SsoPK4 and [γ-^{32}P]-ATP will be applied to screen membranes containing a phage display library comprised of recombinantly expressed proteins and protein fragments. DNA inserts from phages encoding phosphorylated, radiolabeled substrates will be cloned, overexpressed, and their protein products assayed *in vitro* with SsoPK4 to determine potential substrate capability.

Specific Aim 2: ***Characterize the potential substrate(s).***

Characterization of the potential substrate(s) will be necessary to determine baseline function. Protein sequences will be inspected for motifs or domains diagnostic for molecular functions. Informed by this information, assays will be implemented, developed, or modified to analyze any substrate(s) discovered through phage display screens of the *S. solfataricus* genome.

Specific Aim 3: ***Examine the relationship between the substrate and SsoPK4 to determine the effects, if any, phosphorylation has on substrate function.***

Once a baseline characterization of the substrate has been obtained, changes in substrate activity will be determined via *in vitro* methods involving, but not limited to, radiolabeled [γ-^{32}P]-ATP and mutagenic alteration of the potential substrate. Ultimately, any changes in substrate activity through its phosphorylation by SsoPK4 will be examined by *in vivo* analysis of *S. solfataricus* cultures that have been genetically modified to either overexpress or repress the expression of SsoPK4 and/or its possible substrate.

Chapter II: Materials and Methods

General Instrumentation

Unless otherwise indicated, all culture media and general laboratory reagents were purchased from Fisher Scientific (Pittsburgh, PA) or Sigma-Aldrich (St. Louis, MO). [γ-^{32}P]-ATP was purchased from PerkinElmer Life and Bioanalytical Sciences (Boston, MA). Electronic autoradiography was performed using a Packard Instant Imager (Meridan, CT). Liquid scintillation counting was performed with a Beckman-Coulter LS 6500 Multi-purpose Scintillation Counter (Atlanta, GA). Light absorption was measured with a Hitachi UV-2000 Spectrophotometer or a Shimadzu UV-265FW Spectrophotometer, depending upon availability. Fluorescence was measured using an RF-1501 Spectrofluorophotometer (Kyoto, Japan). The pH of solutions was determined using an Accumet Basic AB15 pH meter from Fisher Scientific. PCR amplifications were performed using a PCR Sprint Thermal Cycler from Thermo Electron Corporation (Milford, MA). Bacterial cells were harvested by centrifugation on a Sorvall Superspeed RC-2B or RC-5B centrifuge equipped with an SS-34 or GSA rotor from DuPont Instruments (Newton, CT) or, alternatively, a Marathon 12 KBR centrifuge from Fisher Scientific. Cells were lysed with a Sonifier Cell Disruptor, Model W185, equipped with a microprobe from Heat Systems-Ultrasonics (Plainview, NY). Thin layer electrophoresis was performed on a Multiphor II electrophoresis unit equipped with a Multi Temp II thermostatic circulator (both Pharmacia LKB, Uppsala, Sweden) and an EC4000P Series 90 programmable power supply (E-C Apparatus Corporation, Holbrook, NY). This power supply was sometimes used for performing SDS-polyacrylamide gel elecrophoresis (SDS-PAGE). A Bio-Rad PowerPac 200 power supply and a Trans-Blot

Cell electrophoretic blotting unit (Hercules, CA) were used for SDS-PAGE and Western blotting, respectively. Densitometric scans of stained gels were obtained with the Umax (Fremont, CA) Astra 1220S scanner or with a ChemiDoc XRS 170-8070 gel box from Bio-Rad (Richmond, CA) equipped with Quantity One software. Agarose gel electrophoresis was performed on an Easy-Cast Electrophoresis System from Owl Scientific, Inc. (Portsmouth, NH).

Materials

Materials for molecular biology

Custom oligonucleotide primers were synthesized by Life Technologies (Rockville, MD) and Sigma-Genosys (St. Louis, MO). Genomic *S. solfataricus* P2 DNA was from the American Type Culture Collection (ATCC) (Manassas, VA). *Pfu* Turbo DNA polymerase, *Pfu* Ultra HF DNA polymerase, and QuickChange II Site-Directed Mutagenesis Kit were supplied by Stratagene (La Jolla, CA). pET21d and pET29b expression vectors were obtained from Novagen, now EMD Chemicals (Madison, WI). Restriction enzymes *Nco*I, *Sal*I, and *Dpn*I were obtained from New England BioLabs (Ipswich, MA). S.O.C. media (Super Optimal broth with Catabolite repression) was from Invitrogen (Carlsbad, CA). Shrimp alkaline phosphatase, T4 DNA ligase, and sequencing-grade trypsin were from Promega (Madison, WI). Alpha-Select Gold Efficiency *E. coli* cells were from Bioline (Taunton, MA). QIAquick Spin PCR Purification and QIAprep Spin Miniprep Kits were from QIAGEN (Valencia, CA). DNA sequencing was performed by the Core Laboratory Facility in the Virginia Bioinformatics Institute (Blacksburg, VA).

Materials for protein purification and enzyme characterization

Recombinant proteins were expressed in BL21-CodonPlus(DE3)-RIL competent cells from Stratagene (La Jolla, CA). Complete, mini, EDTA-free protease inhibitor cocktail tablets were from Roche Applied Science (Mannheim, Germany) and IPTG was obtained from Bioline (Taunton, MA). Chelating Sepharose Fast Flow was purchased from Amersham Biosciences (Piscataway, NJ). Coomassie Plus Protein Assay Reagent was ordered from Pierce (Rockford, IL). SDS-PAGE was performed on a Mini-PROTEAN II Cell system using Precision Plus Dual Color pre-stained molecular weight standards, both from Bio-Rad (Hercules, CA). Immobilon-P PVDF (polyvinylidine fluoride) transfer membranes were purchased from Millipore (Billerica, MA). Anti-mouse IgG Alkaline Phosphatase Antibody and SIGMA*FAST*™ BCIP®/NBT (5-Bromo-4-chloro-3-indolyl phosphate/nitro blue tetrazolium) tablets were from Sigma-Aldrich (St. Louis, MO). His-tag monoclonal antibody was obtained from Novagen (Madison, WI). 3MM CHR chromatography paper was obtained from Whatman (Florham Park, NJ) and 10% (w/v) solution of trichloroacetic acid (TCA) in water from Ricca Chemical Company (Arlington, TX). Cellulose thin layer plates (20 x 20cm) were purchased from EMD Chemicals (Gibbstown, NJ).

General Methods

Solutions and procedures for growth of cells

Luria-Bertani (LB) liquid medium and LB agar plates as well as stock solutions of antibiotic, and IPTG were prepared as described in the appendices of *Molecular Cloning: A Laboratory Manual* (Sambrook, Fritsch et al. 1989). Cultures of *Escherichia coli* (*E. coli*) were incubated overnight in liquid LB media with or without

antibiotic. Cells for daily use were streaked on LB agar plates containing the appropriate antibiotic and stored at 4°C. For long-term storage 800 µl portions of an overnight culture were mixed with 200 µl of sterile 80% (v/v) glycerol and stored at -80°C.

Agarose gel electrophoresis

Agarose gel electrophoresis of samples of plasmid and genomic DNA as well as the products of PCR reactions was performed as described by Sambrook, Fritsch et al. Agarose gels at 0.8% (w/v) were cast by melting 0.8 g of high-melt agarose in 100 ml of Tris-acetate EDTA (TAE) buffer to which 5 µl of 10mg/ml ethidium bromide (EtBr) in H_20 was added. DNA samples were prepared by mixing five volumes of sample with one volume of 5x Nucleic Acid Loading Buffer (Bio-Rad). Electrophoresis in TAE buffer was performed at 100 volts for 30-45 minutes. EtBr-stained oligonucleotides were visualized by illumination with a UV light source.

Cloning of open reading frames (ORFs)

Numerous oligonucleotide primers were designed for the amplification of ORFs of interest by PCR using *S. solfataricus* genomic DNA as a template. For each reaction, 5 pmol each of forward primer (5'-3') and reverse primer (3'-5') was combined with 100-200ng of genomic *S. solfataricus* DNA, 200 µM each of dNTP mix (dATP, dTTP, dGTP, dCTP), 5 µl of 10x *Pfu* reaction buffer, and 2.5 units of *Pfu* Turbo DNA polymerase. The final volume was adjusted to 50 µl with sterile, E-pure H_20. Occasionally the PCR reaction was supplemented with 5 µl of 25 mM $MgCl_2$. Reactions were performed in a thermal cycler programmed to maintain a temperature of 95°C for 5 min to denature

the genomic DNA, followed by 30 cycles of: 1) 30 seconds at 95°C, 2) 30 seconds at 58°C, 3) 1 minute per kb of predicted product at 72°C in order to denature, anneal and elongate the PCR product, respectively. The reaction was concluded with a 5-minute incubation at 72°C for further elongation of the DNA segment. The presence of a PCR product was verified by agarose gel electrophoresis using a 10 µl sample of the reaction mixture. The remaining 40 µl were purified using the QIAquick Spin PCR Purification kit.

PCR products were prepared for ligation into pET expression vectors as follows. For a 50 µl reaction, 50 units each of *Nco*I and *Sal*I restriction enzymes were added to a 35 µl sample of purified PCR product to which 5 µl of 10x restriction enzyme buffer and 5 µg of bovine serum albumin (prepared as a 1:100 dilution from 10x stock supplied by the manufacturer). The mixture was incubated for 4-16 hours at 37°C. A sample of pET vector (2000 ng) was also treated with *Nco*I and *Sal*I restriction enzymes, in the same manner as described for PCR product treatment, to ensure directional cloning of the *S. solfataricus* DNA fragment. Next, the vector was incubated with shrimp alkaline phosphatase (SAP) to remove the terminal phosphate group and thus prevent self-ligation of the vector. A portion, 5 µl, of 1x SAP buffer and 5 units of SAP (5 µl of 1 U/µl stock) were added to 40 µl of the restriction digest mixture. The mixture was incubated for 15 min at 37°C, then immediately heated at 65°C for 15 min to inactivate the phosphatase. The digested PCR product was ligated into the SAP-treated vector by combining 9.5 µl of restriction digest containing the PCR product with 3 µl of mixture containing the digested, SAP-treated vector, 3 units of T4 DNA ligase (1 µl of 3 U/µl stock), 1.5 µl 10x DNA ligase buffer in a total volume of 15 µl and incubating for 16 hr at 4°C.

The ligation reaction was used to transform Alpha-Select Gold Efficiency *E. coli* cells (genotype: F- *deoR endA1 recA1 relA1 gyrA96 hsdR17*(r_k^-, m_k^+) *supE44 thi-1 phoA* Δ(*lac*ZYA *arg*F)U169 Φ80*lacZ*ΔM15 λ-), a strain optimized for plasmid production. A 2 to 4.5 µl aliquot of the ligation reaction was added to 25 µl of competent cells and the mixture incubated on ice for 30 min. The cells were incubated at 42˚C for 30 sec ("heat shocked"), then put back on ice. Next, 175 µl of S.O.C. media was added to the cooled cells and the mixture incubated at 37˚C with horizontal shaking (225 rpm) for 30 min. A 100 µl portion of the resulting cell culture was spread on LB plates supplemented with 50 µg/ml Kan when cloning into the pET29b vector or 100 µg/ml Amp for pET21d and the plates incubated overnight at 37˚C.

Plasmid isolation and sequence verification

Selected colonies were used to inoculate, via a sterile toothpick, 5 ml portions of LB media containing either 100 µg/ml Kan or 50 µg/ml Amp for pET29b or pET21d vectors, respectively. Following incubation overnight at 37°C with continuous agitation, an aliquot of the culture was withdrawn for preparation of glycerol permanents for long-term storage (described previously). Plasmid DNA was isolated from the remainder of each culture using a QIAprep Spin Miniprep kit as directed by the manufacturer. The plasmid DNA was eluted with 35 µl of sterile, E-pure H_20. A 10 µl portion of the eluate, which generally contained 50-100 ng/µl of isolated plasmid, was submitted to the Virginia Bioinformatics Institute's (VBI) Core Laboratory Facility for determination of the sequence of the DNA insert using the flanking T7 promoter and T7 terminator sequences of the pET vector system for priming.

Site-directed mutagenesis

Mutant variants of expression plasmids were generated using the QuikChange II Site-Directed Mutagenesis kit according to the manufacturer's protocol. In brief, mutagenic primers (5' – 3' and 3' – 5') were designed to flank the area selected for mutation (see Table 1b). Mutagenic primers, 5 pmol each, were added to 5 µl 10x *Pfu* Ultra HF buffer, 200 µM of dNTP mix, 5-10 µl of template plasmid (2 ng/µl) and sterile, E-pure H_20 was added to a final volume of 50 µl. Next, 2.5 units of *Pfu* Ultra HF DNA polymerase (1 ul of 2.5 U/µl stock) were added and the mixture incubated in a thermocycler as follows. An initial denaturing step of 30 sec at 95°C was followed by 16 cycles of 1) 30 sec at 95°C, 2) 1 min at 55°C, 3) 1 min/kb of plasmid at 68°C. Following completion, 10 units (1 µl of 10 U/µl stock) of the restriction enzyme *Dpn*I were added and the reaction was incubated at 37°C for 1 hr in order to degrade the methylated parent strands lacking the desired mutation. The mutant DNA was transformed into Alpha-Select Gold Efficiency *E. coli* cells and the mutant plasmids isolated and submitted for sequence verification as described in the previous sections.

Expression of recombinant proteins

Isolated plasmid DNA was routinely transformed into BL21-CodonPlus DE3-RIL Competent Cells (genotype: *E. coli* B F^- *ompT hsdS*(r_B^- m_B^-) *dcm*$^+$ Tet^r *gal* λ(DE3) *endA* Hte [*argU ileY leuW* Cam^r]) designed for high-level expression of recombinant proteins in *E. coli*. One µl (~ 100 ng/ul) of plasmid sample was combined with 75 µl of competent cells and incubated on ice for 30 min. The cells were heat shocked for 30 sec at 42°C and placed back on ice. S.O.C. media, 175 µl, was added to cells and the mixture was incubated 30 min at 37°C with horizontal shaking at 225 rpm. The contents of the

tube were then added to 5 ml LB containing 34 µg/ml Cam and 50 µg/ml Kan for pET29b constructs or 100 µg/ml Amp for pET21d constructs and the mixture incubated overnight at 37˚C with shaking at 225 rpm.

Following overnight growth, an aliquot of the culture was removed for preparation of a glycerol permanent for long-term storage as described previously. The remaining culture was used to inoculate 250 ml of LB media supplemented with 34 µg/ml Cam, 50 µg/ml Kan for pET29b recombinant proteins or 100 µg/ml for pET21d. In addition, 2 ml of 0.5 M L-arginine were added to give a final concentration of 4 mM L-arginine. The culture was incubated at 37˚C and 225 rpm until its OD_{600} reached 0.5 to 0.8 (about 2 hours). At that point, expression of the recombinant protein was induced by addition of 200 µl of 1 M IPTG to give a final concentration of 0.8 mM IPTG. The culture was incubated for an additional 4 hours at 37˚C and 225 rpm and the cells were harvested by centrifugation at 4400 x g for 10 min at 4-8˚C. Cell pellets were stored at -20˚C until needed.

Purification of histidine-tagged recombinant proteins

Protein purifications from cell pellets were adapted from established protocols (Ray, Keith et al. 2005). The cell pellet was thawed on ice and resuspended in 5 ml of purification buffer A (50 mM MOPS at pH 7 containing 150 mM NaCl, 20 mM imidazole, 10 mM ß-mercaptoethanol) containing lysozyme (250 µg/ml) and protease inhibitor cocktail (Roche). The cell suspension was incubated on ice for 30 min and then lysed by sonication with the Heat-Systems Ultrasonics microprobe using 5 x 30 sec rounds of sonic disruption, each separated by one min incubation on ice. The cell debris was removed from the lysate by centrifugation for 10 minutes at 4400 x g at 4-8˚C. The

supernatant liquid was transferred to a pre-chilled 15 ml glass centrifuge tube and centrifuged at 10,000 x g for 20 min at 4°C in order to further clarify it. The supernatant was transferred to a 15 ml conical tube and incubated in a 65°C water bath for 10 min in order to denature remaining *E. coli* proteins. The heated solution was cooled on ice for 10 min and clarified by centrifugation at 4400 x g for 20 min at 4-8°C.

The histidine-tagged recombinant proteins generated by the pET expression vectors were purified by immobilized metal affinity chromatography (IMAC). One ml of Chelating Sepharose Fast Flow resin (Amersham Biosciences) was charged with Ni^{2+} as instructed by the manufacturer. The Ni^{2+}-charged medium was then washed twice with 5 ml purification buffer A (described above) by tumbling end-over-end rotation for 5 min each. The resin was collected by centrifugation at 500 x g for 5 min and the supernatant liquid was discarded. Approximately 5 ml of the supernatant from the heat denaturation step described above containing the His-tagged protein was added to the Ni^{2+}-charged resin and incubated at room temperature for 30 min with end-over-end rotation.

The resin was collected by centrifugation at 500 x g for 5 min and the supernatant was decanted and saved for later analysis with SDS-PAGE. The resin was further washed with 2 x 12.5 ml of buffer A, each with rotation and sedimentation of medium as described above. The resin was resuspended in 5-10 ml of buffer A and packed in a 7 ml column. Adherent protein was eluted from the column using 5 ml of buffer B (50 mM MOPS at pH 7, containing 150 mM NaCl, 500 mM imidazole, 10 mM ß-mercaptoethanol) and the eluate was collected in a 15 ml glass centrifuge tube. The eluate was brought to 95% saturation with the slow addition of 3.25 g of ammonium sulfate and constant stirring. The solution was incubated on ice for 20 min and

centrifuged at 10,000 x g for 20 min at 4˚C. The pellet was resuspended in 0.5 – 1 ml of storage buffer, (e.g. for SsoPK4: 50 mM MOPS at pH 7, 10 mM $MnCl_2$, 15% (v/v) glycerol). The solution was divided into 100 µl aliquots and stored at -80˚C for further use.

Determination of protein concentration

Protein concentrations were routinely determined with the method of Bradford assay (Bradford 1976) using Coomassie Protein Assay Reagent and BSA standards (0.2 µg/µl) both supplied by Pierce. A protein standard curve was generated by detecting the absorbance at 595 nm produced from a linear gradient of 0-16 µg of BSA. The standard curve was used to determine the unknown concentration of the IMAC-purified protein. Assays in which absorbances fell within the linear range of the BSA standard curve were averaged to estimate protein concentration.

SDS-PAGE

Resolving gels containing 10, 12, and 15% (w/v) acrylamide, stacking gels containing 5% (w/v) acrylamide, and running buffer (25 mM Tris, 192 mM glycine, 0.1% (w/v) SDS) were prepared according to Laemmli (Laemmli 1970). Polymerized running gels could be stored wrapped in cellophane for up to two weeks at˚C prior to use. Protein samples were prepared for SDS-PAGE by mixing 3 volumes of sample with 1 volume of 4x-SDS loading buffer, which consisted of 200 mM Tris, pH 8.0, containing 400 mM DTT, 8% (w/v) SDS, 40% (w/v) glycerol and 0.4 % (w/v) bromophenol blue (Sambrook, Fritsch et al. 1989). The sample mixtures were then heated for 5 min at 100˚C and collected by centrifugation before loading, unless otherwise indicated.

Samples were resolved by electrophoresis at 150 continuous volts for 1-1.5 hours or until dye front entered the running buffer using a Bio-Rad Power Pac 200 power supply. Gels were removed from the cassette and prepared for further analysis.

Native-PAGE

Resolving gels of various acrylamide percentages and stacking gels were poured as described above except 10% (w/v) SDS was omitted from the gel solutions. Protein samples were prepared for native-PAGE by mixing 3 volumes of sample with 1 volume of 4x-native-PAGE loading buffer consisting of 200 mM Tris, pH 8.0, containing 40% (w/v) glycerol and 0.4 % (w/v) bromophenol blue and were loaded without heating. Samples were resolved by electrophoresis as described above.

Detection of proteins on SDS-polyacrylamide gels

Molecular weights of polypeptides were estimated by comparison to Precision Plus Dual Color molecular weight standards from Bio-Rad. Gels were removed from the cassette and stained for 1 hr by immersion in approximately 30 ml of 50% (v/v) methanol, 40% (v/v) E-pure H_20 and 10% (v/v) acetic acid containing 0.075% (w/v) Coomassie R-250 Brilliant Blue; followed by soaking overnight in 30 ml of 50% (v/v) methanol, 40% (v/v) E-pure H_20, and 10% (v/v) acetic acid to remove free dye (Fairbanks, Steck et al. 1971). A Kimwipe was added to the destaining solution and the container gently agitated on a horizontal shaker in order to help remove excess stain. Stained gels were preserved in plastic wrap, scanned, and stored at room temperature. Alternatively, ^{32}P-labeled proteins were identified by autoradiography of a plastic-wrapped gel using the Packard Instant Imager.

Western blotting to transfer proteins on PVDF membranes

Proteins contained within an SDS-polyacrylamide gel were occasionally transferred to a membrane for further analysis using a wet-transfer electophoretic process, or Western blot procedure. Following SDS-PAGE, described above, an SDS-polyacrylamide gel containing protein(s) of interest was equilibrated in transfer buffer (10 mM CAPS, pH 11, containing 10% (v/v) methanol). An Immobilon-P PVDF membrane was prepared by soaking for 15 sec in 100% methanol, then for 2 min in E-pure H_2O and 5 min in transfer buffer. The Bio-Rad Trans-Blot Cell cassette transfer apparatus, containing the prepared PVDF membrane and the SDS-polyacrylamide gel, was prepared according the manufacturer's user guide. The electrophoretic transfer was carried out for 1 hour at 1.oo amp (100 constant volts) at 4°C using a Bio-Rad Power Pac 200 power supply. Afterwards, the membrane was removed and allowed to air dry for several hours or, when used immediately, was soaked in 100% methanol for 10 sec and allowed to air dry an additional 15 min.

Immunological detection of proteins on PVDF membranes

To visualize the proteins immobilized on PVDF membranes, the proteins were exposed to antibodies that were conjugated to enzymes (e.g. horseradish peroxidase) detectable through a simple colorimetric assay. Following protein transfer, the dried PVDF membrane was placed in a tray containing 10 ml of blocking buffer: Tris-buffered saline, a.k.a. TBS (10 mM Tris-Cl, pH 7.5, 150 mM NaCl) containing 0.1% (v/v) Tween-20 and 1% (w/v) BSA. A dilution of the required primary antibody was prepared in blocking buffer in which the membrane was immersed. For the His-tag antibody from Novagen for example, a 1:5000 dilution was prepared by diluting 2 µl of His-tag

antibody in 10 ml of blocking buffer. Following incubation on a horizontal shaker at room temperature for 1 hr, the antibody solution was decanted and saved at 4°C. The membrane was washed with 2 x 20 ml TBS buffer. Next, 2 µl of a solution of a secondary antibody, Anti-Mouse IgG Alkaline Phosphatase antibody (Sigma), was added to 10 ml of TBS-T (TBS as prepared above plus 0.1% (v/v) Tween-20). The membrane was incubated with this mixture for 30 min at room temperature with horizontal shaking. Afterwards, the membrane was rinsed with 4 x 20 ml TBS buffer. A SIGMA*FAST*™ BCIP®/NBT tablet was dissolved in 10 ml E-pure H_20 and the membrane incubated in this solution until bands of a purple precipitate appeared indicating where the phosphatase activity of the secondary antibody was present. Rinsing the membrane thoroughly with E-pure H20 terminated the colorimetric reaction. The membrane could then be scanned and stored for future use.

Assay of protein kinase activity

The protein kinase SsoPK4 was routinely assayed for phosphotransferase activity using an adaptation of the method developed by Walsh (Walsh, Brostrom et al. 1972). For each 50 µl reaction, 1 µg of SsoPK4 was incubated with 10 µg of protein substrate in SsoPK4 activity buffer consisting of 50 mM MOPS, pH 7, and 4 mM $MnCl_2$. A 1 mM ATP stock solution was prepared containing the radioisotope [γ-^{32}P]-ATP at a concentration of≈ 3 µCi/µl in order to trace the transfer of phosphate. The phosphorylation reaction was initiated by addition of 5 µl of the radioactive ATP stock solution followed by incubation at 65°C for 30 min. The liquid was collected in the bottom of the tubes by brief centrifugation on a microcentrifuge and 15 µl of each mixture was spotted on 2 x 2 cm squares of Whatman 3MM filter paper. The filter

papers were washed, with continuous agitation, in 250-300 ml of 10% TCA (v/v) containing 4% $NaPP_i$ (w/v). Next, the radioactive liquid waste was discarded and the filter papers were washed several times more, with continuous agitation, in 5% TCA (v/v) containing 2% $NaPP_i$ (w/v) solution in increments of 20 min. The washed filter papers were dried, transferred to liquid scintillation vials and 1 ml of Fisher ScintiSafe 30% or Fisher ScintiSafe 50% Liquid Scintillation Fluid (LSF) was added. The quantity of ^{32}P-radioactivity associated with the filter papers was then determined as counts per minute (cpm) using a Beckman-Coulter LS 6500 Multi-purpose Scintillation Counter.

In-gel digestion of proteins with trypsin

In order to analyze protein samples contained in acrylamide gels following SDS-PAGE, gel sections were incubated with a protease to generate peptides capable of diffusing out of the gel matrix. In-gel tryptic digestion of proteins was performed following procedures developed by Shevchenko (Shevchenko, Wilm et al. 1996) with modifications. The section of the gel containing the protein band(s) of interest was excised, cut into 1-2 mm^2 slices, and placed in a 1.5 ml tube. The volume of the gel pieces was estimated visually (e.g. 50 µl). The gel acrylamide fragments were washed for 5 min in three volumes (e.g. 150 µl) of 100 mM ammonium bicarbonate with agitation on a vortex mixer. Following sedimentation by low-speed centrifugation (200-300 x g), the free liquid was removed and discarded and the gel slices further washed, with agitation, for 15 min in three volumes of 100 mM ammonium bicarbonate. If excess Coomassie stain remained in the slices following these washes, the pieces was incubated for 30 min at 37˚C in three volumes of a 1:1 ammonium bicarbonate:HPLC-grade acetonitrile solution. The slices were collected by centrifugation and the free liquid

discarded. Acetonitrile, three volumes, was added and the mixture incubated at 37˚C for 15 min. The preceding two steps were repeated and the gel slices were kept dry by incubation at 37˚C while the trypsin solution was prepared. A trypsin solution was prepared by adding 1 ml of pre-chilled 100 mM ammonium bicarbonate to the contents of a fresh tube of sequencing-grade modified trypsin (20 µg, Promega). A volume of trypsin solution approximately equal to that of the original gel slices was added to the desiccated gel slices. The slices were incubated on ice for 30-45 min to allow them to rehydrate. Additional trypsin solution then was added to cover the rehydrated gel slices and the mixture incubated for 12-16 hr at 37˚C.

The slices were collected by low-speed centrifugation and the supernatant liquid transferred to a fresh 1.5 ml tube. The gel slices were combined with two volumes of 0.5% (v/v) trifluoroacetic acid (TFA) and the mixture agitated by immersion in a Fisher Scientific Ultrasonic Cleaner water bath for 15 minutes to promote diffusion of tryptic peptides out of the gel matrix. Slices were sedimented by centrifugation and the supernatant liquid removed and combined with the previously saved fraction. The slices were subjected to three more rounds of extraction using 0.5% (v/v) TFA plus 20%, 40% or 60% (v/v) HPLC-grade acetonitrile. The pooled supernatants were evaporated by incubation 100˚C with the tube caps removed to concentrate the peptides for further analysis (e.g. phosphoamino acid analysis) and stored at -20˚C until needed.

Phosphoamino acid analysis

Phosphoamino acid analysis was performed using an adaptation of the method from Mahoney (Mahoney, Nakanishi et al. 1996). In brief, an aliquot of the radiolabeled peptide fragments generated from an in-gel digest (as described above), containing

approximately 10,000 cpm of ^{32}P-radioactivity, was evaporated to dryness. The dried residue was resuspended in 200 µl of 6 M HCl and incubated in a heat block set for 100˚C until desiccated. The resulting peptide hydrosylate was resuspended in 5 µl of pH 1.9 buffer (2.5% (v/v) formic acid, 7.8% (v/v) glacial acetic acid) and 5 µl of a phosphoamino acid standard mix (5 mM each p-Tyr, p-Thr, p-Ser in pH 1.9 buffer).

The individual phosphoamino acids in the hyrdrolysate were resolved from one another by 2D-electrophoresis and thin-layer chromatography (TLC). The flatbed LKB Multiphor II electrophoresis unit was cooled to˚C with the thermostatic circulator. Using a pencil, a 20 x 20 cm TLC plate was marked with a 1.5 cm border on all four sides and divided into 10 x 10 cm quadrants Two 0.5 µl aliquots of xylene cyanol (1 µg/µl stock in pH 1.9 buffer, as prepared above) were spotted at the 1.5 cm border on the upper and lower left-side quadrants as guidelines. Portions of the resuspended sample/standard mix, containing 1000-2000 cpm of ^{32}P radioactivity each, were spotted in 0.5 µl increments at origins to the right of each quadrant and approximately 1 cm above the 1.5 cm pencil border from the bottom of the plate. Next, the TLC plate was wetted using Whatman 3MM filter paper soaked in buffer pH 1.9. Wetting was arranged so the flow of buffer tended to concentrate the spotted samples. The first dimension was run for one hr at 1000 constant volts. The plate was then dried thoroughly—preferably overnight—rotated 90˚ clock-wise, and the plate rewetted with buffer pH 3.5 (0.5% (v/v) pyridine, 5% (v/v) glacial acetic acid) and run in this same buffer for 20 min at 1000 constant volts. Again, the plate was dried thoroughly. A solution of ninhydrin (0.2% (w/v) in acetone) was evenly misted over the plate. Next the plate was heated at 80˚C for 5 min to visualize the amino acid standards, which appear as a trio of purple spots. Phosphorylated species were detected by autoradiography of the TLC plate.

Library Screening Procedures

Materials, solutions, and preparations for library screens

Two undergraduate researcher students, Richard Dunham and Dustin Hite, generated a phage display library from *S. solfataricus* P2 genomic DNA following protocol from the Lambda ZAP II Predigested *EcoR* I/CIAP-Treated Vector Kit from Stratagene (La Jolla, CA). The *E. coli* XL1-Blue MRF' bacterial host strain (genotype: Δ(*mcrA*)183 Δ(*mcrCB-hsdSMR-mrr*)173 *endA1 supE44 thi-1 recA1 gyrA96 relA1 lac* [F′ *proAB lacI*^{q}ZΔM15 Tn*10* (Tet^{r})]) was also supplied as part of the Lambda Zap II kit. NitroPure nitrocellulose membranes (0.45 micron, 137mm) were from GE Osmonics (Trevose, PA). Pure*Taq* Ready-To-Go PCR Beads were from Amersham Biosciences, now GE Healthcare (Piscataway, NJ). Oligonucleotide primers complementary to the T7 promoter (5'-TAATACGACTCACTATAGGG-3') and M13 reverse sequence (5'-CAGGAAACAGCTATGAC-3') were from Invitrogen (San Diego, CA).

XL1-Blue MRF' host cells were maintained by weekly streaking onto fresh LB agar plates supplemented with 12.5 μg/ml of tetracycline (Tet). SM buffer for λ-phage dilutions was prepared as described in appendix A.7 of Molecular Cloning: A Laboratory Manual (Sambrook, Fritsch et al. 1989). "Top agar" was prepared by dissolving 3.15 g of Difco NZYM Broth (Detroit, MI) in 150 ml E-pure H_2O and adding Difco Bacto-agar to a concentration of 0.7% (w/v) before sterilizing. The LB agar plates used for determining phage titers and screens were prepared in large, 150 x 15 mm Petri dishes (Fisher). Blocking buffer (2o mM Tris-HCl, pH 8.0, containing 150 mM NaCl and 1% (w/v) BSA) was prepared by combining 20 ml of 1 M Tris-HCl, pH 8.0, with 30 ml of 5 M NaCl, adding 10 g of BSA, and bringing to a final volume of 1 L with E-pure H_2O. Kinase Reaction Buffer (KRB) at 10x concentration was prepared by combining 125 ml 1 M

Tris-HCl, pH 7.0, with 2.47 g $MnCl_2$, and 0.77 g DTT in E-pure H_20 to a final volume of 250 ml. RWB at 1x concentration was made by mixing 50 ml 10x RWB in 450 ml E-Pure H_20 to give a final concentration of 50 mM MOPS, pH 7, 5 mM $MnCl_2$ and 2 mM DTT. Triton Wash Buffer (TWB) was prepared as a 5x concentrated stock by combining 100 ml of 1 M Tris-HCl, pH 7.5, with 150 ml of 5 M NaCl, 100 ml of 0.5 M EDTA, pH 8, 2.34 g of EGTA, 0.77 g of DTT, 25 ml of Triton X-100 and, finally, E-pure H_2O to 1 L. TWB in 1x concentration (20 mM Tris-HCl, pH 7.5, containing 150 mM NaCl, 10 mM EDTA, 1 mM EGTA, 1 mM DTT, and 0.5% (v/v) Triton X-100) was made by diluting 200 ml 5x TWB in 800 ml H_2O. Reaction wash buffer (RWB; 20 mM Tris-HCl, pH 7.5, containing 150 mM NaCl, 10 mM EDTA, and 1 mM EGTA) was prepared with and without Triton X-100 at a final concentration of 0.1% (v/v). Masking buffer was prepared by dissolving ATP in RWB to a final concentration of 25 µM.

Determining the titer of the phage library

An aliquot of the amplified *S. solfataricus* genomic library was titered to determine the concentration of viable phage particles present as described in the manual for the Lambda ZAP II Predigested *EcoR* I/CIAP-Treated Vector Kit. In brief, a colony of XL1-Blue MRF' host cells was selected and used to innoculate 5 ml LB supplemented with tetracycline (Tet, 12.5 µg/ml). The cell culture generally reached mid-log phase following incubation at 30˚C for 10-12 hrs, with shaking. At this point, the host cells were collected by centrifugation at 2000 x g for 10 min and resuspended in 10 mM magnesium sulfate (MgSO4) to an OD_{600} of approximately 0.5. Next, the phage library was thawed and serial dilutions prepared (1:1000, 1:10,000, etc.) in SM buffer. An aliquot (1-10 µl) of each serial-dilution was added to a round-bottom culture tube

containing 600 µl of the XL1-Blue MRF' host cell resuspension and incubated for 15 min at 37°C. Top agar, 6.5 ml, was added to each tube. The contents were quickly mixed and evenly poured onto pre-warmed 150mm LB-plates. The plates were incubated for 8-12 hrs at 37°C to permit formation of lytic plaques. The number of plaques was determined and the titer was expressed as plaque-forming units (pfu) per µl of solution according to the following formula:

[(Number of plaques (pfu) * dilution factor) / Volume of dilution added (µl)]

Plating the phage library and preparing plaque lifts

Plaque lifts were performed following protocols derived from the Lambda ZAP II Predigested *EcoR* I/CIAP-Treated Vector Kit manual. XL1-Blue MRF' host cells cultured in LB-Tet media were collected by centrifugation and resuspended in $MgSO_4$ as described above. For primary screens, 600 µl of resuspended host cells were inoculated with a portion of the phage library containing 20,000 pfu, as determined by the above titer procedure, and incubated for 15 min at 37°C to allow the phage to attach to the cells. Top agar, 6.5 ml, was added to each tube, the contents mixed and poured onto a pre-warmed (37°C) 150 mm LB-plate. The plate was incubated at 37°C for 4 hrs to allow time for plaque formation. Next, a 137 mm nitrocellulose membrane soaked in 10 mM IPTG was overlaid on the agar plate and the overlaid plate incubated for an additional 4 hrs at 37°C. The membrane, labeled A, was lifted, wrapped in plastic wrap and stored at 4°C. A second membrane, also soaked in 10 mM IPTG, was placed on the agar plate and the combination incubated 4 hrs at 37°C. This membrane, labeled B, was also wrapped in plastic and stored at 4°C until needed. The LB -agar plate was also stored at 4°C.

Preliminary identification of potential phosphoproteins

Membranes A and B from the plaque lifts were routinely developed by a modification of a procedure developed by Fukunaga (Fukunaga and Hunter 1997). Each membrane was placed in a separate 150 x 15 mm empty Petri dish and incubated in 15 ml of Blocking Buffer (prepared as described above) with horizontal shaking for 1 hr at room temperature. The buffer was discarded and the membranes washed with 2 x 5 ml TWB (described above). After the second TWB wash was discarded, membranes A and B were incubated for 10 min in 5 ml SsoPK4 kinase activity buffer (see Assay of Protein Kinase Activity, above). The activity buffer was discarded and the membranes were incubated 1 hr at room temperature in 5 ml of masking buffer (described above). Masking buffer was discarded and membranes were rinsed for 10 min in 5 ml of kinase activity buffer. The kinase activity buffer was discarded and the membranes were transferred to 150 x 25 mm Petri dishes for incubation with a protein kinase and [γ-^{32}P]-ATP. Radioactive reaction mixtures containing [γ-^{32}P]-ATP were made for each membrane as follows. Reaction A was composed of 4 ml kinase of activity buffer containing 25 µM ATP, 5 µCi/ml of [γ-^{32}P]-ATP, and 2 µg/ml of SsoPK4 (8µg total). Reaction B also contained 4 ml kinase activity buffer, ATP, and radiolabeled ATP but received H_2O instead of kinase in an amount equal to the volume of kinase added to Reaction A. Reaction A was added to membrane A, reaction B to membrane B, and the membranes were incubated for 2 hrs at 37°C with gentle shaking. Afterwards, the radioactive liquid was discarded and the membranes were rinsed in 5 x 5 ml RWB with Triton (see above) to remove free [γ-^{32}P]-ATP. The membranes were rinsed a final time in 5 ml RWB without Triton and allowed to air-dry.

Membrane imaging and secondary screens

Electronic autoradiography of the membranes was performed using a Packard Instant Imager. The autoradiogram was compared to its corresponding LB-agar plate to match areas that contained ^{32}P on the kinase-treated membrane with areas of plaque formation. The radiolabeled regions unique to plate A should, in theory, contain immobilized proteins and protein fragments that were phosphorylated by SsoPK4. In turn, these proteins should correspond to phage-expression products derived from the *S. solfataricus* genome. Segments of agarose containing plaques that aligned with radiolabeled spots were excised using a 1 ml pipet tip, with the tapered-end cut off, as a punch and the phage plugs were placed in 1.5 ml tubes. Each plug was covered with 1 ml SM buffer and incubated for 12-16 hrs at $4^{\circ}C$ to permit phage particles to diffuse from the matrix. The free liquid containing the suspended phage particles was decanted and titered, as described previously, to determine the number of phage particles (pfu/µl) present. A secondary screen was performed for each excised phage, but using much lower quantities of phage per plate (250 or 500 pfu). Plaque lifts, membrane development and imaging were performed as described above for the primary screen.

Determination of phage insert sequence

In order to determine the sequence of the *S. solfataricus* fragment inserted within the pBluescript phage vector, phages isolated from a secondary screen were subjected to PCR using Pure*Taq* Ready-to-go PCR beads following manufacturer recommendations. In brief, each 0.2 ml PCR tube contained 1 Ready-to-go PCR bead, 1 µl of excised, isolated phage product (approximately 10,000 pfu), 5 pmol each of T7

promoter primer and M13 reverse primer and sterile, E-pure H_2O to a final volume of 25 µl. The PCR reaction was performed using the PCR Sprint Thermal Cycler as described previously with the following modifications. The initial denaturation step was increased to 6 min to break phage coats followed by 35 cycles of denaturation, annealing, and elongation. The final elongation step was increased to 8 min to account for the average DNA insert length of 4 kb. The presence of PCR products was verified by agarose gel electrophoresis. The PCR products were then purified using the QIAquick Spin PCR Purification kit, and submitted to VBI for DNA sequencing, all as described previously.

AtpA/ATPase Characterization Methods

Malachite green assay for inorganic phosphate

Initially, the formation of inorganic phosphate resulting from the hydrolysis of ATP was measured colorimetrically via the Malachite green assay (Lanzetta, Alvarez et al. 1979). On the day of use, the malachite green color reagent was prepared by combining three volumes of a 0.045% (w/v) solution of malachite green with one volume of 4.2% (w/v) ammonium molybdate in 4 N HCl. After mixing, the color reagent was allowed to stand for 20 min or until a light, yellow-brown color developed. For each 50-µl reaction, subunit AtpA was combined with subunit AtpB in activity buffer (50 mM MES, pH 5.5, 4 mM $CaCl_2$). The reaction was initiated with the addition of 250 µM ATP (5 µl of 2.5 mM ATP stock). The mixtures were incubated for 30 min at 65°C and the liquid collected at the bottom of the tube by brief centrifugation. Color reagent, 800 µl, was added, followed by agitation on a vortex mixer. Next, 200 µl of a 34% (w/v) sodium citrate solution was added, the mixture agitated on a vortex mixer, and the liquid collected in the bottom of the tube by brief centrifugation. After standing at room

temperature for 15 to 30 min to permit full color development, the absorbance of the mixture at 660 nm was measured. The production of inorganic P_i via ATP hydrolysis was quantified by comparison to a K_2HPO_4 standard curve.

Assay of inorganic phosphate by molybdate extraction

A second method of detecting inorganic phosphate produced by the ATPase-catalyzed hydrolysis of ATP routinely employed the molybdate extraction procedure of Martin and Doty (Martin and Doty 1949) with modifications (Schacter 1984). In brief, samples of the ATPase subunits AtpA and AtpB were combined in a total volume of 30 µl of ATPase activity buffer (50 mM MES, pH 5.5, 4 mM $CaCl_2$). Reaction was initiated by adding 20 µl of a solution of 125 µM ATP (50 µM final) supplemented with 1.25 µCi/µl of [γ-^{32}P]-ATP (0.5 µCi/µl final). The mixture was incubated for 30 min at 65°C and liquid collected at the bottom of the tube by centrifugation. The reaction was terminated by addition of 150 µl 20% (v/v) TCA followed by agitation with a Vortex mixer. Precipitated proteins were pelleted by a 3 min centrifugation at 16,000 x g and 74 µl of the supernatant liquid transferred to a fresh 1.5 ml tube. To this 74 µl aliquot, 200 µl of Molybdate Reagent (1.5% (w/v) ammonium molybdate in 25 mM H_2SO_4) were added, followed by 10 µl of 4 mM K_2HPO_4 and, lastly, 200 µl of a 1:1 isobutanol:toluene mixture. The mixture was thoroughly agitated using a Vortex mixer for 30 sec and the organic and aqueous layers separated by centrifugation at 11,750 x g for 3 min. A portion, 50 µl, of the organic layer was added to 1 ml of LSF and counted for ^{32}P radioactivity. The use of radiotracers enabled the detection of much smaller quantities of P_i by this technique than was possible using Malachite Green.

Chemical cross-linking of ATPase subunits

Subunits of the ATPase were chemically linked with EDC (1-ethyl-3-(dimethylaminopropyl)) as described (Schäfer, Rössle et al. 2006) In a 1.5 ml reaction tube, 20 µg each of ATPase subunits were pre-incubated in a final volume of 45 µl of ATPase activity buffer (50 mM MES at pH 5.5, 4 mM $CaCl_2$) containing 2 mM ATP for 10 min at 65°C. After pre-incubation, cross-linking was induced by the addition of 5 µl of 50 mM EDC (5 mM final concentration) in water followed by end-over-end rotation for 30 min at room temperature. The reaction was terminated by the addition of 15 µl of 4x SDS-PAGE loading buffer. Samples were heated for 1 min at 100°C, 20 µl free liquid collected at the bottom of the tube by centrifugation, and a 20 µl portion loaded onto 12% SDS-polyacrylamide gels for SDS-PAGE analysis as previously described. Samples were stained and destained as described previously. Species of high M_r (relative molecular mass) corresponding to presumed cross-linked polypeptides were submitted to the Mass Spectrometry Research Incubator in Blacksburg, VA for identification of their constituent proteins.

Identification of mis-folded proteins by partial proteolysis

In order to compare protein folding between wild type SsoATPase subunits and its mutant variants, tryptic digests were performed following established procedures (Kennelly, Starovasnik et al. 1990; Coulter-Mackie and Lian 2008). The ratio of protein:trypsin required for detecting intermediate species generated during proteolytic cleavage was empirically determined by incubation of the AtpA subunit in a solution of ATPase activity buffer (50 mM MES, pH 5.5, 4 mM $CaCl_2$) for various times and at

several temperatures. Following a 10 min pre-incubation at 65°C of AtpA (3 µg/µl), AtpB (3 µg/µl), and 1 mM ATP in activity buffer, it was determined that incubation at room temperature for 15 min with a 45:1 ratio of protein to trypsin was sufficient for approximately 50% of native AtpA to undergo cleavage. Each reaction was terminated by mixing 3 volumes of the reaction with one volume of 4x SDS-PAGE loading buffer and heating at 100°C for 3 min. Protein digests were resolved by SDS -PAGE on 12% SDS-polyacrylamide gels followed by Coomassie staining as described previously.

Instrinsic tryptophan fluorescence

The intrinsic tryptophan fluorescence of *S. solfataricus* ATPase subunits was measured following established methods (Biukovic, Rossle et al. 2007). In brief, ATPase subunits, with or without addition of the nucleotide ATP, were pre-incubated for 10 min at 65°C in activity buffer (50 mM MES at pH 5.5, 4 mM $CaCl_2$). Once cooled to room temperature, the samples were analyzed using the RF-1501 Spectrofluorophotometer from Shimadzu. Samples were excited at 295 nm with the emission range set to record from 310 to 380 nm. Data was collected at 5-10 nm intervals. Fluorescence titration experiments required a fixed emission wavelength set to 335 nm.

Chapter III:

Screening of a *S. solfataricus* Expression Library for Potential Protein Kinase Targets

Preliminary Research

SsoPK4: cloning, overexpression, and protein kinase activity

The ORF *sso3182* was predicted to encode a protein-serine/threonine kinase based on homology searches of the *S. solfataricus* genome. To test this assumption, W. K. Ray cloned *sso3182* into the pET vector system and overexpressed the encoded ligation product as a recombinant protein in *E. coli* BL21-CodonPlus(DE3)-RIL cells as described in Materials and Methods. The protein product, SsoPK4, was assayed for protein kinase activity against exogenous protein substrates as described previously. SsoPK4 phosphorylated histone 2A (H2A) *in vitro* on serine and threonine residues (Chapter I, Figures 1-4 and 1-5).

Construction of phage expression libraries from *Sulfolobus solfataricus* P2

Richard Dunham and Dustin Hite, undergraduate researchers in the Kennelly laboratory, constructed two phage display libraries from *S. solfataricus* P2 genomic DNA as described in Material and Methods. The two libraries differed in the identity of the restriction enzyme used to fragment the genomic DNA. Digestion conditions were optimized to produce fragments of 2-6 kilobases (Kb) in length for ligation into the λ-phage vector. *EcoR*I produced larger fragments for phage packaging than did *Tsp509*I, which cut *S. solfataricus* DNA more frequently. Successful ligation of *S. solfataricus* DNA and subsequent packaging of the recombinant vector into phage coats was verified

by blue/white color selection in the presence of X-gal (5-bromo-4-chloro-3-indolyl beta-galactoside) and IPTG (isopropyl ß-D-1-thiogalactopyranoside). The libraries were labeled "Sulf-Eco" and "Sulf-Tsp" based on the restriction enzyme (*EcoR*I or *Tsp509*I, respectively) used to generate the DNA fragments. Dustin Hite determined that the Sulf-Eco library had a titer of 7×10^5 pfu/µl and the Sulf-Tsp library contained 1.2×10^6 pfu/µl based on the calculation procedure described in Chapter II.

Library Screens

Primary screening with purified SsoPK4

A high concentration of plaque forming units (pfu) per agar plate was desired in order to ensure a broad representation of phage library expression products to be immobilized during membrane lifts. Based on the original library titer results (previous section), it was calculated that 2 µl of a 1:100 dilution of the Sulf-Eco library was sufficient to generate approximately 24,000 pfu per 150mm x 15 mm LB-agar plate:

Sulf-Eco (1:100 dilution): 1.2×10^4 pfu/µl * 2 µl = 2.4×10^4 pfu

For Sulf-Tsp, 3 µl of a 1:100 dilution of the original library concentration was required for an estimated 21,000 pfu:

Sulf-Tsp (1:100 dilution): 7×10^3 pfu/µl * 3 µl = 2.1×10^4 pfu

Duplicate samples of the "high pfu" aliquots of each library were incubated in resuspended XL1-Blue MRF' host cells prepared from overnight cultures as described in Materials and Methods. The phage-infected host cells were combined with Top Agar and layered over a total of four LB-agar/phage plates: Sulf-Eco (plates 1 and 2) and Sulf-Tsp (plates 3 and 4) libraries.

Plates 1-4 were incubated for 4 hrs at 37°C to allow plaque formation, then overlaid with nitrocellulose membranes that had been soaked in a solution containing IPTG in order to induce expression of the *S. solfataricus* phage inserts. The plates were returned to the incubator. Four hours later the membranes were lifted, labeled 1-4A, rinsed with TWB as described, and stored at 4°C for later use. A second set of membranes was overlaid on the plates and the combination incubated for 4 hrs at 37°C as before. The second, duplicate, set of membranes—labeled 1-4B—were lifted, rinsed and stored at 4°C. Closer inspection of the four plates showed that the bacteriophage had formed a lawn with indistinct plaque separation. The membranes were discarded without development since individual plaques could not be identified for excision from the corresponding LB-agar plate.

The primary screen plating procedure was repeated with two different aliquots of each library containing lower pfu to produce distinct plaques as opposed to a continuous bacteriophage lawn. Table 3-1 summarizes the pfu applied to each plate, the library used, the corresponding plate number, and the labels for the phage subsequently excised. The membranes containing immobilized phage expression products were incubated with [γ-^{32}P]-ATP in Kinase Reaction Buffer (KRB) as described in Library Screening Procedures of Chapter II. Membranes 1-4A were incubated with purified SsoPK4; membranes 1-4B were negative controls that lacked the protein kinase. Following incubation, the membranes were rinsed to remove excess radioactive ATP and analyzed by electronic autoradiography in order to detect any regions containing high levels of ^{32}P radioactivity (Fukunaga and Hunter 1997). The autoradiographic images in Figure 3-1 show membranes from plate 3 with phage populations #5 and #6. The regions of the upper agarose layer containing the plaques that aligned with the

Plate	Dilution	Pfu/µl (in dilution)	µl of dilution	Approx Pfu/plate	Phage isolated
Sulf-Tsp (7×10^5 pfu/µl)					
1	1:100	7000	2	14,000	#1, #2, #3
2	1:200	3500	3	10,500	#4
Sulf-Eco (1.2×10^6 pfu/µl)					
3	1:100	12,000	1.5	18,000	#5, #6
4	1:1000	1200	10	12,000	#7

Table 3-1. Plaque-forming units (pfu) per LB-agar plate in primary screen.

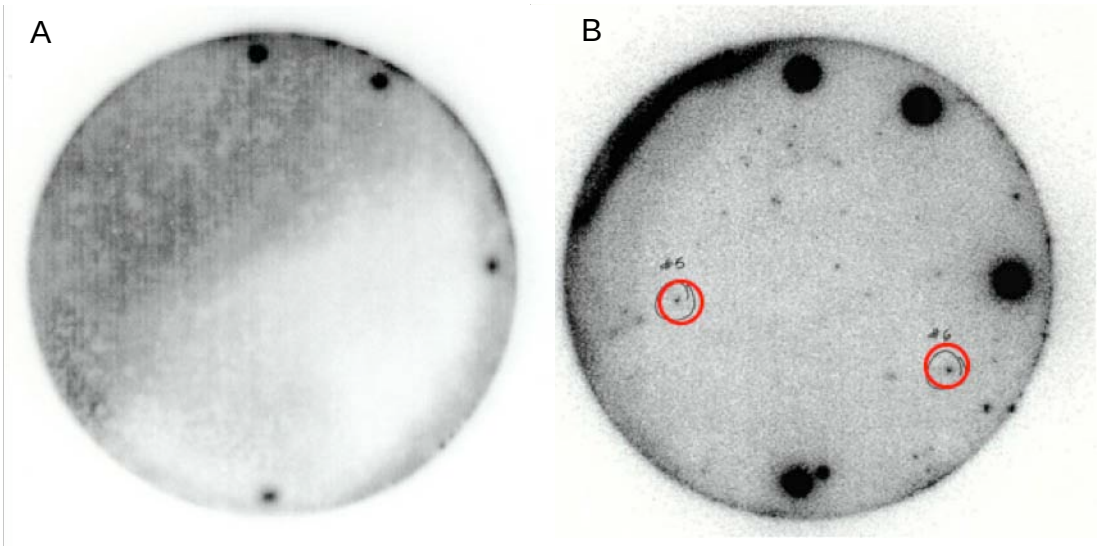

Figure 3-1. Autoradiogram results for Sulf-Eco library plate 3. Membranes were incubated in kinase reaction buffer (50 mM MOPS, pH 7, 5 mM $MnCl_2$, 2 mM DTT) and 25 µM ATP with 5 µCi/µl [γ-^{32}P]-ATP. A. Control membrane; plaque-lift membrane was incubated without SsoPK4. B. Small dark spots represent phage expression products phosphorylated with ^{32}P by SsoPK4. Numbered circles 5 and 6 outline phage populations that were excised for phage isolation and secondary screening. Dark circles on right edges of image correspond to marks made to orient the membrane to the plate.

autoradiographic “hot spots” were excised and dispersed into SM buffer following the protocol outlined in chapter II. The pfu concentration of excised primary phage populations #1-7 are shown in Table 3-2.

Secondary screen results

The secondary screening of isolated bacteriophage populations followed the same protocol as for initial library plating except each LB-agar plate contained approximately 250-500 pfu. Plating at a much lower pfu helps to ensure excision of monophage populations. Phages #4 (Sulf-Tsp) and #5 (Sulf-Eco), at 250 and 500 pfu each, were selected for secondary plating giving a total of four LB-agar plates. The pfu calculations were based on titer results shown in Table 3-2. A large portion of the top agar pulled away from the LB-agar plate during the final membrane lifts for #4 (250 and 500 pfu) and #5 (250 pfu). Only membranes #5A and B at 500 pfu were developed as described previously.

SsoPK4 phosphorylated numerous immobilized phage expression products as shown in the autoradiogram (Figure 3-2B). The circled areas numbered 1-5 correspond to the radiolabeled membrane images excised from the LB agar plate. These isolated phage populations should contain the protein or peptide products of the *S. solfataricus* insert that were expressed, trapped on the membrane, and ultimately phosphorylated by SsoPK4. A few phosphorylated spots were visible on the control membrane (Figure 3-2A). These could be the result of autophosphorylation by immobilized expression products as no kinase was added to solutions in development of control membranes.

Phage #	pfu/10^{-3} dil	pfu/10^{-4} dil	pfu/10^{-5} dil	pfu/µl
1	241	34	8	2.8×10^4
2	61	3	2	6.8×10^3
3	74	9	0	4.9×10^3
4	41	3	2	6.8×10^3
5	253	26	5	3.4×10^4
6	127	16	1	1.3×10^4
7	182	29	3	2.6×10^4

Table 3-2. Pfu concentration (pfu/µl) for primary phage titers. Excised phages #1-7 from primary screens of both *S. solfataricus* libraries were titered on LB-agar plates and the resulting plaques counted to determine pfu/µl.

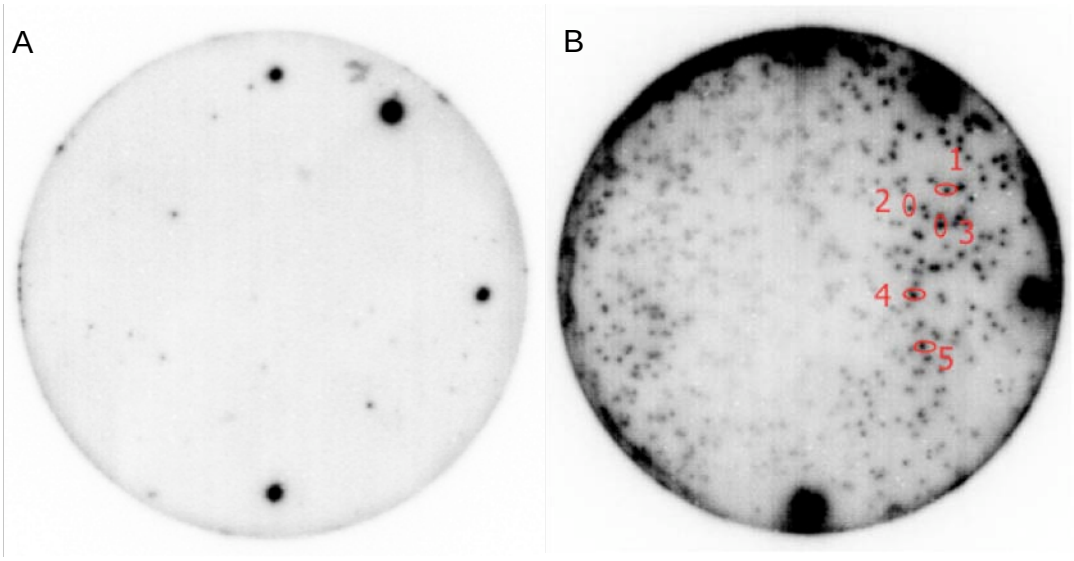

Figure 3-2. Autoradiogram results for secondary screening of phage #5 isolated from primary screen plate 3. Membranes were incubated in kinase reaction buffer (50 mM MOPS, pH 7, 5 mM $MnCl_2$, 2 mM DTT) and 25 µM ATP with 5 µCi/µl [γ-^{32}P]-ATP. A. Control membrane; plaque-lift membrane was incubated without SsoPK4. B. Small dark spots represent phage expression products phosphorylated with ^{32}P by SsoPK4. Numbered circles, 1-5, outline phage populations that were excised for genomic sequencing of the *S. solfataricus* insert region. Dark circles on right edges of image correspond to marks made to orient the membrane to the plate.

The five phages in Figure 3-2B were isolated for genomic DNA sequencing of the *S. solfataricus* insert. The insert region of each isolated phage was amplified by PCR using oligonucleotide primers complementary to the T7 promoter (5'-TAATACGACTCACTATAGGG-3') and M13 reverse sequence (5'-CAGGAAACAGCTATGAC-3'). These primers form cohesive ends by which the *S. solfataricus* genomic insert can be annealed to and ligated in the cloning vector (Figure 3-3). Each *Pure*Taq Ready-to-Go PCR reaction (Amersham Biosciences) contained 1 µl of the solution containing dispersed phage, 5 pmol T7 promoter primer, 5 pmol M13 reverse primer and 22.5 µl sterile E-pure H20 for a final volume of 25 µl. Thermocyler parameters were as described in Chapter II.

The PCR products were resolved by agarose gel electrophoresis. The presence of a single band in each amplified insert region was observed for each phage 1-5, suggesting that each contained a homogeneous, clonal phage population (Figure 3-4). The PCR products were purified utilizing the QIAquick Spin PCR Purification kit from QIAGEN according to manufacturer's protocol. 10 µl of each PCR product (~10 ng/µl) were submitted to the Virginia Bioinformatics Institute's (VBI) Core Laboratory Facility for DNA sequencing with the T7 promoter primer.

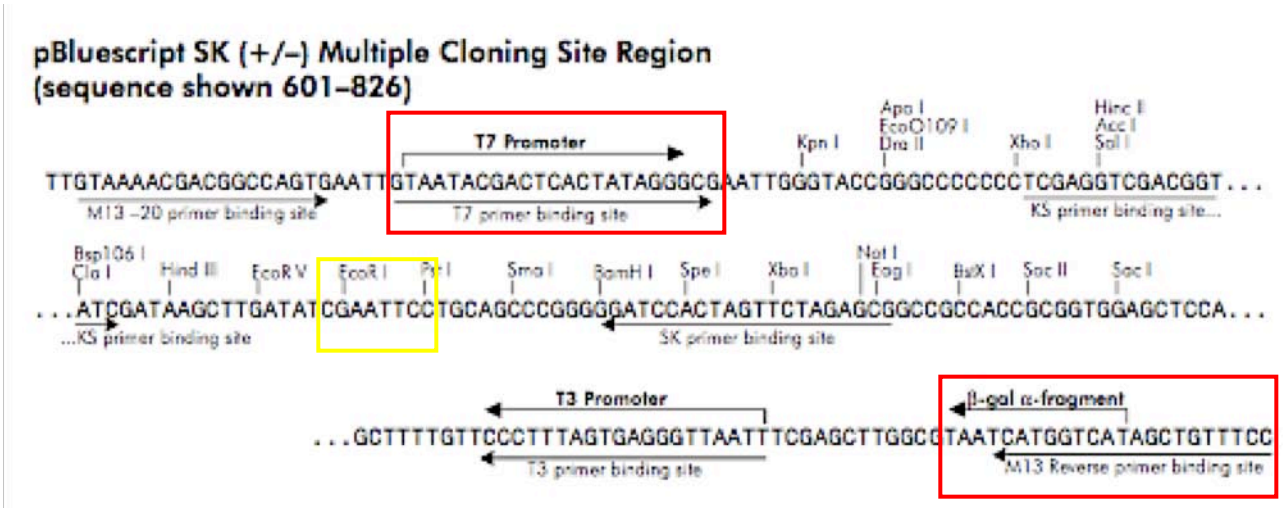

Figure 3-3. Multiple Cloning Site Region for pBluescript SK (-) vector. Red boxes outline the T7 forward primer and M13 reverse primer binding sites used in PCR for phage insert sequence determination. The yellow box highlights the *Eco*RI region where *S. solfataricus* genomic DNA ligation into the phagemid occurred. Figure obtained from "Lambda ZAP II Predigested *EcoR* I/CIAP-Treated Vector Kit Instruction Manual" from Stratagene (La Jolla, Ca).

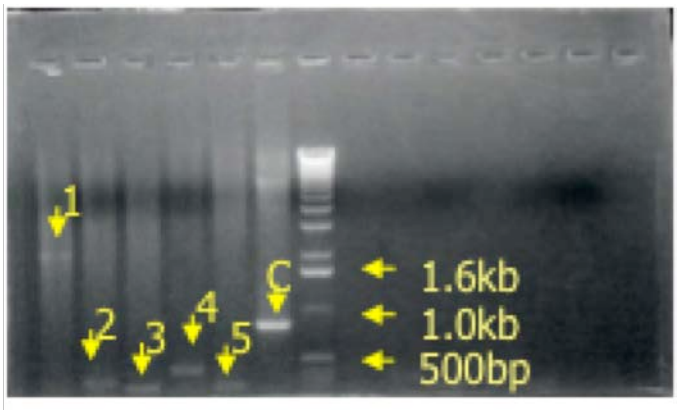

Figure 3-4. Agarose gel separation of *S. solfataricus*-insert fragments following PCR amplification of isolated phagemids 1-5. Lanes 1-5 correspond to excised phages 1-5 labeled in figure 3-2B. Lane 6: C, positive control reaction using primers and a plasmid previously cloned in the Kennelly laboratory. Lane 7: 10 µg of 1 Kb DNA Ladder (Invitrogen, Carlsbad, CA).

Identification of Potential SsoPK4 Substrates

S. solfataricus insert-sequence results

Examination of the sequences of the five PCR products indicated that three of them contained ORFs coding for four potential *S. solfataricus* proteins as determined by BLAST comparisons of the nucleotide sequences to the *S. solfataricus* genome (Table 3-3). A 144 base pair sequence from ORF *sso0563* in phage 2 encoded the following 48 amino acid peptide fragment:

ILVPPYVHGTLKEVVAEGDYTVEDPIAIVDMNGDEVPVKLMQKWPVRI

This was the only ORF encoding a protein product with a readily assayed function—the catalytic subunit, AtpA, of the soluble A_1 portion of A_1A_o-ATPase/ATP-synthase. Therefore ORF *sso0563* was chosen as the focus for subsequent experiments. The DNA sequence, corresponding amino acid translation of *sso0563* (AtpA), and primers used in cloning are shown in Figure 3-5.

Cloning *S. solfataricus* ORF sso0563

If the 48 amino acid fragment of AtpA, was the peptide phosphorylated by SsoPK4 in plaque 2, then the protein kinase should phosphorylate the isolated protein fragment *in vitro*. Moreover, if AtpA itself is a target for the enzyme, it too should be phosphorylated when combined with SsoPK4 and ATP. In order to determine this, we set out to generate both AtpA and AtpA-T (a truncation of AtpA containing the N-terminus and the phage-insert region) via recombinant expression.

Phage	ORF	Amino Acids	Function
1	*sso9378*	91	Putative: transcriptional regulator
	sso1969	132	Putative: nucleic acid binding protein
2	*sso0563*	592	ATP synthase subunit A
3	Unidentifiable	___	___
4	*sso0119*	506	Putative: pilus assembly protein
5	Unidentifiable	___	___

Table 3-3. Results of phage-insert sequencing. ORFs correspond to *S. solfataricus* sequences identified via BLAST.

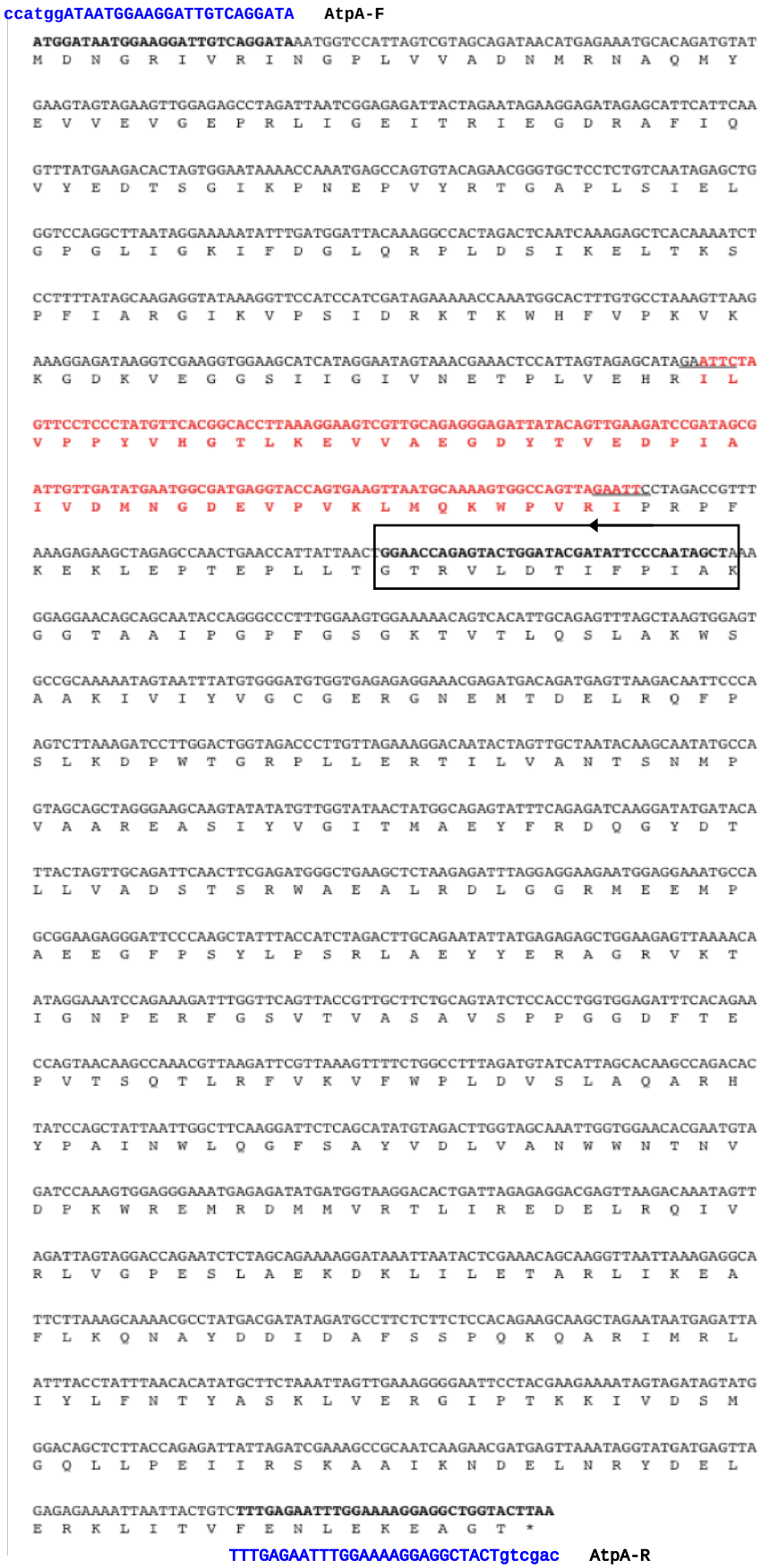

Figure 3-5. ORF *sso0563* and amino acid translation. AtpA (1779 bp, 592 aa). The sequenced insert region is highlighted in red. *Eco*RI regions flanking the insert are underlined. Shown in blue bold-type are the forward and reverse primer regions for cloning using *Nco*I and *Sal*I restriction enzymes (lowercase). Bold-type in boxed region corresponds to the truncated AtpA reverse primer sequence T-AtpA-R; arrowhead signifies end of coding region. Upstream and downstream primer sequences for AtpA-F and AtpA-R are not shown.

A forward primer, AtpA-F, and two reverse oligonucleotide primers, AtpA-R and T-Atp-R, for *sso0563* were designed with the *Nco*I and *Sal*I restriction enzyme sequences (underlined, below) for directional cloning into the pET vector system as described in Materials and Methods from Chapter II.

AtpA-F: 5'-TAAGTAACCATGGATAATGGAAGGATTGTCAGGATA-3'

AtpA-R: 5'-CGCTTAGTCGACAGTACCAGCCTCCTTTTCCAAATTCTCAAA-3'

T-AtpA-R: 5'-AGCTATGTCGACTATCGTATCCAGTACTCTGGTTCC-3'

ORF *sso0563* was initially cloned into the pET29b vector and eventually cloned into the pET21d vector using the same forward and reverse primers as above. The salient attributes of the pET29b and pET21d cloning and expression regions are depicted in Figure 3-6.

A single DNA fragment was observed following PCR amplification for each of the AtpA-F/AtpA-R and AtpA-F/T-AtpA-R primer sets. The product labeled AtpA was approximately 1800 bp in length and the AtpA-T (AtpA-truncated) DNA segment containing the phage insert region was approximately 650 bp. AtpA and AtpA-T were purified using a kit from QIAGEN before being incubated with the restriction enzymes *Nco*I and *Sal*I as described in Chapter II. The digested DNA fragments were combined with *Nco*I/*Sal*I-treated pET21d vector and T4 DNA ligase for directional insertion within the cloning vector. The recombinant plasmid was transformed in Alpha-Select Gold Efficiency *E. coli* cells for growth on LB-kanamycin (50 µg/ml) plates. Clones were selected from the plates to culture in LB-kanamycin (50 µg/ml) liquid media. Plasmid DNA was isolated from the culture cell pellets with the QIAprep Spin Miniprep kit from QIAGEN. 1000 ng of each plasmid were submitted to the Core Laboratory Facility at VBI for DNA sequencing with T7 promoter (5'-3') and T7 terminator (3'-5') primers.

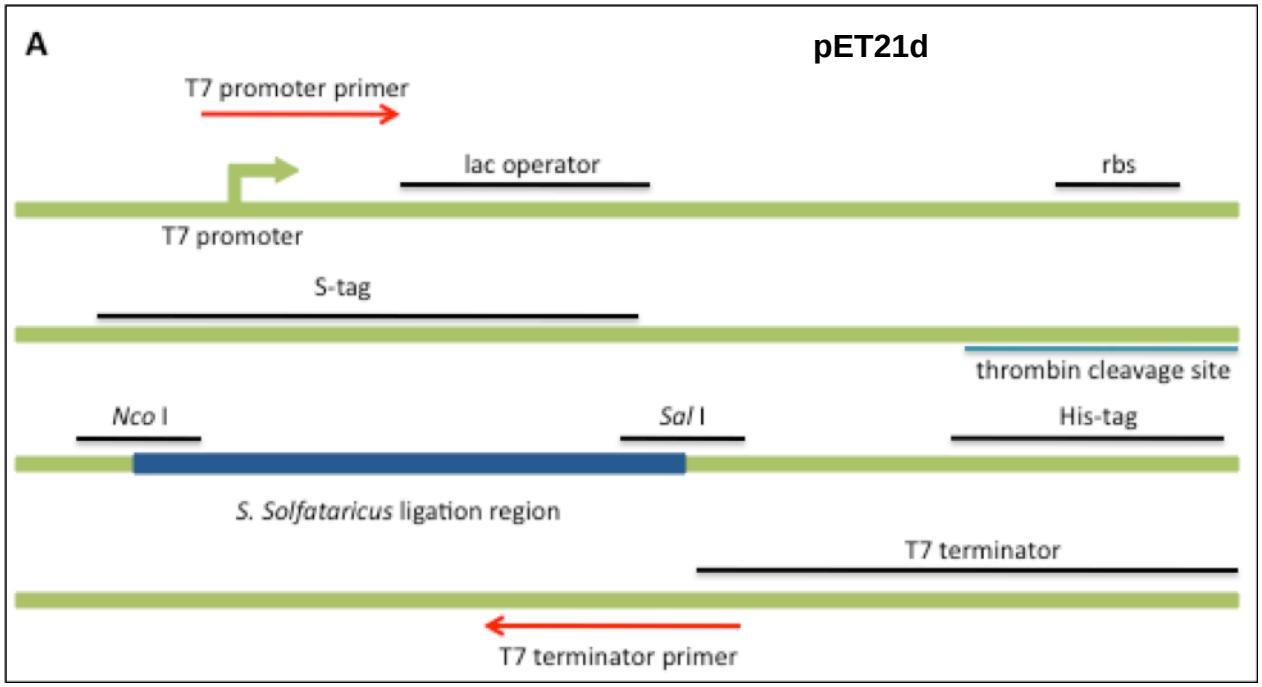

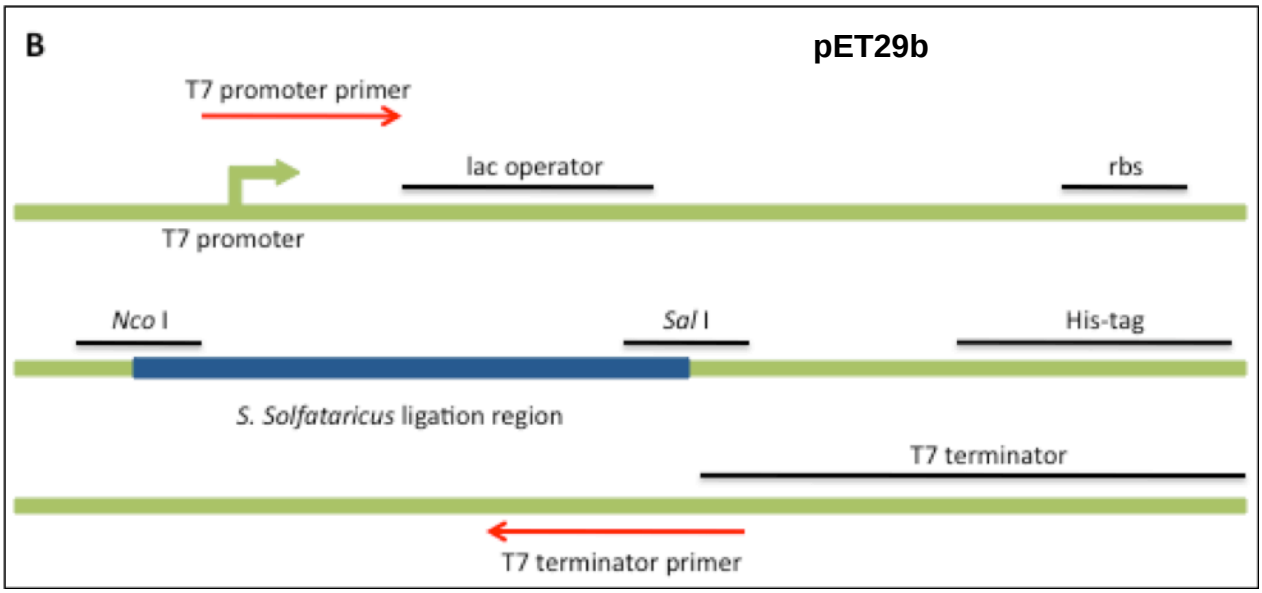

Figure 3-6. Illustration of pET vector cloning and expression regions. A. Depiction of pET21d vector with key features: N-terminal S-tag coding region, downstream thrombin cleavage site, cloning and ligation region, and C-terminal His-tag. B. The pET29b vector is similar to pET21d except it lacks the S-tag nucleotide sequence and thrombin recognition site. Adapted from pET vector system manual (Novagen/EMD Biosciences).

The sequence results for AtpA and AtpA-T were free of mutations and contained the S-tag at the N-terminus and C-terminal His-tag of the pET29b vector.

Overexpression, purification, and detection of AtpA and AtpA-T

The recombinant plasmids encoding AtpA and AtpA-T were transformed into BL21-CodonPlus DE3-RIL Competent Cells for recombinant protein overexpression as described in Chapter II. Overexpression cell pellets were resuspended and purified also as described in Chapter II based on protocol used to purify other *S. solfataricus* recombinant proteins in *E. coli* (Ray, Keith et al. 2005). During the initial purification of AtpA and AtpA-T the ammonium sulfate precipitation step was carried out overnight with the reactions on a stir plate at 4°C in order to fully dissolve all salt. The following morning the precipitate formed in each ~ 5 ml tube was pelleted by centrifigution for 20 min at 10,000 x g. The pellets were resuspended in 1 ml of protein storage buffer (50 mM MES pH 6.5, 10 mM $MnCl_2$, 2 mM DTT, 15% (v/v) glycerol), divided into aliquots, 75 µl each, and stored at -80°C until further use. AtpA had an estimated protein concentration of 9.7 µg/µl and AtpA-T of 6.9 µg/µl.

Samples of AtpA and AtpA-T were saved at various points during the purification procedure to be analyzed by SDS-PAGE (Materials and Methods, Chapter II). AtpA was resolved by 12% SDS-PAGE and AtpA-T by 15% SDS-PAGE; the results are depicted in Figure 3-7. Full-length AtpA purified from both pET vectors failed to yield the expected single band product as observed on SDS-PAGE. AtpA was predicted to have a molecular weight of 66 kDa and the results in Figure 3-7A show AtpA migrating between 50 and 75 kDa. The large band migrating at the predicted M_r for AtpA was accompanied by several

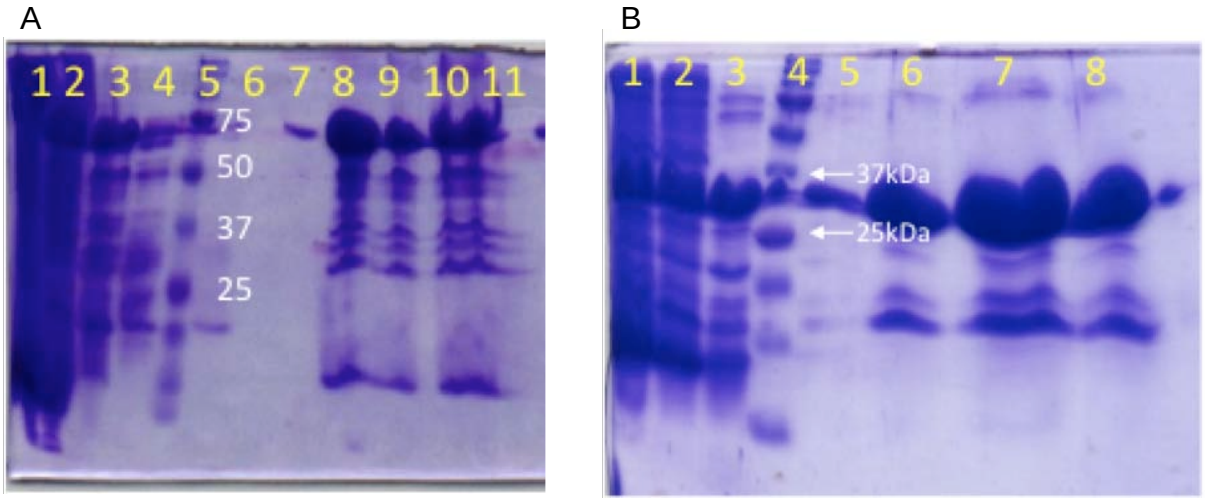

Figure 3-7. SDS-PAGE results for AtpA and AtpA-T overexpression. Both gels were Coomassie-stained to visualize proteins. A. Lanes 1-4: 10 µl each of sonicated-lysate, centrifigution supernatant, heat-shock supernatant and IMAC column eluate from initial His-tag protein binding, respectively. 5: Precision Plus Dual Color standards. 6-7: IMAC wash buffer (50 mM MOPS pH 7, 150 mM NaCl, 20 mM imidazole), 40 µl. 8-9: His-tag elution (50 mM MOPS pH7, 150 mM NaCl, 500 mM imidazole), 40 µl. 10-11: 10 and 40 µl of AtpA in protein storage buffer. B. Lanes 1-3: 10 µl each of sonicated-lysate, centrifugation supernatant, heat-shock supernatant. 4: Precision Plus Dual Color standards. 5: IMAC wash buffer, 40 µl. 6: His-tag elution, 40 µl. 7 and 8: 40 µl and 10 µl of AtpA-T in storage buffer, respectively.

bands of lower relative molecular mass. Western blot analysis using a primary antibody directed against the N-terminal His-tag domain engineered into the recombinant ATPase indicated that all the polypeptides present were His-tagged (not shown). Subsequent MS analysis detected only AtpA-derived peptides in the sample. It thus appeared that some portion of the recombinantly expressed AtpA had been degraded post-translationally. In Figure 3-7B, AtpA-T was located between 25 and 37 kDa standards, consistent with the predicted MW of 24.5 kDa.

In vitro SsoPK4 kinase activity with phosphorylation of AtpA and AtpA-T

When AtpA and AtpA-T were incubated with SsoPK4 and [γ-^{32}P]-ATP, *in vitro,* phosphotransfer to the proteins was observed (Figure 3-8). The rate at which SsoPK4 phosphorylated AtpA and AtpA-T was approximately 0.08 and 0.2 that of an equivalent concentration of histone H2A, respectively. In order to determine that the radioactive phosphate detected in the TCA-precipitates formed using our standard assay for protein kinase activity was in fact bound to the target proteins, samples of AtpA and AtpA-T that had been incubated with SsoPK4 and [γ-^{32}P]-ATP were resolved by 12% SDS-PAGE and ^{32}P detected by electronic autoradiography (Figure 3-9). If ^{32}P interacted with the precipitates in a noncovalent fashion, the radioactivity should not remain associated with the target protein following gel electrophoresis under denaturing conditions.

Figure 3-9 indicates that direct, covalent transfer of phosphate had occurred to both AtpA and AtpA-T at levels that compared favorably with the positive control, histone H2A. A low level of affinity for radiolabeled ATP by full-length AtpA was also present, as evidenced in lane 8 of Figure 3-9B where AtpA was incubated with [γ-^{32}P]-ATP in the absence of SsoPK4.

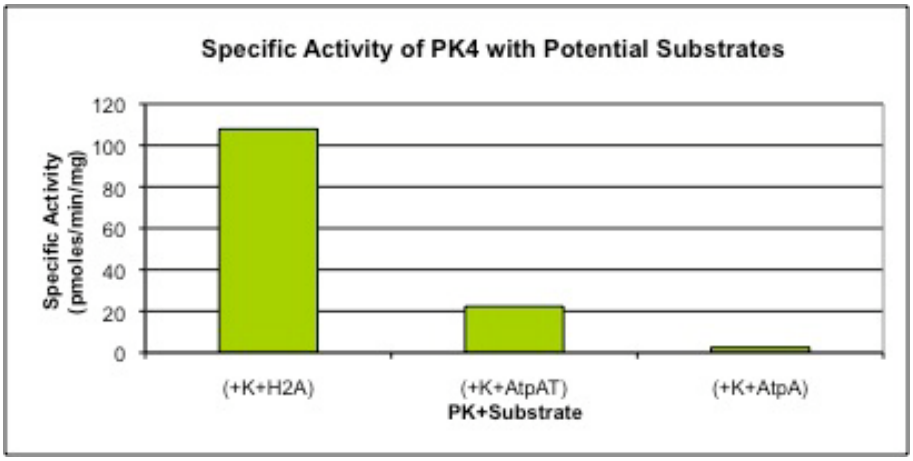

Figure 3-8. SsoPK4 phosphorylates AtpA-T (truncated AtpA) more readily than the full-length version of AtpA. AtpA-T is phosphorylated approximately 10-fold over AtpA. The specific activities for AtpA-T phosphorylation are 5-fold less than for the exogenous histone substrate, H2A. "+K" refers to SsoPK4 addition.

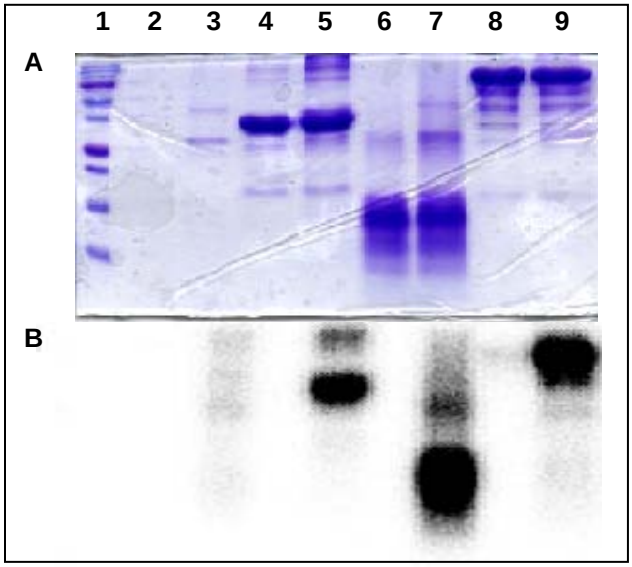

Figure 3-9. Phosphorylation of AtpA and AtpA-T by SsoPK4. Histone H2A and AtpA along with its truncated variant were incubated with SsoPK4 and [γ-^{32}P]-ATP and the protein mixtures were analyzed by SDS-PAGE. Shown are the Coomassie-stained gel (A) and its autoradiogram (B). Lane 1: molecular weight standards; Lane 2: empty; Lane 3: SsoPK4 (~34kDa); Lane 4: AtpA-T (~37kDa); Lane 5: SsoPK4 and AtpA-T; Lane 6: H2A; Lane 7: SsoPK4 and H2A; Lane 8: AtpA (~70kDa); Lane 9: SsoPK4 and AtpA.

SsoPK4 phosphorylates AtpA on threonine residues.

We next determined the nature of the amino acid(s) that SsoPK4 was phosphorylating on AtpA. It was known that SsoPK4 phosphorylated the exogenous substrate, H2A, on serine and threonine residues (Chapter I, Fig. 1-5) so one would expect to find phosphoserine and/or phosphothreonine in ^{32}P-labeled AtpA. Phosphoamino acid analysis of revealed that the protein kinase SsoPK4 phosphorylated AtpA solely on threonine residues (Figure 3-10).

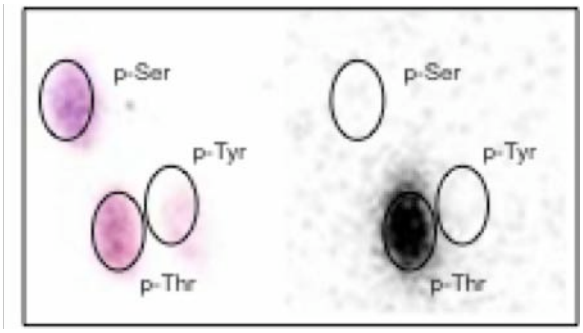

Figure 3-10. Phosphoamino acid analysis of AtpA. On left is the ninhydrin-stained TLC plate showing the position of amino acid standards following 2D-electrophoresis. At right is an autoradiograph of the same TLC plate showing ^{32}P-labeled amino acids following hydrolysis of SsoPK4-phosphorylated AtpA.

Chapter IV:

Functional Characterization of AtpA

The A-/V-/F-ATP Synthase/ATPase family

What is the function of AtpA in *S. solfataricus*? Once we identified an endogenous protein substrate for SsoPK4, it became important to find a way to characterize its activity and interactions *in vitro* as a means of searching for a functional difference between the phosphorylated versus unphosphorylated state of the protein. Identification of a functional impact of phosphorylation *in vitro* would strongly buttress the argument that AtpA is targeted for modification *in vivo.*

As discussed in Chapter III, the predicted product of ORF *sso0563* within the *S. solfataricus* genome encodes the catalytic protein subunit AtpA. AtpA, along with several other proteins, comprises the soluble A_1 sector of the bilobular A_1A_O-ATP synthase complex; A_O forms the hydrophobic membrane lobe responsible for proton/ion transport (Forgac 1999; Kish-Trier and Wilkens 2009). The archaeal A-type ATP synthases are more closely related, evolutionarily and structurally speaking, to the vacuolar, or V-ATPase, enzyme complexes found in eukaryotes, than to the F-type ATPases (Hilario and Gogarten 1998). The A- and V-type A subunits share an insert of approximately 80 amino acid residues located near the N-termini of the A subunits (Bickel-Sandkötter, Wagner et al. 1998; Maegawa, Morita et al. 2006). This insert region is called the non-homologous region (NHR) due to its lack of homology to the α or β subunits in F-type ATP synthases (Grüber and Marshansky 2008).

On the other hand, the A-type enzymes are functionally similar to F-ATP synthases found in prokaryotes and eukaryotes as they both can utilize electrochemical

gradients to generate ATP (Gruber, Wieczorek et al. 2001) or function reversibly to hydrolyze ATP to ADP and Pi (Grüber and Marshansky 2008). The V-type complexes strictly hydrolyze ATP to produce proton motive forces for a variety of intracellular purposes (Wieczorek, Brown et al. 1999). A representation of all three classes of ATPase is shown in Figure 4-1.

The A-/V-/F-ATPase superfamily of proton or sodium trans-locating enzymes is present in every life form. They share approximately 25% sequence identity between the major nucleotide-binding subunits: A and B of the A_1/V_1 sector and the corresponding β and α subunits of the F_1 sector (Nelson 1992). Figure 4-2 illustrates the presence of the phosphate-binding (P-loop) consensus sequence GXXXXGKT for the A-/V-/F-type complexes, suggesting a common ancestral relationship, yet highlights the diversity among the three ATPases and the potential for varying regulatory mechanisms (Kumar, Manimekalai et al. 2010).

Recombinant Expression of S. solfataricus *ATPase Subunits*

The minimal functional unit of the A_1A_0-ATP synthase that can be reconstituted *in vitro* is an AB subunit complex (Gruber, Wieczorek et al. 2001; Lemker, Ruppert et al. 2001; Wilkens 2001; Müller 2003; Schoenhofen, Li et al. 2005). Other proteins are also associated with the A_1 complex (e.g. AtpE, AtpG) although the composition varies among organisms and, as mentioned, suggests evolutionary transitions between V-, F-, and A-type ATPases (Hilario and Gogarten 1998; Gruber, Wieczorek et al. 2001; Müller 2003; Mulkidjanian, Makarova et al. 2007).

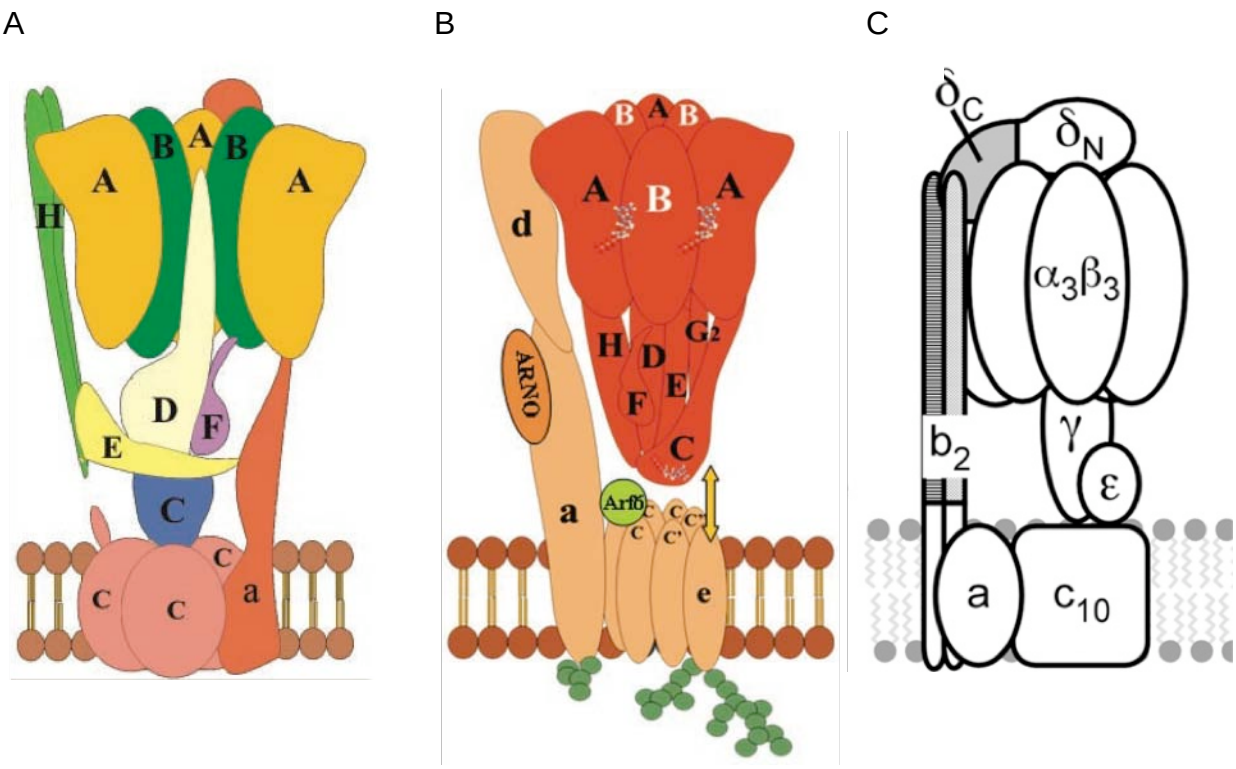

Figure 4-1. The A-/V-/F-type ATPase superfamily. Depicted are subunit arrangements of the A) A-ATP synthase, B) V-ATPase and C) F-ATP synthase. Note the structural similarities of knob-like regions on the A subunits of the A- and V-ATPases. The A- and F-type enzymes function to synthesize ATP while V-type enzyme hydrolyzes ATP. Figures A and B are taken directly from "New insights into structure-function relationships between archeal ATP synthase (A1A0) and vacuolar type ATPase (V1V0)," (Grüber and Marshansky 2008). Figure C was taken directly from "The Stator Complex of the A1A0-ATP Synthase--Structural Characterization of the E and H Subunits," (Kish-Trier, Briere et al. 2008).

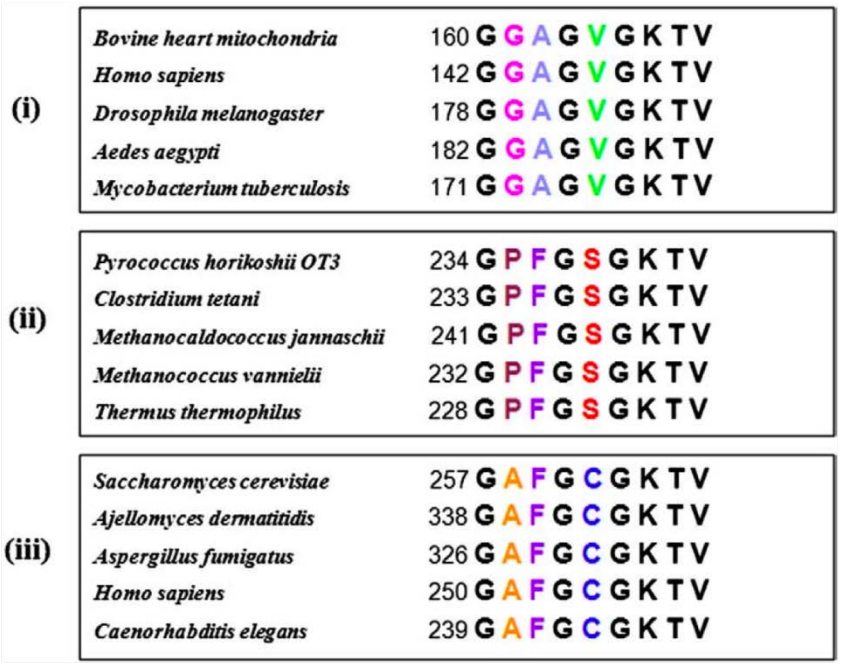

Figure 4-2. Multiple-sequence alignments of the nucleotide-binding P-loop region in A-/V-/F-type ATPases. A comparison of the ß-subunits from F-ATP synthases is shown in (i), A-ATP synthase subunit A comparisons in (ii) and V-ATPase comparisons of the A subunit are shown in (iii). *S. solfataricus* P2 AtpA shares approximately 55% sequence identity to *P. horikoshii OT3* in (ii). Taken from "Nucleotide Binding States of Subunit A of the A-ATP Synthase and the Implication of P-Loop Switch in Evolution" (Kumar, Manimekalai et al. 2010).

Subunit AtpB was known to interact with AtpA to form an A_3B_3 catalytic hexamer while the auxiliary subunits AtpG and AtpE are also believed to interact with AtpA based on structural models of A-ATP synthase organization (e.g. Figure 4-1A). The ORFs encoding the *S. solfataricus* equivalents of these proteins, *sso0564* (AtpB), ORF *sso6175* (AtpG), and ORF *sso0561* (AtpE), were therefore cloned and their polypeptide products overexpressed. Note that AtpG is the homologue of AtpH depicted in Figure 4-1A. Table 4-1 lists primers used to clone ORF *sso0564* (AtpB), ORF *sso6175* (AtpG), and ORF *sso0561* (AtpE). A section of the *S. solfataricus* ATPase operon and results of recombinant expression and purification are shown in Figure 4-3.

Reconstituting a Functional ATPase

ATPase activity was measured by incubating various subunits from the *S. solfataricus* ATPase with ATP. Initial attempts employed the Malachite Green assay (Lanzetta, Alvarez et al. 1979) to detect hydrolyzed phosphate as described in Chapter II. Subunit AtpA alone was not sufficient to catalyze hydrolysis although subunits, while adding AtpA and AtpB together yielded activity (Figure 4-4A). The inclusion of potential auxiliary subunits AtpE and AtpG along with AtpA and AtpB had no apparent effect on activity (Figure 4-4A). Optimal conditions for the assay of ATPase activity using the Malachite Green method were as follows: 1.5 µg each of AtpA and AtpB in HEPES, pH 7.5, 4 mM $CaCl_2$, 200 µM ATP with incubation for 30 min at 65°C. The truncation of AtpA used in SsoPK4 kinase activity assays yielded no detectable activity, either alone or in combination with AtpB (Figure 4-4B), presumably due to loss of catalytic motifs needed for nucleotide binding (Figure 4-5).

ORF – (Primer)	Oligonucleotide Sequence (5'-3')	Product	MW (kDa)
sso0564 – (For)	GGTACTCCATGGTAAGCGTAAGGGAATTTTCAAACA	AtpB	50
sso0564 – (Rev)	CTTTTTGTCGACTTTCTTACCCCTATAATTCGGATG		
sso6175 – (For)	GAGGGACCATGGATCAAGATAAATATTTACAAATTT	AtpG	12
sso6175 – (Rev)	AGAAAAGTCGACTGACAATTCCTTTAAAAC		
sso0561 – (For)	GTGAAATCCATGGATTTCGAACAGTTGTTGGATAAATCC	AtpE	26
sso0561 – (Rev)	TATCCAGTCGACCTTACCTCCAAACAACATGTCTGA		

Table 4-1. Oligonucleotide primer sequences for recombinant protein expression of ATPase subunits AtpB, AtpG, and AtpE. The adherent sequences for *Nco*I (CCATGG) and *Sal*I (GTCGAC) to induce forward and reverse directional insertion in the pET vector system (Novagen) are underlined.

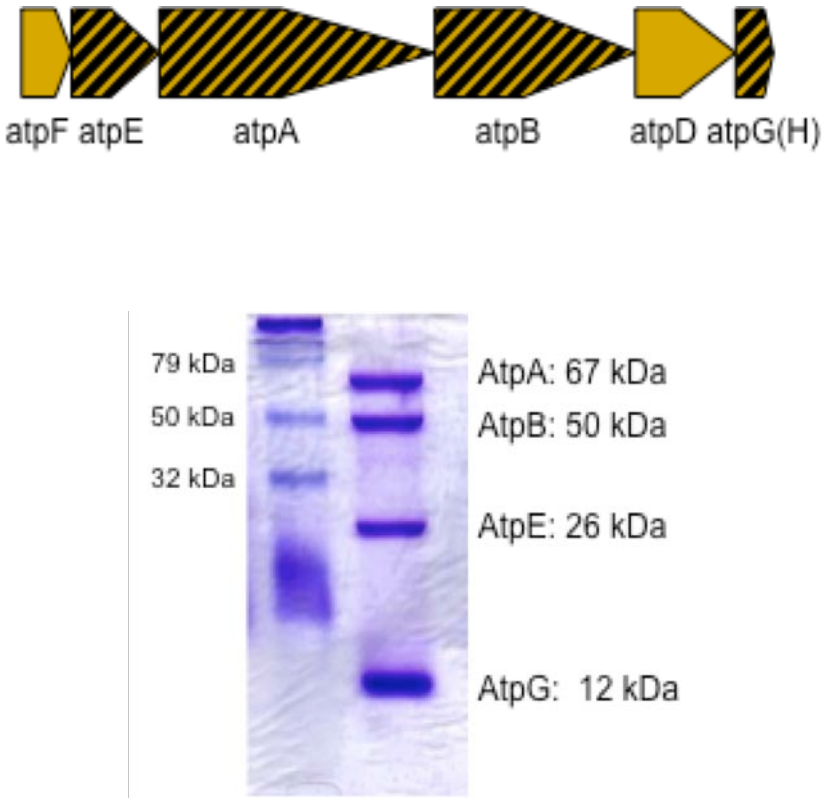

Figure 4-3. The *S. solfataricus* A-ATP synthase. Shown on top is a schematic diagram of operon organization for most of the A1 (soluble) portion of the A_1A_o-ATP synthase. Crosshatched arrows designate recombinantly-expressed subunits. Below: results of 15% SDS-PAGE of overexpressed and purified ATPase subunits. For each putative subunit, 5 µg of protein was applied to the gel.

A

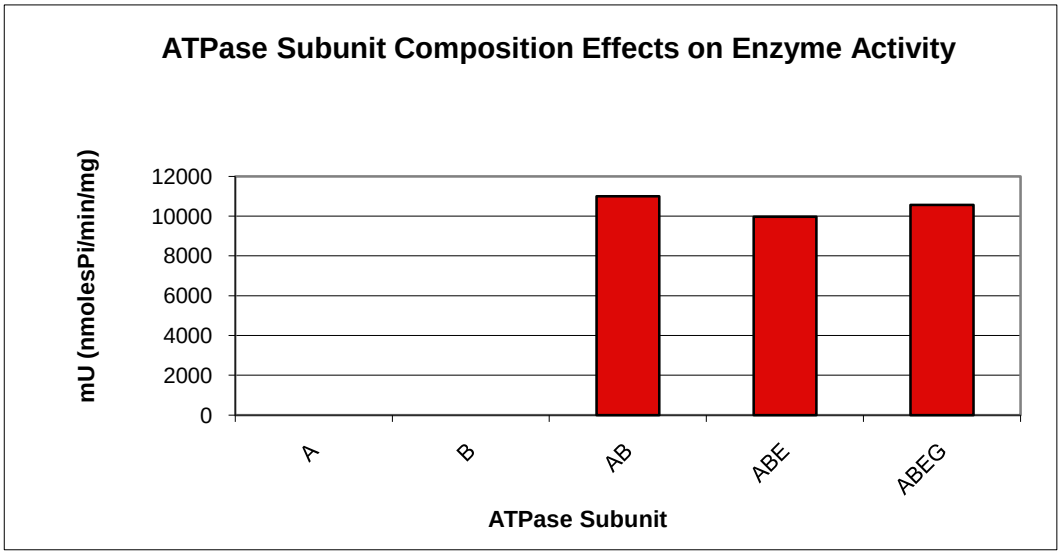

B

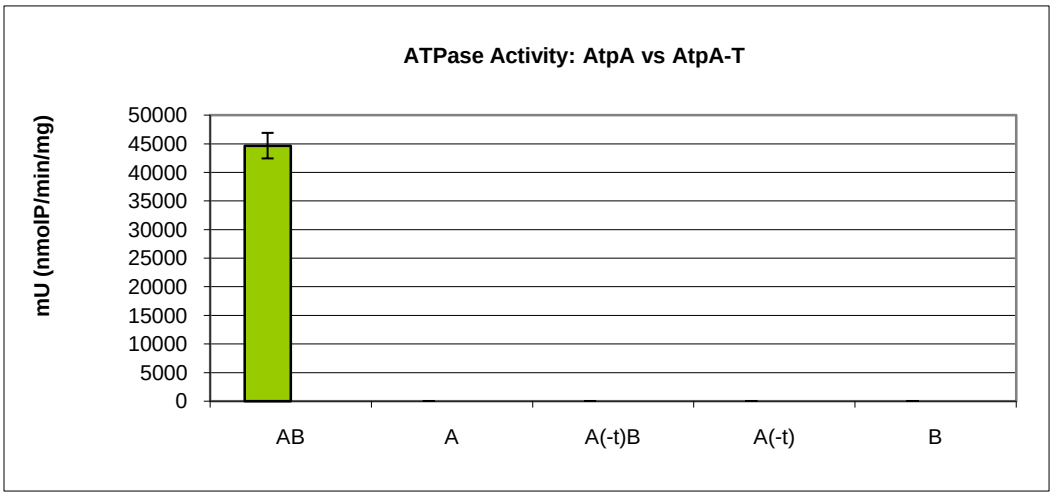

Figure 4-4. An active ATPase was generated with subunits AtpA and AtpB. A) AtpA and AtpB constitute an active enzyme. 5 µg of each subunit were assayed in SsoPK4 protein storage buffer (50 mM MES at pH 6.5, 10 mM MnCl2, 15% (v/v) glycerol) supplemented with 200 µM ATP. Samples were incubated for 60 min at 65°C before treating with Malachite Green reagent. Results displayed are of single samples. B) Subunits AtpA or AtpB alone, or AtpA-T are not sufficient to generate measurable ATP hydrolysis. 1.5 µg of AtpA, AtpB, or AtpA-T were assayed with 200 µM ATP and incubated for 30 min at 65°C. Results displayed as average of triplicate absorbance readings, ± 5% error.

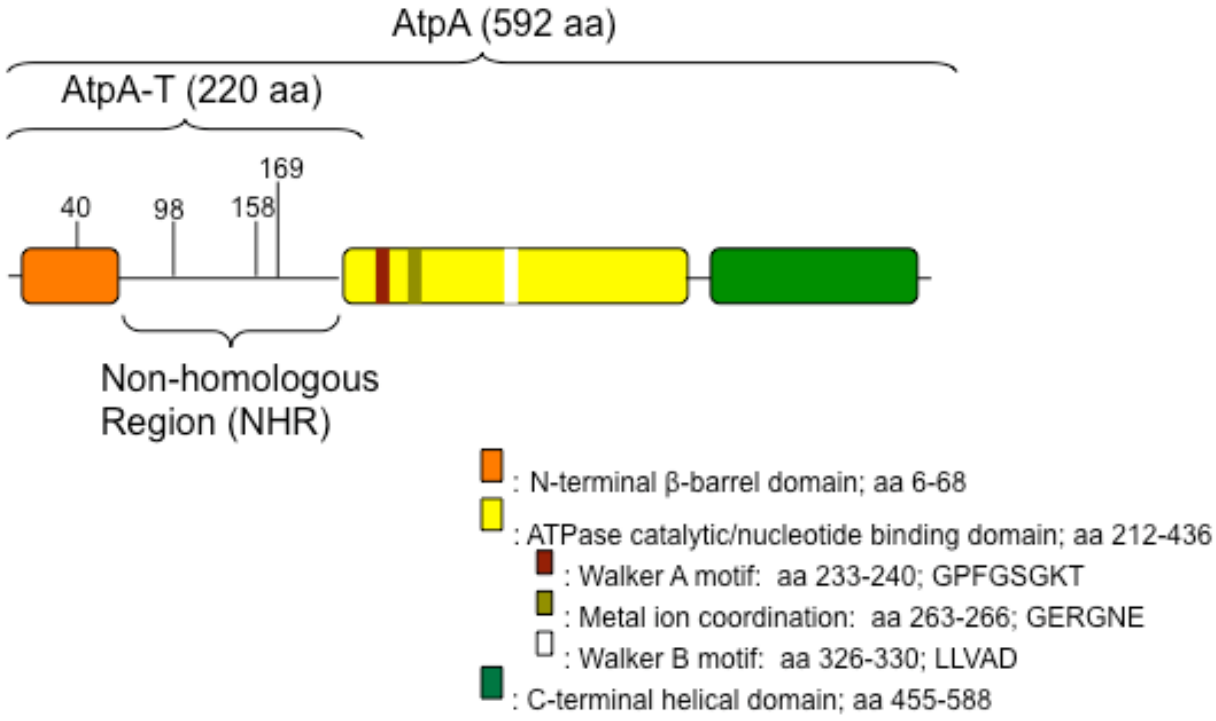

Figure 4-5. Schematic representation of AtpA domains. Shown within the catalytic/nucleotide binding domain (yellow) are the Walker A (red) and Walker B motifs (white) and the conserved GER sequence (brown). The AtpA-T form of AtpA does not contain these regions and therefore is catalytically inactive. Numbered residues near the NHR denote potential sites of phosphorylation by SsoPK4 (see Chapter V).

Characterization of ATPase Activity

The use of ATP as substrate resulted in chronically high backgrounds in the Malachite Green colorimetric-detection method. This problem was overcome by turning to a more sensitive assay through detection of ^{32}P from [γ-^{32}P]-ATP hydrolysis via extraction into organic solvents as a molybdate complex (Martin and Doty 1949; Schacter 1984). The molybdate extraction assay was used for all experiments involving the putative AtpAB complex. The term "± 5% error" refers to the specific percentage above and below each data point in as an indicator of sample agreement in sample averages.

It was observed that SsoPK4 phosphorylated a threonine residue within the S-tag sequence that gave false-positive results when we tested for phosphorylation by SsoPK4. It proved necessary to change the expression vector used to express the ATPase subunits, as well as SsoPK4, to the pET21d vector, which does not encode the S-tag fusion sequence found at the N-terminus of our original constructs (Chapter III, Figure 3-6A).

Altering the expression vector and method for assaying the phosphate produced yielded similar levels of ATPase activity as before. Optimal assay conditions were 65˚C (Figure 4-6A) at pH 5.5 (Figure 4-7A) with the calcium cofactor at a final concentration of 4 mM (Figure 4-7B). Under these conditions, phosphate production was linear for at least 30 min (Figure 4-6B).

A

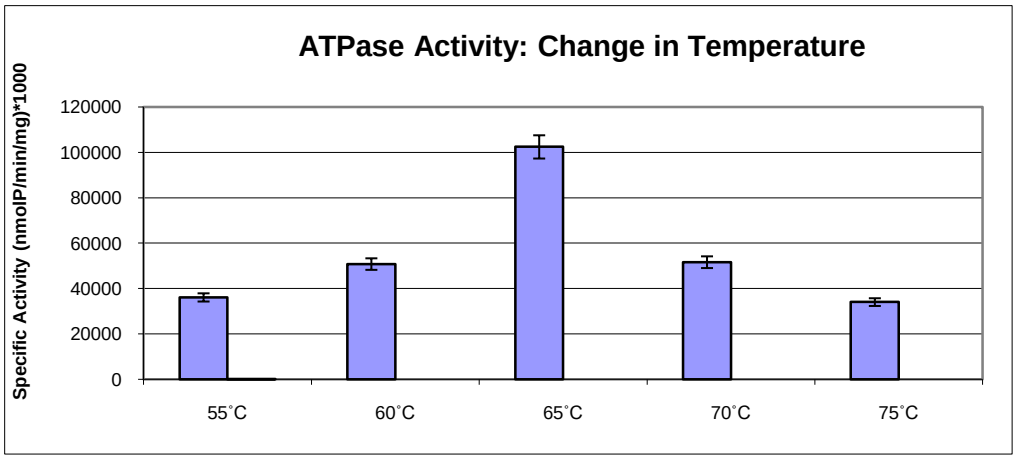

B

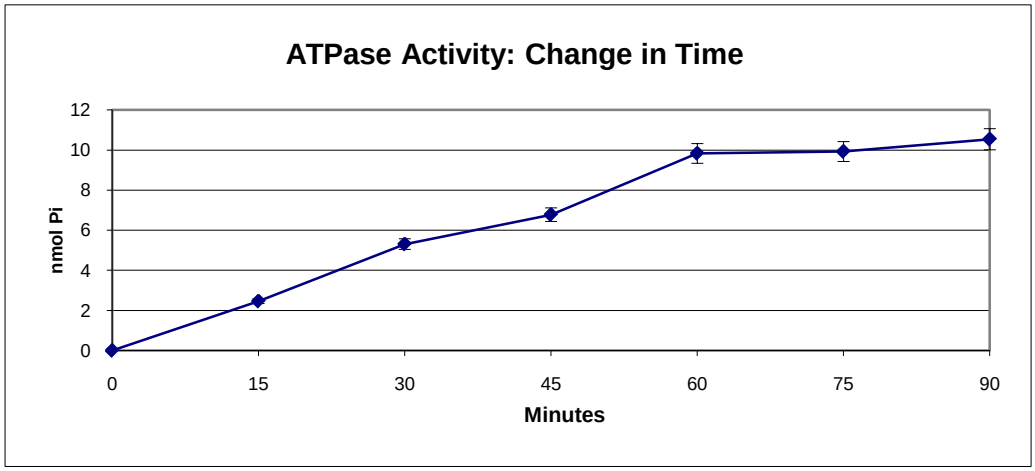

Figure 4-6. ATPase activity as a function of temperature (A) and time (B). AtpA and AtpB were present at 1.5 µg each per 50-µl assay. For both experiments, AB were combined in 50 mM HEPES, pH 7.5 supplemented with 4 mM $CaCl_2$ and 200 µM ATP. In A) peak ATPase activity was observed at incubation for 65˚C, t = 30 min. Results displayed are the average of triplicate samples, ± 5% error. In B) a linear curve was seen for nmoles of phosphate produced from t = 0 to t = 60 min. A period of 30 minutes was chosen as standard since this timepoint fell within the linear range of activity. Results displayed are the average of duplicate samples, ± 5% error.

A

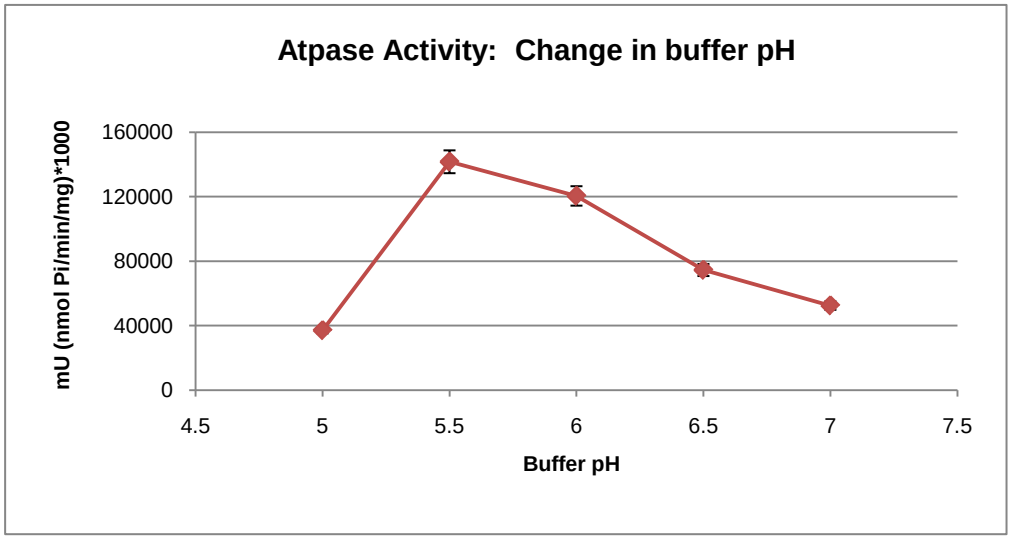

B

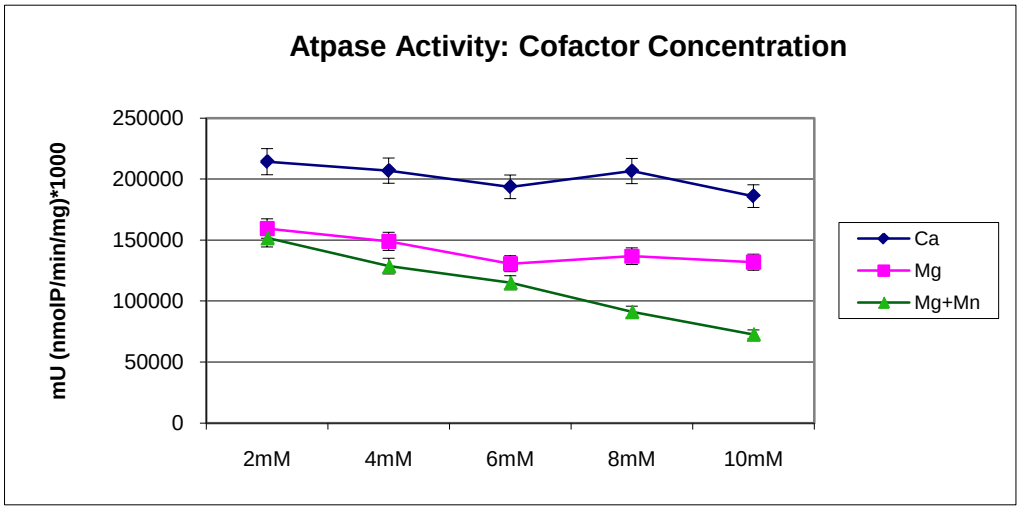

Figure 4-7. ATPase activity with varying pH (A) and cofactors (B). AtpA and AtpB were present at 1.5 µg each per 50-µl assay and incubated with 200 µM at 65°C for 30 min. A) HEPES/MES/Bicine buffer with 4 mM $CaCl_2$ (final concentration) was used to vary the pH range. B) Highest activity levels were attained using a calcium cofactor. ATPase activity did not seem to change as the calcium concentration increased; 4 mM was chosen as the final concentration based on preliminary results with malachite green (not shown). Both graphs display the average of duplicate samples, ± 5% error.

Figure 4-8 demonstrates the 1:1 stoichiometric relationship of AtpA to AtpB. As the amount of AtpA increased, the overall activity of the ATPase increased and leveled out (shown in blue); AtpB was held constant at 1.5 µg (600 nM). In contrast, as AtpA was held constant at 1.5 µg (450 nM) the ATPase activity did not change as the amount of AtpB was increased from 0.5 - 3 µg (shown in pink). These results demonstrated the limiting effect each subunit has relative to the other. The maximum ATPase activity peak at 2 µg of AtpA (red arrow) corresponded to 600 nM of each subunit within the reaction vial.

AtpA and AtpB were varied in equimolar concentrations in order to ascertain the linear range of enzyme activity for the catalytic subunit AtpA (Figure 4-9). An amount equal to 1 µg AtpA (300 nM) was observed to fall within the linear range and was used for the remainder of the characterization assays. The equimolar amount of AtpB at 300 nM corresponded to 0.75 µg of AtpB per reaction.

A final set of ATPase activity assays using the molybdate extraction method focused on varying the amount of ATP. The amount of ATP chosen for further ATPase experiments was considerably less than the 200 µM of ATP previously added to reactions. The specific activity of AtpA at 1 µg with 200 µM ATP neared saturation levels for the AtpAB complex as depicted in Figure 4-10. A final concentration of 50 µM ATP was selected based on its position within the linear range of activity for the ATPase.

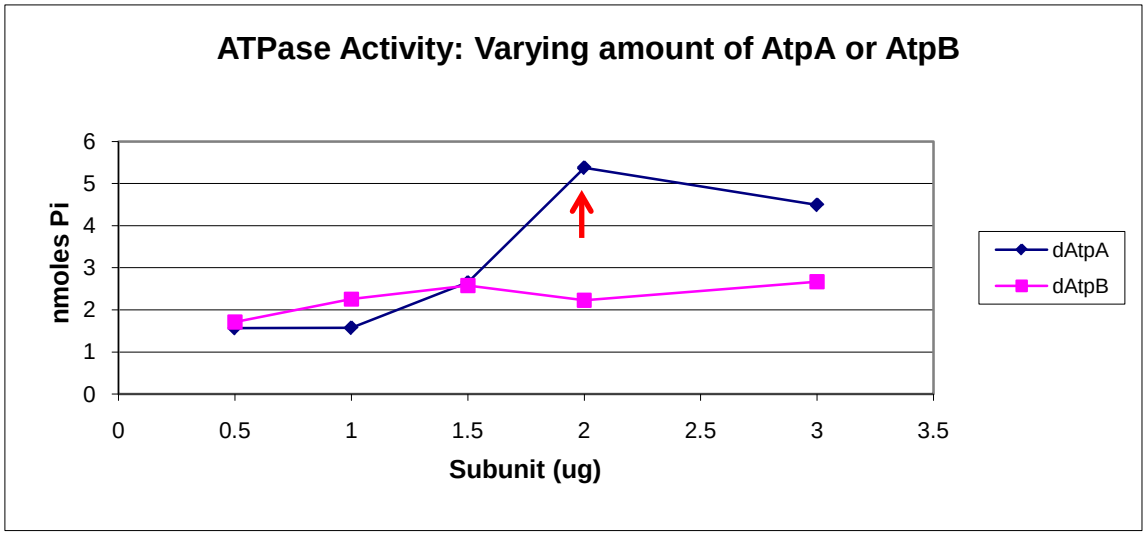

Figure 4-8. The activity of the ATPase depends on a 1:1 stoichiometric amount of AtpA and AtpB. The amount of AtpB was held constant at 1.5 µg (600 nM) while AtpA was increased from 0.5 to 3 µg (◆). Peak activity (red arrow) correlates to 600 nM, or 2 µg, of AtpA to 600 nM of AtpB. Increasing the concentration of AtpB while holding AtpA constant at 1.5 µg (450 nM) did not increase activity above that observed between 1 and 1.5 µg of AtpB; 450 nM of AtpA corresponds to 1.1 µg AtpB (■). Results displayed are of single reactions incubated at 65°C for 30 min in 50 mM MES, pH 5.5, 4 mM $CaCl_2$, and 200 µM ATP.

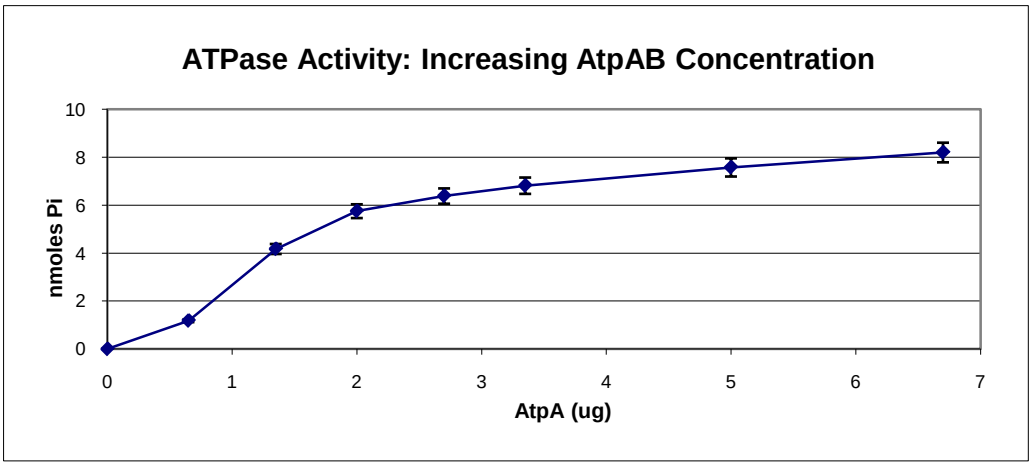

Figure 4-9. ATPase activity curve with increasing equimolar amounts of AtpA and AtpB. Based on these results, AtpA at 1 µg and AtpB at 0.75 µg were chosen for ATPase assay conditions. Both subunits are present at 300 nM for the molybdate extraction assay. All reactions were incubated at 65 °C for 30 min in 50 mM MES pH 5.5, 4 mM $CaCl_2$, and 200 µM ATP. Results displayed are the average of duplicate samples, ± 5% error.

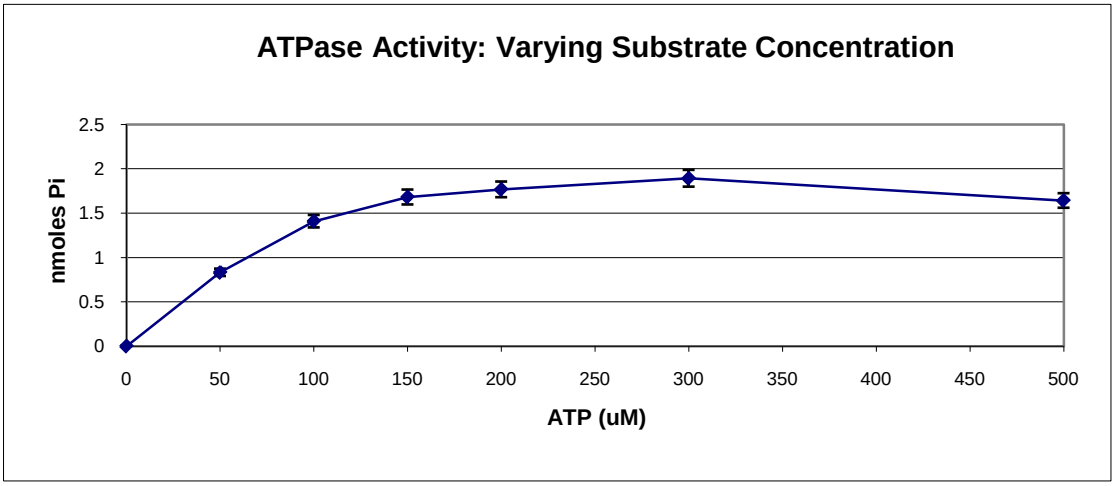

Figure 4-10. ATP at 50 µM was optimal for ATPase activity assays. All reactions were incubated at 65°C for 30 min in 50 mM MES pH 5.5, 4 mM $CaCl_2$, 0.75 µg AtpB and 1 µg AtpA. Results displayed are the average of duplicate samples, ± 5% error.

Postulating ATPase Subunit Interactions with Chemical Cross-Linking

Other archaea have been used as model systems for ATPase/ATP-synthase studies. Chemical cross-linking methods have been employed to better understand the proximity of ATPase subunits in relation to each other within *Methanosarcina mazei* Gö1 and *Methanococcus jannaschii* (Coskun, Grüber et al. 2002). *S. solfataricus* AtpA, AtpB, AtpE, and AtpG were incubated with the zero-length chemical cross-linker EDC (1-ethyl-3-(dimethylaminopropyl)) as described under Materials and Methods, Chapter II. Samples were resolved by 12% SDS-PAGE (Figure 4-11). Bands formed in the presence of EDC were analyzed by mass spectrometry (MS) at the Virginia Tech Mass Spectrometry Incubator (Blacksburg, VA). See Appendix A for information on MS analysis methods and a summary of MS data for EDC cross-linking in Table A-1.

The following linked proteins were identified: a) A-A, b) A-G, c) A-B, e) B-G, f) E-G following MS analysis. AtpE did not form cross-links with AtpA or AtpB. The cross-linked product labeled "d" was not analyzed by MS; it can be inferred that this product represents the AtpB homodimer based on the molecular weight migration of 100 kDa. No dramatically different changes in ATPase activity were evident with addition of AtpE and AtpB (Figure 4-4b). However these subunits could still play a role in ATPase regulation of the soluble A_1 multimer complex as evidenced by A-G and B-G cross-link formation. Based on results of the characterization assays we presumed that AtpA and AtpB act as an AtpAB active-enzyme complex to facilitate hydrolysis of ATP. The results of EDC cross-linking helped support this hypothesis as the subunits AtpA and AtpB interact closely enough to be joined with the zero-length cross-linker.

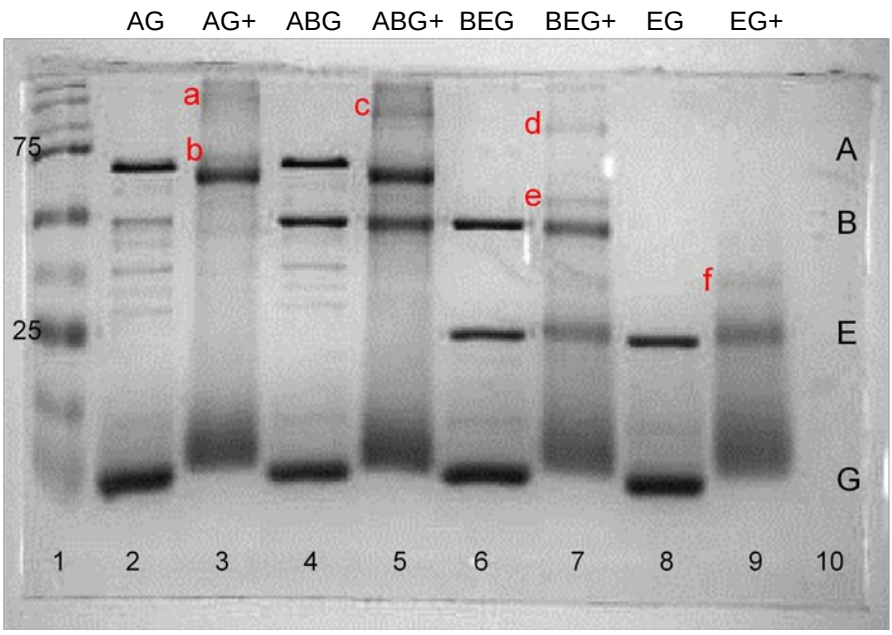

Figure 4-11. Results of EDC cross-linking resolved by 12% SDS-PAGE. Approximately 20 µg of each protein were incubated before addition of 5 µl of 50 mM EDC ("+"). Approximately 6 µg each of subunit (AtpA,B,E, or G) were loaded in each well. Lane 1: Precision Plus standards; lane 2: AG; lane 3: AG plus EDC; lane 4: ABG; lane 5: ABG plus EDC; lane 6: BEG; lane 7: BEG plus EDC; lane 8: EG; lane 9: EG plus EDC; lane 10: empty.

Chapter V:

Phosphorylation of AtpA – Sites Modified and Effects on ATPase Activity

Identification of Phosphothreonine (pThr) Residues on AtpA

The importance of phosphoresidue identification

Identifying an endogenous protein that can be phosphorylated by a protein kinase *in vitro* explains little of their relationship beyond phosphotransfer capabilities. What are the effects of phosphorylation? What structural and functional changes, if any, are induced by the addition of a phosphoryl group to AtpA from *S. solfataricus?* Is its ATPase activity going to be affected? The first step in addressing these questions is to identify the specific phosphoacceptor residues targeted for modification. The identification of specific phosphoresidues on protein substrates, for example, has proven to be an invaluable tool in cancer research and the implementation of therapeutic drug design (Cohen 2002; Ashman and Villar 2009).

We have identified AtpA as a potential endogenous substrate for protein-serine/threonine kinase SsoPK4 from λ-phage expression library screenings of the *S. solfataricus* genome (Chapter III, Table 3-3) and that its ATPase activity could be reconstituted when combined with AtpB (Chapter IV, Figure 4-4). We next decided to determine whether phosphorylation of the AtpA substrate affected the enzyme's ability to hydrolyze ATP. However, it was first necessary to identify the specific residues targeted by SsoPK4 on AtpA in order to probe the effects of phosphorylation on ATPase activity.

Site-directed mutagenesis

Insight into potential regulatory relationships of a protein kinase and its endogenous substrate(s) can oftentimes be deduced from site-directed mutagenesis of the identified or postulated phosphoacceptor residues. For example, substituting the nucleophilic hydroxyl side chain of a serine or threonine residue with a small, non-polar moiety such as the methyl group of alanine removes the potential for a protein kinase to transfer a phosphate to that residue (Dixon, Eydmann et al. 1991; Boldyreff, Meggio et al. 1994; Du, Perry et al. 2008). Likewise, altering the hydroxyl group of threonine to an acidic functional group such as aspartate may potentially mimic the effect of the negative electrostatic force an added phosphoryl group imposes upon a protein (Pei and Shuman 2003; Ray, Keith et al. 2005; Lee, Lee et al. 2008). All primers required for site-directed mutagenesis of various AtpA amino acid residues are listed in Appendix B.

Examining the phage-expression product: Thr-158 and Thr-169

The nucleotide sequence of the phage-insert isolation encoded a 48-amino acid fragment of AtpA containing two threonine residues at positions 158 and 169 (Chapter III). The following AtpA variants, T158A, T158D, T169A, and T169D, were constructed and incubated with SsoPK4 kinase activity and [γ-^{32}P]-ATP. If SsoPK4 targeted either Thr-158 or Thr-169, substitution by nonphosphorylatable residues such as alanine should abrogate phosphorylation. The results of these assays are shown in Figure 5-1.

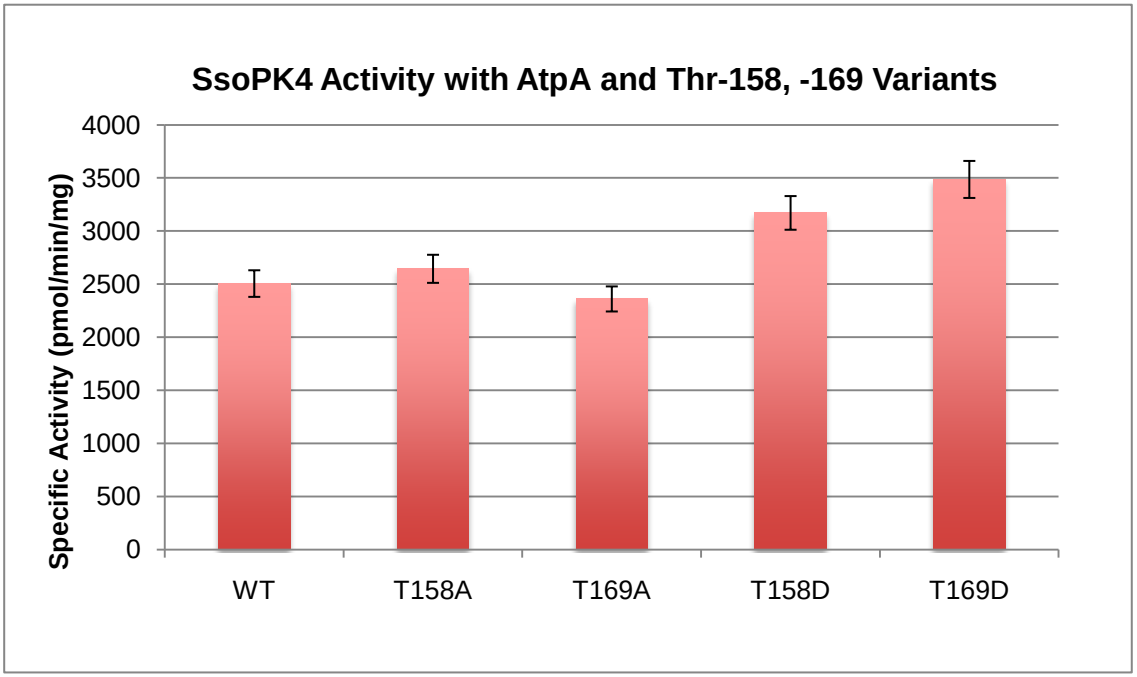

Figure 5-1. Comparison of wild-type AtpA phosphorylation to Thr-158 and Thr-169 variants. SsoPK4 was assayed for protein kinase activity with Thr-158 and Thr-169 variants in 50 mM MOPS at pH 7, 4 mM Mn^{2+} for 90 min at 65°C as described in Chapter II. Results displayed are the average of duplicate samples, ± 5% error.

Little variation was observed between the level of phosphorylation of AtpA wild-type (WT) and the variants (Figure 5-1). In fact, slight increases in protein bound radioactivity of ~25% and ~40% were noted for T158D and T169D respectively. We postulated that phosphorylation might be taking place on both threonine residues—perhaps SsoPK4 phosphorylated Thr-158, for example, when the residue at 169 was occupied by an alanine, and vice-versa. It is a common occurrence for phosphoproteins to be phosphorylated on more than one residue with multiple phosphorylation sites situated in close proximity to each other (Roach 1991). Double mutations at 158 and 169 were therefore constructed. The double-mutants were labeled "T→A dm" (double mutant) and "T→D dm" then assayed again for SsoPK4 kinase activity. Similar results were obtained as those in Figure 5-1, with no remarkable changes in phosphorylation levels compared to AtpA WT (not shown).

The catalytic competence of the Thr-158 and Thr-169 variants was assayed using molybdate extraction with radiolabeled ATP as described previously. As shown in Figure 5-2, ATPase activity did not vary dramatically compared to AtpA WT; mutations at Thr-158 and Thr-169 did not alter ATPase activity *in vitro*.

Identification of phosphoresidues on AtpA: Thr-40 and Thr-98

It was hoped that removal of the proposed phosphorylation site residue(s) Thr-158 and -169 would eliminate phosphotransfer on AtpA by SsoPK4. However phosphorylation was still detected, indicating that phosphorylation of the complete protein by SsoPK4 must be occurring at other location(s) than was the case with the phage display product. AtpA-T was phosphorylated by SsoPK4 in a 1:20 ratio of kinase

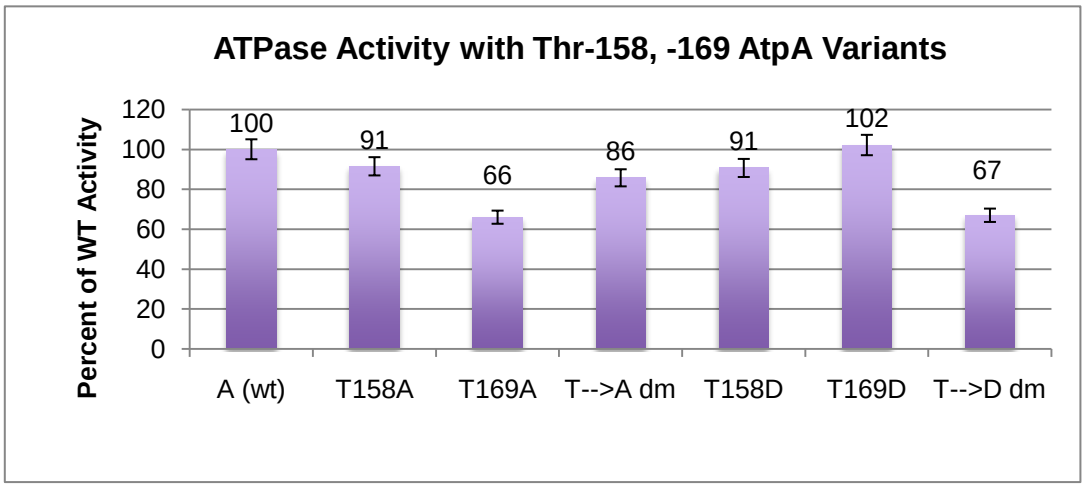

Figure 5-2. Comparison of ATPase activity with AtpA WT to Thr-158 and Thr-169 AtpA variants. In this assay, 1.5 µg of AtpB and 1.5 µg of each AtpA variant were combined in ATPase activity buffer (50 mM MES, pH 5.5, 4 mM Ca^{2+}) and assayed 30 min at 65°C using molybdate extraction as described in Chapter IV. Results displayed are the average of triplicate samples, ± 5% error.

to substrate using non-labeled ATP in order to locate phosphoresidues via mass spectrometry (MS). The lower protein kinase to substrate ratio was used to minimize background due to SsoPK4. AtpA-T was chosen over full length AtpA due to its higher levels of phosphorylation *in vitro* to aid in detection of phosphopeptides. Also, AtpA-T encompasses approximately 1/3 of the catalytic subunit and contains the 48-amino acid phage insert sequence (Figure 4-5, Chapter IV). Two sites of phosphorylation were identified at the Virginia Tech Mass Spectrometry Incubator (Blacksburg, VA): Thr-40 and Thr-98. Figure 4-5 highlights locations of these residues on AtpA; Appendix A, Figure A-1 and Table A-3 describe pThr-98 MS results. In order to verify these assignments and probe their functional role, oligonucleotide primers were again designed for site-directed mutagenesis (Appendix B) to generate the following recombinant variants: T40A, T98A, T40D, T98D, T40/98D dm (double mutant). The full-length AtpA variant with a double-mutation for threonine to alanine proved refractory to cloning.

The Thr-40 and Thr-98 variants were assayed with SsoPK4 to determine levels of phosphorylation as compared to AtpA WT (Figure 5-3). A more than 50% decrease in phosphate incorporation was exhibited for the T98D and T40/98D double mutants. The T98A mutation also displayed lower levels of phosphorylation: 56% of WT. Although phosphorylation was not completely eliminated by the simultaneous alteration of both threonine residues, and ^{32}P was still detected in the Thr-40 mutants, it appeared SsoPK4 primarily phosphorylated AtpA at Thr-98. No matter what nonphosphorylatable residues were substituted for it, and regardless of whether Thr-40 was altered, the maximum level of phosphate that could be incorporated into Thr-98 variants was less than 50% that of wild-type under comparable conditions.

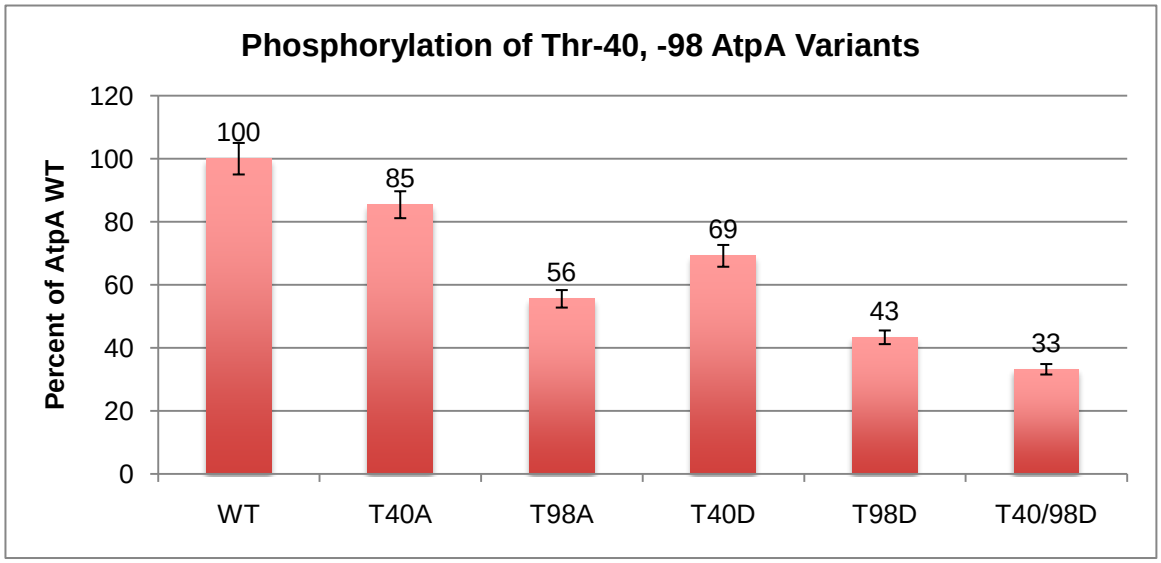

Figure 5-3. Comparison of wild-type AtpA phosphorylation to Thr-40 and Thr-98 variants. SsoPK4 was assayed for protein kinase activity with Thr-40 and Thr-98 variants in 50 mM MOPS at pH 7, 4 mM Mn^{2+} for 90 min at 65°C as described in Chapter II. Results displayed are the average of two independent assays with duplicate samples, ± 5% error.

Does SsoPK4 Phosphorylate Full-length AtpA on Additional Residues?

Mutations of AtpA catalytic regions

The ~ 30% phosphorylation remaining on AtpA T40/98D compared to AtpA WT needed to addressed to be certain that Thr-40 and Thr-98 were the target residues for SsoPK4 phosphotransfer. Apparent autophosphorylation was detected at low levels on the full-length product of AtpA (Figure 3-9); pThr-40 and pThr-98 were detected from MS analysis of the AtpA-T variant. The protein substrate itself has nucleotide binding domains and uses ATP as a substrate; these domains are absent in the truncation (Figure 4-5, Chapter IV). It seemed reasonable that full-length AtpA was binding and retaining [γ-^{32}P]-ATP within the catalytic regions not present in the truncated variant.

Oligonucleotide primers for AtpA were designed to insert mutations within three conserved sequences important to ATPase activity (Futai, Sun-Wada et al. 2004). Four mutant variants of full-length AtpA were generated within the Walker-A and Walker-B motifs and the GER region depicted in Figure 4-5 (Chapter IV). The T240A mutation altered the consensus sequence for the Walker-A/P-loop motif (GFPGSGK<u>T</u>). Mutant D330A perturbed the Walker-B motif (LLVA<u>D</u>). Both the R263G and E266A mutations occur in the conserved GE<u>R</u>GN<u>E</u> sequence.

Catalytic-site mutations on AtpA result in an inactive ATPase

All catalytic-site mutations exhibited little or no catalytic activity as expected (Figure 5-4). Surprisingly, the levels of phosphate incorporation were elevated by 20-60% following incubating with SsoPK4 and [γ-^{32}-P]-ATP as shown in Figure 5-5.

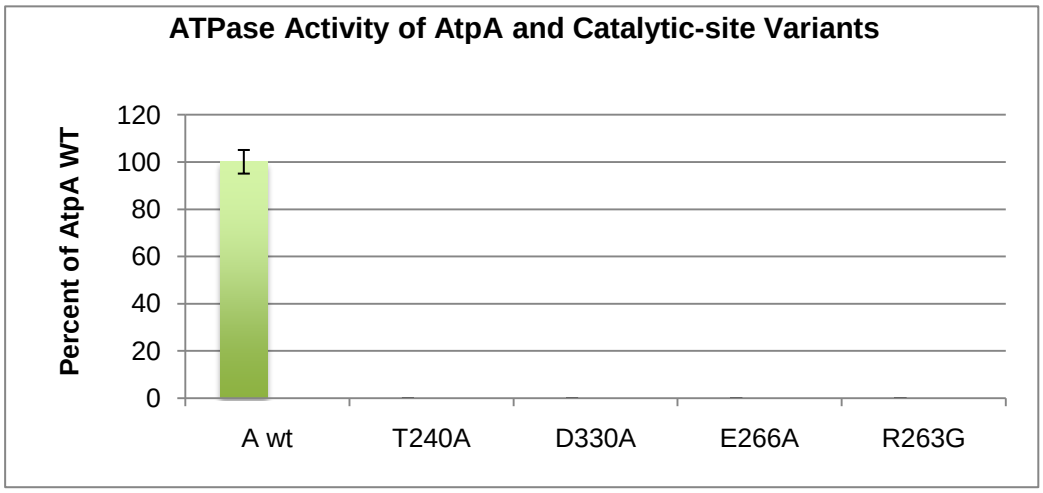

Figure 5-4. ATPase activity of AtpA and catalytic mutant-variants. In this assay, 1.5 µg of AtpB and 1.5 µg of each AtpA variant were combined in ATPase activity buffer (50 mM MES, pH 5.5, 4 mM Ca^{2+}) and assayed 30 min at 65˚C using the malachite green method as described in Chapter IV. Results displayed are the average of triplicate absorbance readings, ± 5% error.

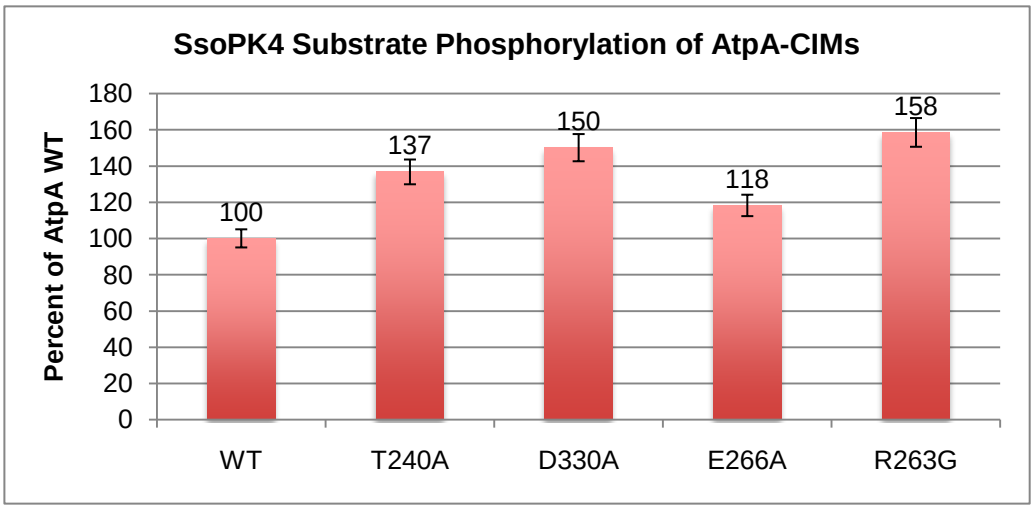

Figure 5-5. SsoPK4 phosphorylation of catalytically inactive mutants (CIMs). SsoPK4 was assayed for protein kinase activity with CIM variants and compared to AtpA WT. Assay conditions were as described in Chapter II. Results displayed are the average of duplicate samples, ± 5% error.

We theorize that the loss of ATP binding by the inactive AtpA variants may have promoted higher levels of phosphorylation at other sites by decreasing competition for ATP, the shared nucleotide substrate utilized by SsoPK4 and the ATPase.

Elimination of AtpA "autophosphorylation"

A final mutant variant of the ATPase catalytic subunit was constructed and overexpressed in hopes of verifying that covalent phosphorylation on AtpA threonine residues was attributable to SsoPK4. It has been established that the lysine residue of the P-loop region of AtpA (GFPGSG<u>KT</u>$_{240}$) binds the γ phosphate of ATP (Yohda, Ohta et al. 1988) while the threonine coordinates the divalent cation, typically Mg^{2+}, with a resultant "tightening" of the nucleotide-binding pocket (Burgard, Nett et al. 1994). It follows that the T240A substitution disrupts the ability to retain ATP in the binding pocket. A triple mutant variant (TripM) was created containing the T40D, T98D and T240A residues using previously designed oligonucleotide primers for T240A and T40/98D plasmid DNA. Recombinant TripM was incubated with SsoPK4 and [γ-^{32}-P]-ATP and the levels of phosphate incorporation compared to AtpA wild-type, Thr-40, and Thr-98 variants.

The results of the assay are shown in Figure 5-6. Included in the experiment were two AtpA-T variants: AtpA-T wild-type (A-T), and AtpA-T with T40D and T98D mutations (A-T dm) shown in Figure 5-6A. The level of phosphate incorporation into AtpA-T wild-type (shown in gray) was over 4-fold greater than that for AtpA WT, as observed in previous SsoPK4 assays, while the AtpA-T double mutant exhibited the least amount of phosphorylation at 11%, relative to AtpA WT. For clarity, Figure 5-6B presents the results obtained for the full-length variants of AtpA alone.

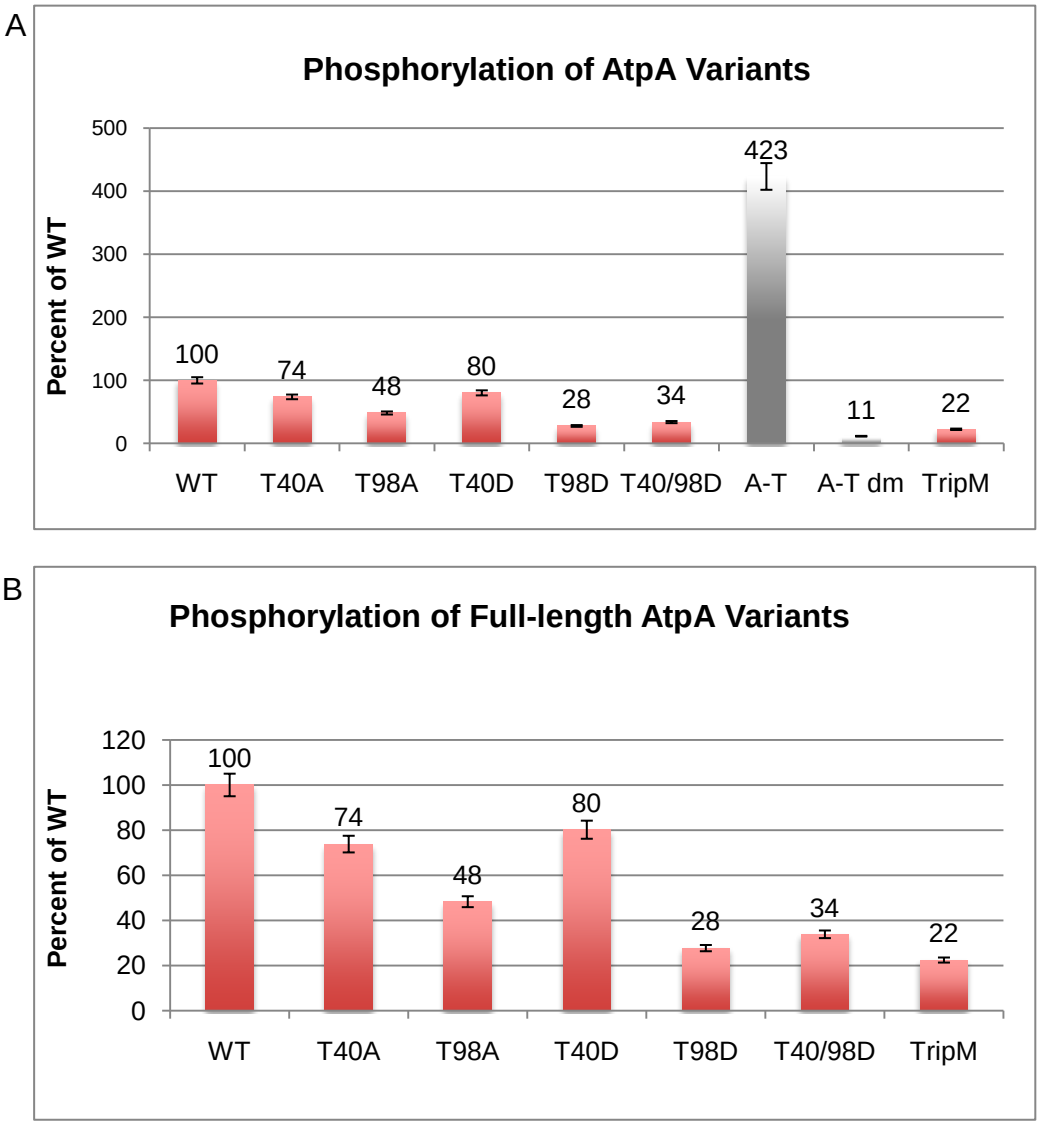

Figure 5-6. SsoPK4 phosphorylation of AtpA and phosphorylation-site variants. SsoPK4 was assayed with various Thr-40 and Thr-98 mutants and compared to AtpA WT. A) The two truncated variants (gray) represent highest and lowest levels of phosphorylation. B) Comparison of full-length AtpA variants; a similar trend was observed in Figure 5-3. Assay conditions were as described as described in Chapter II. Results displayed are the average of duplicate samples, ± 5% error.

The amount of phosphate incorporation catalyzed by SsoPK4 into the numerous AtpA variants was as follows:

AtpA-T > CIMs > AtpA > T40D ≈ T40A > T98A > T40/98D > T98D > TripM > A-T dm

As discussed in Chapter III, any covalently bound ^{32}P transferred by SsoPK4 will remain on the target protein following SDS-gel electrophoresis. The protein-bound ^{32}P can then be detected by electronic autoradiography of the polyacrylamide gel. Therefore, in an effort to ascertain whether all of the ^{32}P radioactivity associated with the protein precipitates was covalently associated, aliquots of the assay samples depicted in Figure 5-6 were resolved by 12% SDS-PAGE and the gels analyzed by electronic autoradiography.

As expected, the highest level of phosphorylation by SsoPK4 was observed with AtpA-T WT (Figure 5-7A, lane 8). The high level of radioactivity visualized for the AtpA-T double mutant in lane 9 could be attributed to background levels of radiation detected from AtpA-T WT that was resolved in the neighboring lane. The amount of detectable ^{32}P on AtpA, as visualized by "hot" gel bands, decreased in the following order:

AtpA-T > AtpA ≈ T40A ≈ AtpA-T dm > T40D > T98A > T98D > T40/98D > TripM

The AtpA triple mutant exhibited a deficiency of ^{32}P associated with the protein with the concomitant appearance of free ^{32}P near the dye-front at bottom of gel (lane 10, Figure 5-7A). Based on these results, it appeared that AtpA does not autophosphorylate, per se. Rather it appeared Thr-240, responsible for binding divalent cations to tighten the nucleotide-binding pocket, acted in conjunction with the lysine residue at 239 to coordinate and retain [γ-^{32}P]-ATP in the catalytic site.

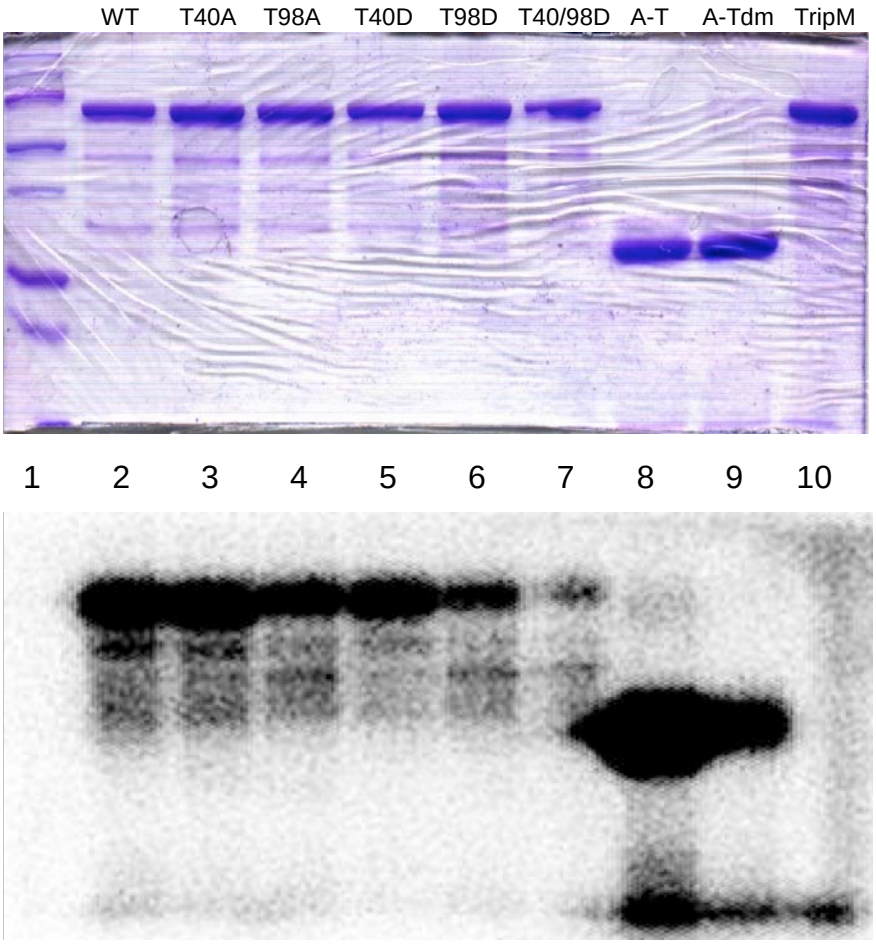

Figure 5-7. Visual comparison of ^{32}P-phosphorylated AtpA variants. 1.5 µg of ^{32}P-labeled samples assayed in Figure 5-6 were resolved by 12% SDS-PAGE, top, and the resulting Coomassie-stained gel was imaged by autoradiography, bottom. Lane 1: Precision Plus Dual Color standards; 2: AtpA WT; 3: T40A; 4: T98A; 5: T40D; 6: T98D; 7: T40/98D; 8: AtpA-T; 9: AtpA-T dm; 10: TripM.

ATPase Function: Effects of Threonine Mutations on AtpA

Mutations at Thr-40 and Thr-98 alter ATPase activity

Based on the results summarized in the previous section, we can assert with confidence that SsoPK4-catalyzed phosphotransfer to AtpA at Thr-98 and, to a lesser extent, on Thr-40. Now that SsoPK4-related phosphorylation sites on AtpA had been identified, we wanted to evaluate the effects, if any, of the various T40X and T98X substitutions on ATPase activity (as with phage-insert mutants, Figure 5-2). None of the variants exhibited ATPase activity on their own. All T40 and T98 variants evidenced lower ATPase activity levels when combined with AtpB than WT (Figure 5-8A). The T40A and T40/98D mutants exhibited 21% and 33% the ATPase activity of wild-type AtpA, while T40D and T98A were approximately 75% as active. Most surprisingly, the T98D mutant exhibited no detectable ATPase activity. The assay was repeated comparing T40/T98 mutant activity with TripM (T40/98D, T240A) and CIMs with results compared as a percentage of AtpA WT (Figure 5-8B). Table 5-1 summarizes the results of SsoPK4 phosphorylation of, and ATPase activity for, the full-length threonine mutants as a percentage of AtpA wild-type activity.

As discussed, the aspartate-for-threonine mutation oftentimes behaves as a phosphate-mimic by substituting a negatively charged residue for the non-polar hydroxyl group. As it was previously determined that SsoPK4 preferentially phosphorylates Thr-98 over Thr-40 (Figure 5-3), I decided to focus on T98D as a model for the phosphorylation of Thr-98 by SsoPK4.

A

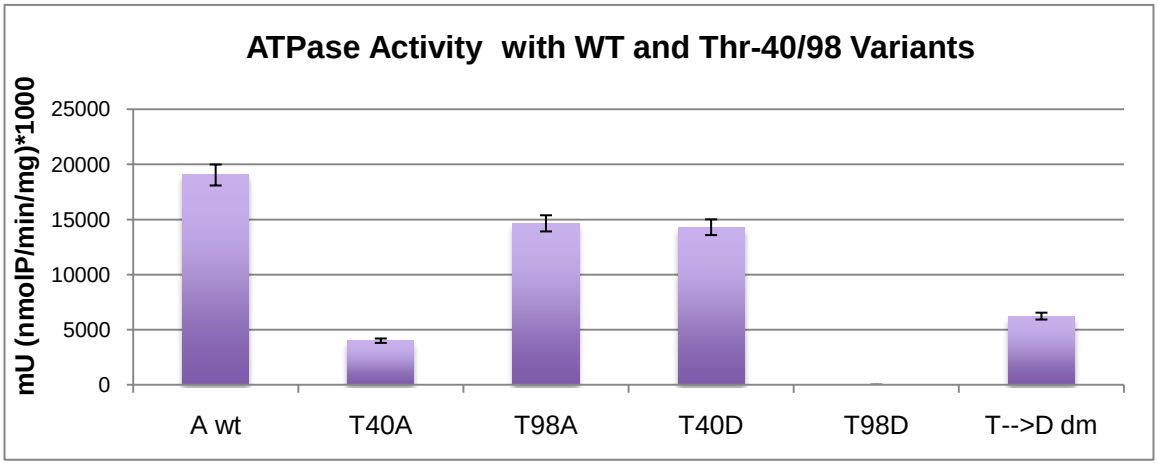

B

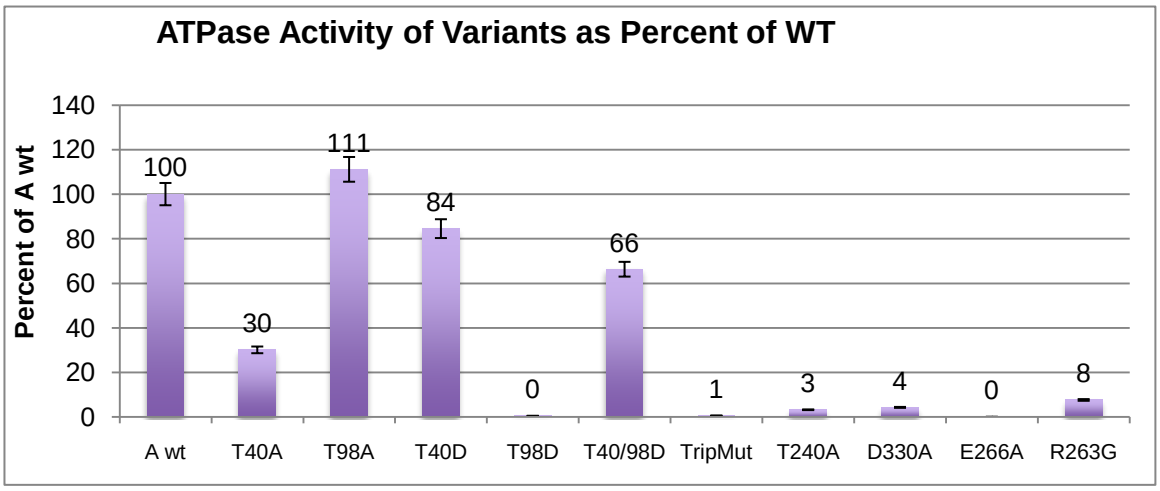

Figure 5-8. ATPase activity with MS-identified-pThreonine variants and CIM variants of AtpA. In both A) and B), AtpA variants (1 µg) and AtpB (0.75 µg) at 300 nM each were combined in ATPase activity buffer (50 mM MES, pH 5.5, 4 mM Ca^{2+}) and assayed 30 min at 65°C using molybdate extraction as described in Chapter IV. In A), T→D dm refers to the T40/98D double mutation variant. Results displayed in A: average of triplicate samples, B: average of duplicate samples, ± 5% error.

Phage-insert Threonine Mutants (Percent of AtpA WT)						
	T158A	T169A	T→A dm	T158D	T169D	T→D dm
SsoPK4	106	94	n.d.	127	139	n.d.
ATPase	91	66	86	91	102	67
Catalytic Site Mutants (Percent of AtpA WT)						
	T240A	R263G	E266A	D330A	---	---
SsoPK4	137	158	118	150	---	---
ATPase	3	4	0	8	---	---
MS-Identified Threonine Mutants (Percent of AtpA WT)						
	T40A	T98A	T40D	T98D	T40/98D	TripM
SsoPK4	74	48	80	28	34	22
ATPase	30	111	84	0	66	1

Table 5-1. Summary of SsoPK4 activity and ATPase activity with full-length AtpA variants. Results are presented as percentage relative to AtpA wild-type at 100%.

Partial proteolysis of AtpA and AtpA variants

We wanted to examine the possibility that protein misfolding might account for the decrease of ATPase activity associated with the AtpA variants of T40X and T98X. To test this, full-length AtpA and its variants were subjected to partial proteolysis with trypsin. Rates and sites of proteolysis should differ compared to wild-type protein if the mutation destabilizes gross protein morphology (Kennelly, Starovasnik et al. 1990; Coulter-Mackie and Lian 2008).

First, appropriate tryptic-digest conditions were determined using wild-type AtpA. It was necessary to observe a time-course for complete hydrolysis in order to compare rates of hydrolysis with the mutants. Because the activity of AtpA depends on the presence of AtpB, trypsin digests were performed under conditions as close as possible to those used to assay ATPase activity as described in Chapter II. Trypsin digest conditions are described in Materials and Methods.

Complete proteolysis of AtpA was observed at t = 30 min without ATP (Figure 5-9A) and at t = 60 min with 1 mM ATP (not shown). Approximately 50%-cleavage of AtpA was achieved at t = 15 min in the presence of 1 mM ATP (Figure 5-9A). AtpB was resistant to trypsin hydrolysis under these conditions (not shown). These conditions and time-points were then used to compare hydrolysis of AtpA variants (Figure 5-9B). Shown in red-boxed regions are the results obtained for AtpA WT and T98D. At t = 15 min, the intensity of the band at 67 kDa had decreased by roughly 50%. These results suggest that the conformation of the T98D variant was similar to wild-type. Similar polypeptide profiles were obtained for the remaining p-Thr variants (Figure 5-9B).

A

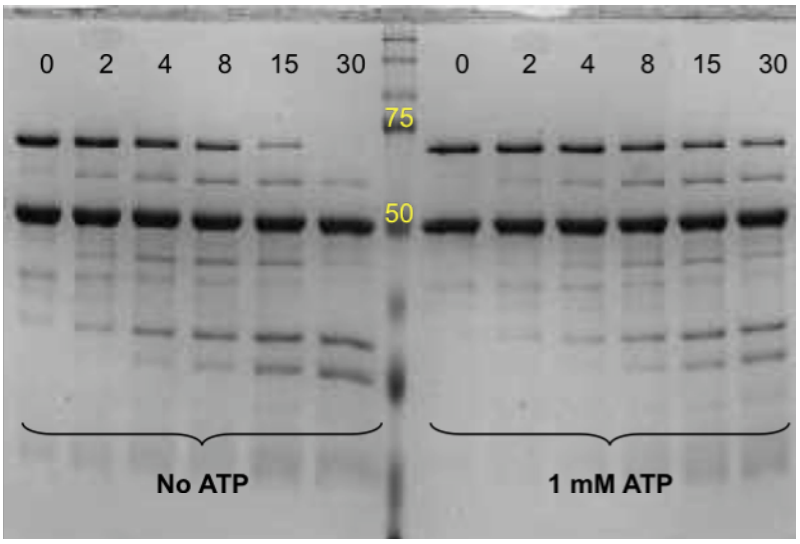

B

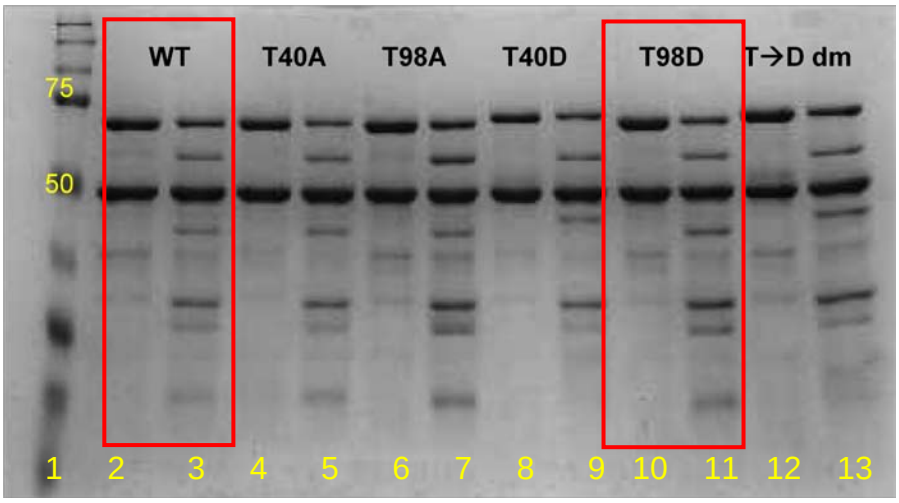

Figure 5-9. Proteolytic trypsin cleavage comparison of AtpA to T40 and T98 full-length variants. For both A) and B) a 45:1 ratio of AtpA (67 kDa) to trypsin was incubated at room temperature in ATPase activity buffer; AtpB (50 kDa) was not affected by trypsin under these conditions (not shown). A) Wild-type AtpA with and without 1 mM ATP for t=0 to t=30 min. B) Comparison of wild-type (WT) to mutants at t=0 (left) and t=15 min (right) with 1 mM ATP. Boxed regions highlight WT and T98D proteins. Lane 1: Precision Plus Dual Color standards; Even-numbered lanes: t = 0; odd-numbered lanes: t=15 min.

Wild-type AtpA, T98D, and ATPase activity

It was concluded that the T98D was properly folded with respect to wild-type based on results of partial proteolysis by trypsin. Thus, its lack of catalytic competency must be attributable to some other cause. The minimal active form of all other homologous ATPases is a complex between AtpA and AtpB. As the *S. solfataricus* ATPase required the presence of a stoichiometric quantity of AtpB for activity, it seemed likely that the active form of this enzyme was a complex. In this case, it is possible that either AtpA T98D forms a complex with AtpB, but the complex is not active, or AtpA T98D fails to hydrolyze ATP because it is unable to associate with AtpB. If the former is true, then the T98D should act as a "dominant negative" relative to WT by competing for available AtpB. As evidenced in Chapter IV, the ratio of AtpA to AtpB for ATP hydrolysis occurred in a 1:1 stoichiometric relationship.

For these experiments, AtpB was added to the molybdate extraction assay for ATPase activity in a limiting amount at a ratio of approximately 2:1 AtpA (300 nM) for AtpB (160 nM). We asked whether an inclusion of excess variant T98D over wild-type AtpA reduced the yield of ATPase activity. As shown in Figure 5-10, the addition of T98D variant in equimolar amounts (not shown) or at 5x levels of AtpA wild-type levels had little or no impact on the level ATP hydrolysis (Figure 5-10). This result was independent of the order in which the various proteins were added to the reaction mixture. All ATPase activities were within 5% error for wild-type activity when 5x T98D was combined with AtpB and AtpA regardless of order of addition. As seen in the last two columns, 5x T98D and 1x T98D had similar negligible levels of ATP hydrolysis with AtpB.

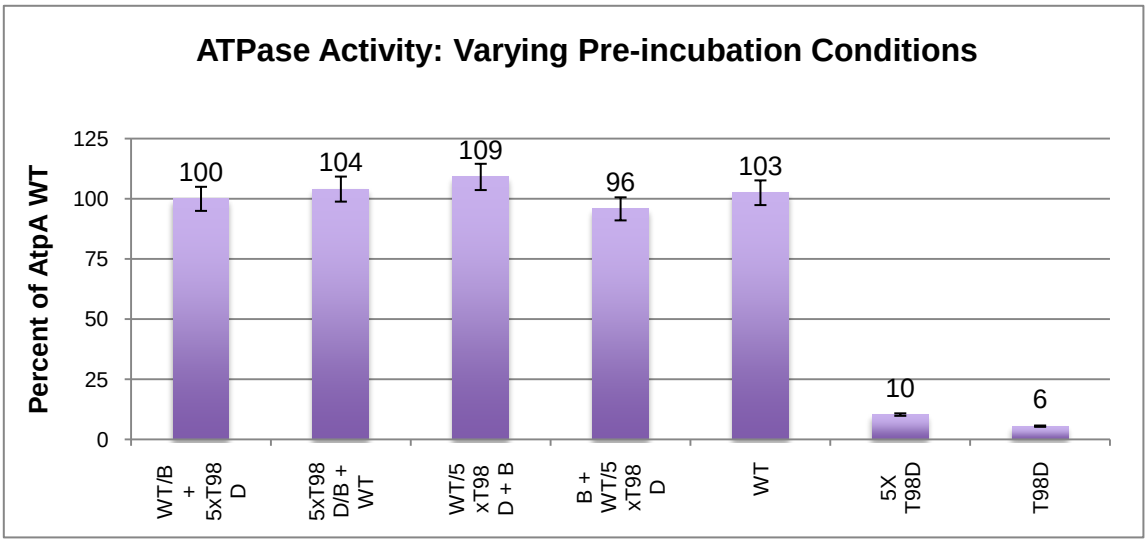

Figure 5-10. ATPase activity with excess (5x) T98D mutant. Columns 1-4 show order of addition where "x/x" were combined in ATPase activity buffer before addition of "+ x" component. 5x T98D and T98D with AtpB without AtpA WT results shown in last two columns. Average of triplicate samples, ± 5% error.

Finally, it the phosphorylated-mimic T98D was pre-incubated with AtpB for 5 min at 65°C before addition of AtpA wild -type. Perhaps pre-incubating under assay conditions would allow T98D and B to form a complex before addition of AtpA. Also 10x T98D (3 µM vs. 300 nM WT) was added to a few sample reactions to see if any recovery of ATPase activity would occur when pre-incubated with AtpB alone. The results of these experiments are presented in Figure 5-11. The pre-incubation of 5x T98D and 10x T98D with AtpB alone did not dramatically increase levels of ATPase activity: 14% and 7% respectively. Moreover, 5x T98D and 10x T98D with AtpA and AtpB did not show a decrease in ATPase activity compared to pre-incubated AtpA and AtpB. The simplest explanation for these observations is that the phosphorylation-mimic mutant T98D would not form an active, catalytic AtpA-AtpB hetero-oligomer as observed via production of free phosphate, presumably because the negative-charge substitution at Thr-98 disrupted AtpAB complex formation.

Protein-protein interactions with native-PAGE

All attempts to rescue or alter ATPase activity with the phosphorylated-mimic T98D proved unavailing. Chemical cross-linking results of the various ATPase subunits pointed to potential complex formation of AtpA and AtpB *in vitro* (Figure 4-11, Chapter IV). The working hypothesis was that the negative charge at Thr-98 prevents assembly of an active AtpA-AtpB complex. Efforts to detect complex formation of AtpAB by intrinsic fluorescence in solution proved indeterminate. Another way to test the working hypothesis was to compare the physical association of wild-type AtpA/AtpB with T98D/AtpB by native-PAGE (Chapter II).

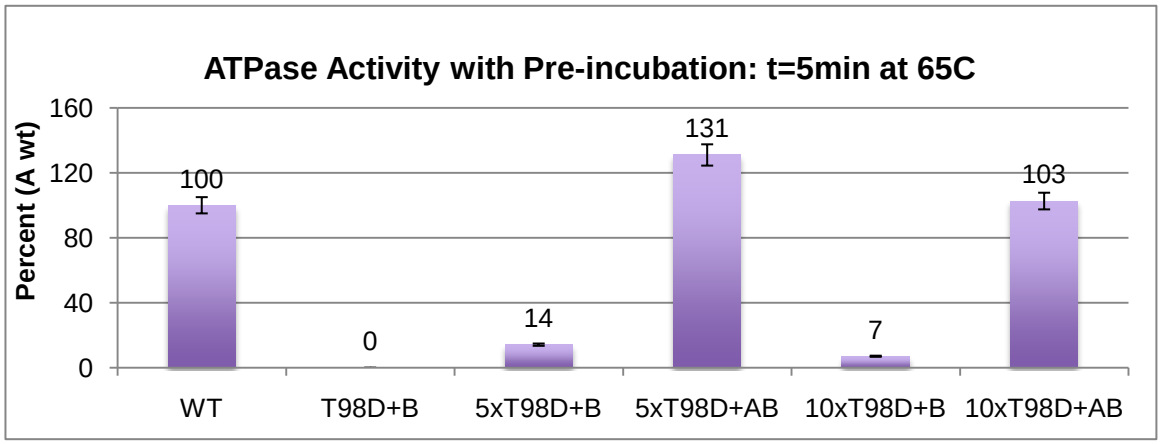

Figure 5-11. ATPase activity with pre-incubation of protein subunits. AtpA WT was pre-incubated with AtpB for 5 min at 65˚C in column 1. The remaining samples were pre-incubated under same conditions before the addition of AtpA WT. AtpA and T98D (1 µg), AtpB (0.4 µg), 5x T98D (5 µg) and 10x T98D (10 µg). Results shown are averages of duplicate samples, ± 5% error.

Duplicate aliquots were removed from each reaction vial and incubated 30 min on ice as a negative control for ATPase activity. The S-tag variant of AtpA, A(s), was included because of its greater molecular weight to help distinguish it from the AtpA WT subunit. The S-tag slowed migration of AtpA compared to tagless AtpA WT. Addition of the S-tag fusion sequence on AtpA did not interfere with ATPase activity (Chapter IV).

Results of native-PAGE with AtpA/T98D and AtpB are shown Figure 5-12. Lanes 2-4 in experimental and control gels contained AtpA or AtpA variants to identify bands associated with AtpA homo-oligomer interactions (Coskun, Rizzo et al. 2004). The boxed region of lanes 5 through 9 in Figure 5-12A highlights the region of interest for possible AtpA-AtpB complex formation. The control gel in Figure 5-12B lacked a well-defined band in the highlighted region of Figure 5-12A.

Within the boxed region of lanes 5 and 7, presumed heterodimers of AtpA(s)-AtpB and AtpA-AtpB form distinct bands. The heteromeric nature of the complex was verified as containing both AtpA and AtpB subunits by MS analysis at the Virginia Tech Mass Spectrometry Incubator. The subunit identification results are summarized in Table A-2 (Appendix A).

A heterodimer band was conspicuously absent in lane 6 (Figure 5-12A), which contains T98D and AtpB. Subsequent MS-identification of the boxed region in lane 6 returned the presence of AtpA (T98D) alone. It was evident that the phosphorylated-mimic T98D and AtpB failed to form a stable hetero-oligomer complex, lending support the to hypothesis that phosphorylation of AtpA by SsoPK4 may regulate ATPase activity.

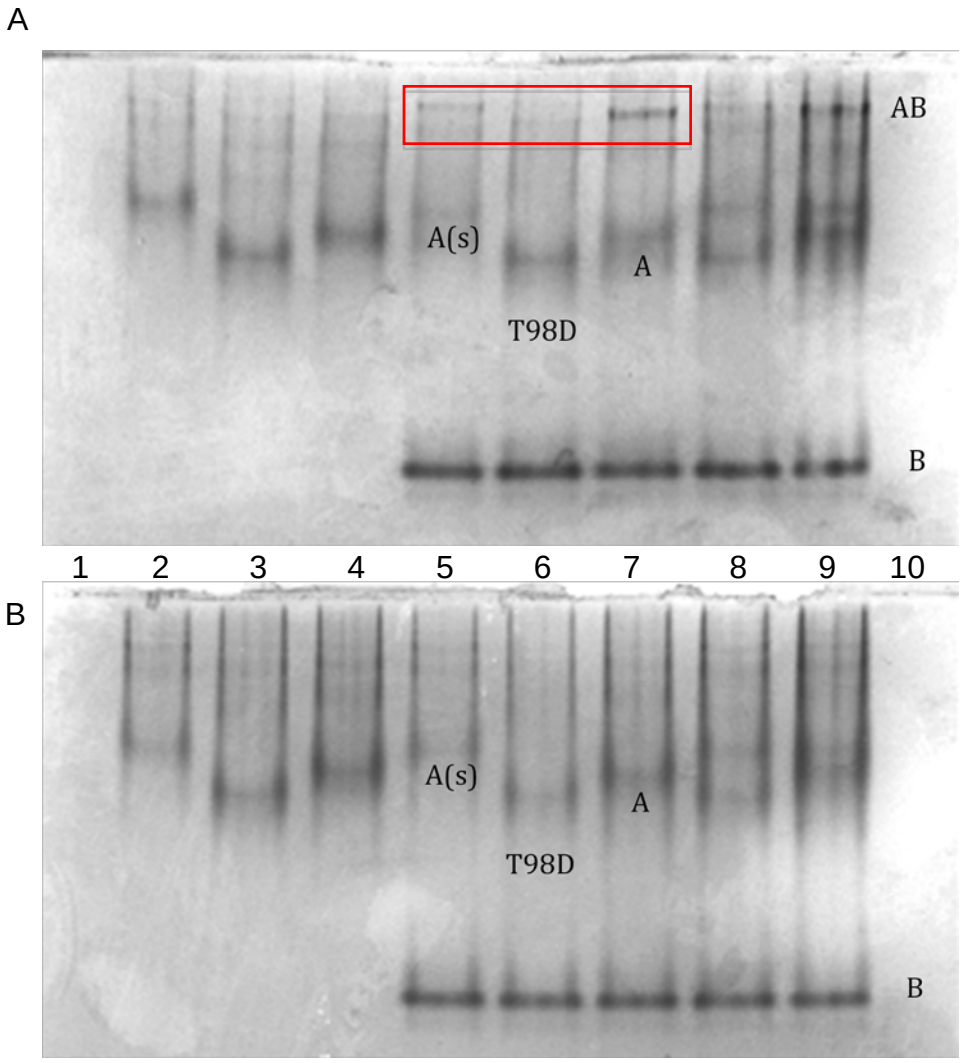

Figure 5-12. AtpA and AtpB subunit interactions resolved by 8% native-PAGE. For each 50 µl reaction, 10 µg of each AtpA variant was combined in ATPase activity buffer with 500 µM ATP. AtpB was added under limiting conditions at 4 µg per 50 µl reaction. A: results of one set of reactions following ATPase activity assay conditions with incubation at 68 for 30 minutes. B: duplicate reactions with incubation for 30 minutes on ice. Loading order: Lanes 1 and 10 are empty. Lanes 2-4 contain AtpA with S-tag, A(s), T98D and AtpA WT, respectively. Lanes 5-6 contain A(s), T98D, and AtpA WT with AtpB, respectively. Lane 8: A(s) and T98D with AtpB. Lane 9: AtpA(s) and AtpA WT plus AtpB.

Chapter VI:

Summary of Results and Discussion

SsoPK4 Phosphorylated the Protein Kinase Substrate AtpA in vitro

Identification of potential SsoPK4 target proteins

Specific Aim 1 of this research project involved utilizing a genomic phage display expression library to identify and overexpress potential SsoPK4 protein substrates. The phage display library was previously constructed using *S. solfataricus* genomic DNA packaged within the Lambda ZAP expression vector. The resultant library was probed with the purified recombinant protein-serine/threonine kinase SsoPk4, encoded by ORF *sso3182*, and [γ-^{32}P]-ATP. Plaque-lift membranes were subjected to autoradiography to detect the presence of "hot spots" indicating phosphotransfer between to kinase to the expression products. The immobilized radiolabeled phage-expressed peptides correlated to monoclonal phage populations on the LB agar plates. The phage insert DNA was isolated from the LB agar plates and PCR-amplified for DNA sequence analysis.

Several ORFs from *S. solfataricus* were identified as potential SsoPK4 target substrates. The ORF *sso0563* (AtpA) was chosen for further examination due to its annotated enzymatic function as the catalytic subunit in the soluble A_1 protein complex of the A_1A_O-ATPase. AtpA and a C-terminally-truncated variant, AtpA-T, were cloned and overexpressed in the pET vector system that includes a C-terminal His-tag for IMAC purification. Initially, recombinant proteins were overexpressed within the pET29b vector also containing a 3 kDa S-tag fusion sequence at the N-terminus. AtpA (~ 67

kDa) and AtpA-T (~ 37 kDa) were purified and found to be soluble and stable when stored at -80˚C.

Assays for protein kinase activity with SsoPK4 and AtpA

SsoPK4 was discovered to phosphorylate a threonine within the S-tag/thrombin cleavage site, leading to false-positive results for protein kinase activity highlighting the sometimes-promiscuous nature of protein kinases *in vitro.* AtpA, AtpA-T and subsequent recombinant proteins were overexpressed using the S-tag deficient pET21d vector to eliminate confounding phosphorylation events. As before, the recombinant protein products AtpA and AtpA-T were soluble and stable when stored at -80˚C.

SsoPK4 phosphorylated both AtpA (67 kDa) and AtpA-T (26 kDa); AtpA-T was phosphorylated at a higher stoichiometric level over AtpA. Subsequent radioactive SDS-PAGE and gel autoradiography determined the covalent [^{32}P]-addition on both AtpA variants. Phosphoamino analysis results showed threonine residues of both AtpA and AtpA-T labeled with [^{32}P].

Functional characterization of AtpA

Specific aim 2—the characterization of potential protein kinase substrates—was addressed in Chapter IV. SsoPK4 was proven to exhibit phosphotransferase activity on both the full-length and truncated variants of AtpA. Next we needed to determine whether we could detect the enzymatic activity of AtpA, specifically ATP hydrolysis, in order to probe any effects SsoPK4 phosphotransfer may have on wild-type AtpA function. By analogy to other ATPases, it was presumed that the protein products of ORFs *sso0564* (AtpB), *sso6175* (AtpG), and *sso0561* (AtpE), which were located in the

same putative operon as AtpA, interacted directly with AtpA. Each of these ORFs was cloned in the pET21d vector and their polypeptide products were successfully overexpressed as recombinant fusion proteins in *E. coli*.

ATPase activity was quantified using the *in vitro* Malachite Green assay and Molybdate Extraction assay; both methods involve the detection of inorganic phosphate hydrolyzed from ATP. The use of [γ-^{32}P]-ATP in the extraction assay was preferred due to its lower background and greater sensitivity. Neither full-length AtpA nor AtpB alone detectably hydrolyzed ATP. However, a functional ATPase was reconstituted upon incubation of full-length AtpA and AtpB with ATP in pH 7.5 buffer and the divalent cations Mg^{2+} and Mn^{2+}. The inclusion of putative auxiliary subunits AtpG and AtpE did not appear to enhance or decrease ATPase activity; hence they were omitted from subsequent assays. AtpA-T could not substitute for AtpA, presumably due to the lack of the conserved Walker A (P-loop), Walker B and GER regions removed in the former, C-terminally truncated, protein.

Optimal ATPase activity was observed at 65°C, which overlaps the end of environmental temperature range for *S. solfataricus*. The preferred pH for ATPase activity, 5.5, is consistent with an intracellular location. Optimal *S. solfataricus* growth occurs at pH 2-4 while the cytosol is maintained near physiological pH (Schäfer 1996). The A_1 lobe of the ATPase is located on the cytosolic side of the plasma membrane and is associated with the membrane-bound A_O sector. The flow of protons from the acidic environment through the A_O sector drives the synthesis of ATP within the A_1 multimeric complex.

The divalent cation Ca^{2+} was the cofactor of choice. In the tobacco hornworm V-ATPase, the presence of calcium was preferred over Mg^{2+} under certain assay conditions

(Coskun, Rizzo et al. 2004). Calcium-dependant ATPase activity has also been exhibited in F-ATPases of *Bacillus firmus* (Hicks and Krulwich 1986) and spinach chloroplasts (McCarty and Racker 1968). An ATP concentration of 50 µM fell within the linear range of activity for the ATPase.

Several lines of evidence suggest that the active form of the ATPase is a heterodimer similar to the A_3B_3-heterohexamer core of other A/V/F-ATPases. First, ATPase activity reached its maximum at a 1:1 stoichiometry of AtpA and AtpB dependence. Second, cross-linking of the *S. solfataricus* subunits AtpA, B, E, and G using the zero-length chemical linker EDC yielded homodimers of AtpA and AtpB as well as the heterodimers A-B, A-G, B-G and E-G. Third, hetero-oligomers of AtpA and AtpB could be resolved on acrylamide gels run under native, i.e. SDS-free, conditions.

Determination of SsoPK4-targeted phosphothreonine residues on AtpA

Chapter V addressed Specific Aim 3 by examining "the relationship between the substrate and SsoPK4 to determine the effects, if any, phosphorylation has on substrate function." It was imperative to first locate the SsoPK4-targeted residues on AtpA. The phosphorylated fragment of the phage insert sequence contained two threonines at residues 158 and 169. Site-directed mutagenesis of each of these residues to alanine or aspartate failed to alter the level of phosphate transferred by SsoPK4 into AtpA, indicating that phosphorylation of AtpA was occurring elsewhere. Also, substitution of Thr-158 and Thr-169 in AtpA by Asp or Ala residues did not affect ATPase activity.

The truncated version of AtpA was incubated with ATP and SsoPK4 then submitted to the Mass Spectrometry Incubator at the Virginia Polytechnic Institute and State University (Blacksburg, VA). The MS analysis detected two phosphorylated

residues in AtpA-T, Thr-40 and Thr-98. These residues are situated near the N-terminal non-homologous region (NHR) common to both V- and A-type catalytic subunits. Substitution of either threonine with aspartate or alanine using site-directed mutagenesis resulted in decreased levels of phosphotransfer into full length AtpA by SsoPK4. For both the T98A and T98D variants, phosphate incorporation was only≈ 50% as compared to wild-type AtpA.

Low levels of phosphotransfer into AtpA were still detected following construction of the T40/98D variant that eliminated both of the phosphoacceptor threonines previously identified via MS. Since apparent autophosphorylation had been observed by SDS-PAGE following incubation of AtpA with [γ-^{32}P]-ATP, we hypothesized that the catalytic regions responsible for nucleotide binding on AtpA were retaining radiolabeled ^{32}P. We therefore asked whether mutagenic alterations designed to perturb these regions would decrease the level of apparent autophosphorylation on AtpA.

Four additional AtpA variants were overexpressed from mutant plasmids containing point mutations within the coding regions for the putative Walker A (T240A), Walker B (D330A), and GER (R263G, E266A) domains. Assays of ATPase activity confirmed that these variants formed less active ATPases when combined with AtpB under standard assay conditions. A triple mutation plasmid was constructed using the T40/98D plasmid as a DNA template and primers for T240A mutagenesis. The purified expression product, TripM, exhibited the lowest level of phosphotransfer (11%) compared to other variants and wild-type AtpA. To determine whether the "background" radioactivity was a consequence of a covalent modification, samples were resolved by SDS-PAGE and the resulting gel subjected to autoradiography. ^{32}P was detected among all AtpA variants except on TripM, indicating that the apparent

background phosphorylation detected earlier in protein precipitation assays was in fact a consequence an ionic association of [γ-^{32}P]-ATP or some product thereof with the catalytic regions of AtpA.

The Phosphorylation-mimic Variant, T98D, Inhibits ATPase Activity

Lower ATPase activity was evidenced by Thr-40 and Thr-98 variants of AtpA

The Thr-40 and Thr-98 variants were assayed for ATPase activity under standard conditions. The T98D variant had no detectable ATPase activity compared to wild-type. The remaining variants exhibited decreased ATPase activity at levels ranging from 75% of wild-type (T40D, T98A) to ~ 25% (T40A, T40/98D). The substitution of the negatively charged aspartate at position 98 in the T98D variant could function as a mimic of the phosphoryl group on the hydroxyl of threonine. The implication, that phosphorylation at Thr-98 abolishes ATPase activity, as well as the preferential targeting of this residue over Thr-40 by SsoPK4 led to the examination of the relationship of Thr-98 and the T98D mutant in more depth.

It then became necessary to rule out the possibility that mutational alterations decreasing ATPase activity acted by disrupting protein conformation. AtpA and the phosphorylation-site variants were treated with trypsin to generate a partial proteolysis time-curve. The proteins were each combined with AtpB and ATP to mimic assay conditions. All variants exhibited a similar band pattern profile to that of AtpA where the protein at 67 kDa was approximately 50% digested at t = 15 min of incubation with trypsin and similar polypeptide fragments were visible on the gel. These results suggest that all variants were properly folded with respect to wild-type AtpA.

T98D does not produce and active ATPase enzyme

Since T98D appeared to be correctly folded it was concluded that this variant either 1) associated with AtpB but the complex was inactive or 2) T98D failed to interact with AtpB and cannot form the catalytic hetero-oligomer. Increasing the concentration of AtpA T98D 5- and 10-fold over AtpB did not dramatically increase ATPase activity levels. T98D was then combined with AtpA in a 1:1 and 5:1 ratio; AtpB was added under limiting conditions. There was no decrease in ATPase activity compared to wild-type alone, indicating T98D did not compete with wild-type for the limited supply of AtpB. The order of addition of T98D, AtpB, or AtpA had no effect on ATPase activity—all levels were same as for AtpA and AtpB alone. Pre-incubation of the T98D variant with AtpB did not affect the outcome; once AtpA was added, ATPase activity levels were at levels of wild-type with AtpB.

These results led us to conclude that T98D cannot form the AtpA-AtpB complex required for ATPase function. Based on cross-linking results we knew that unmodified AtpA and AtpB associate closely enough to be chemically linked. Introduction of a negative charge on residue 98 appeared to interfere with T98D-AtpB interaction. Initially, tryptophan fluorescence signaling was utilized to examine subunit interactions as described in Chapter II, Materials and Methods. This method was chosen based on previous studies involving tryptophan signal quenching on AtpA due to its association with other soluble ATPase subunits (Biukovic, Rossle et al. 2007; Kumar, Manimekalai et al. 2008). However, the sample volume required large quantities of protein, making replicate samples difficult (results not shown).

Native-PAGE techniques were employed to determine whether or not AtpA T98D associated with AtpB. The subunits AtpA-AtpB and T98D-AtpB were incubated under

standard ATPase activity conditions before resolving the proteins via native-PAGE. A control gel was also run containing duplicate samples incubated on ice, rather than 65˚C. AtpA and AtpB formed a complex as evidenced by Coomassie-staining of the gel; the control gel lacked of bands at higher MW regions where potential heterodimer associations would occur. The lane containing AtpA T98D together with AtpB resembled that of the control where no bands at increased MW were detected; this indicated a failure to form the heterodimer complex by the T98D variant.

The addition of AtpA(s), or the S-tagged recombinantly expressed protein, was also included for comparison. The 3-kDa N-terminal tag did not affect ATPase activity or its ability to form a complex with AtpB. The identity of A-B and A(s)-B heterodimers were confirmed by MS analysis of excised gel bands. A band near the region where a T98D-B complex should be observed was identified as AtpB alone, indicating homodimer formation also witnessed in EDC cross-linking experiments. These results confirmed the working hypothesis that the AtpA variant T98D and AtpB cannot interact to form an active complex. Following this logic, it could be reasoned that phosphorylation of AtpA at Thr-98 by SsoPK4 may help regulate the physiological function of the A_1A_O-ATPase.

Phosphoregulation of the S. solfataricus *A_1A_O-ATPase?*

The A/V-ATPase connection

In the 1960s and 1970s, research efforts pioneered by Paul Boyer, among others, revealed the complex structural changes that occurred within F_1F_O-ATPases during the course of ATP hydrolysis and synthesis (Boyer, Cross et al. 1973; Kayalar, Rosing et al. 1977). In 1994 the structure of a β-subunit isolated from bovine mitochondria was

resolved and highlighted key catalytic residues (Abrahams, Leslie et al. 1994); a few years later the rotational movement of the F-ATPase was observed using fluorescence labeling techniques (Noji, Yasuda et al. 1997; Häsler, Engelbrecht et al. 1998). Initial findings on F_1F_O-ATPases mechanisms have since proven applicable to the V- and A-ATPases. Despite decades of structural and mechanistic research on this superfamily of enzymes many questions remain regarding their regulation (Gruber, Wieczorek et al. 2001). Studies of archaeal models, such as the *S. solfataricus* A_1A_O-ATPase, could illuminate activity regulation of this complex multimeric enzyme in other organisms (Grüber and Marshansky 2008).

The archaeal ATPase has been described as "chimeric" since it shares properties of both F- and V-type ATPases (Gruber, Wieczorek et al. 2001); however, the link between archaeal and vacuolar (eukaryotic) ATPases has been studied in relatively greater detail. The A/V-ATPase comparisons are warranted due to their close evolutionary relationship (Nelson 1992; Schafer, Engelhard et al. 1999) and the inclusion of a highly conserved non-homologous region (NHR) in the A subunit (Bowman, Tenney et al. 1988; Zimniak, Dittrich et al. 1988) that accounts for ~ 50% of the sequence identities between A subunits of A/V-ATPases (Bowman, Tenney et al. 1988). The F_1 β subunit lacks this region. It shares ~ 25% identity with the A subunits of the vacuolar and archaeal catalytic proteins.

The non-homologous region

It has been proposed that the NHR may be involved in regulation of ATPase activity since mutations within this region have been shown to decrease V-ATPase activity in yeast by 50-80% relative to wild-type (Shao, Nishi et al. 2003; Shao and

Forgac 2004). It has been postulated that NHRs in V-ATPases may be responsible for A_1-A_O dissociation—a feature unique to V-ATPases—or changes in the coupling efficiency of the V_O sector via subunit associations bridging the soluble and membrane-bound lobes of the ATPase (Shao and Forgac 2004; Cipriano, Wang et al. 2008). Coupling efficiency refers to the "differences in the efficiency with which protons are pumped during ATP hydrolysis" (Jefferies, Cipriano et al. 2008).

Figure 6-1 shows a structural comparison of the F1-β subunit of bovine heart mitochondria (Abrahams, Leslie et al. 1994) to the A subunit, PhoA, from archaeal *Pyrococcus horikoshii* (Maegawa, Morita et al. 2006). In Pho A, Domain I refers to the N-terminal domain, Domain II contains the NHR, Domain III consists of the nucleotide-binding region, and Domain IV is the C-terminal domain. The NHR of Domain II is highlighted in red (Figure 6-1B) and projects away from the central A-B assembly core region as shown in Figure 6-1C.

A model of *S. solfataricus* AtpA was constructed using Swiss Model Workspace (Peitsch 1995; Arnold, Bordoli et al. 2006; Kiefer, Arnold et al. 2009) and labeled with similar domain coloring as in Figure 6-1B. The result, shown in Figure 6-2, was modeled after homology alignments to the A subunit of the archaeal *P. horikoshii,* (PDB: 1VdzA, ~ 55% sequence identity) and β-subunits of two thermophilic bacteria, *Thermotoga maritima* (PDB: 2r9vA, ~ 23%) and *Thermophillic bacillus* P53 (PDB: 1skyE, ~ 18%). Since the two bacterial species lack the NHR, the region shown in red corresponds to the PhoA subunit depicted in Figure 6-1. Arrows highlight threonines 40 and 98 of *S. solfataricus*. Thr-40 is located in the N-terminal Domain I while Thr-98 resides in or near the NHR region of Domain II.

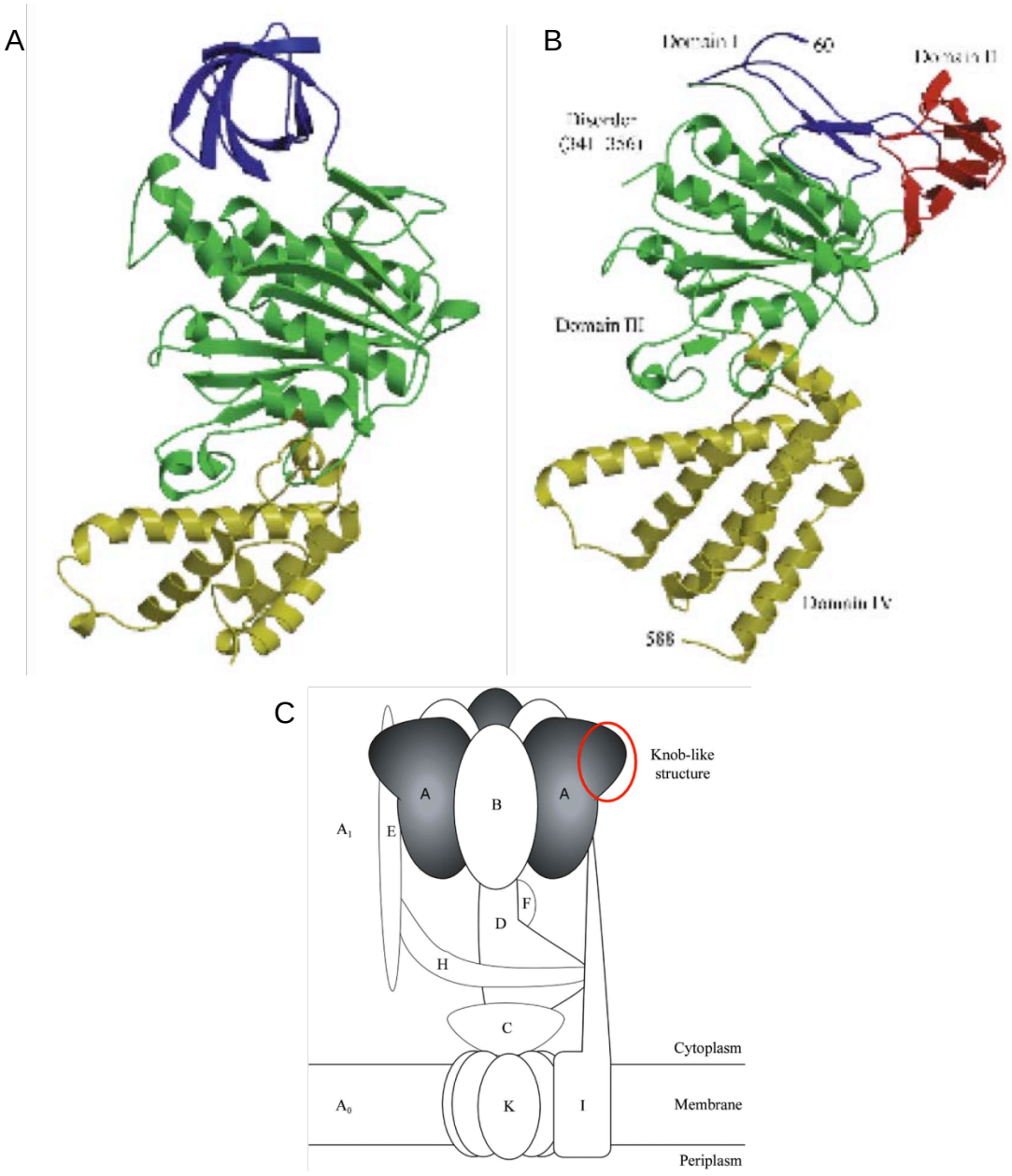

Figure 6-1. Comparison of F- and A-ATPase catalytic subunit crystal structures. The β-subunit structure derived from bovine mitochondria (Abrahams, Leslie et al. 1994) in A lacks the non-homologous region (NHR) seen in B for *P. hirokoshii* catalytic subunit PhoA. Shown in C is a depiction of archaeal ATPase subunit arrangement. All images are from "Structure of the catalytic nucleotide-binding subunit A of A-type ATP synthase from Pyrococcus horikoshii reveals a novel domain related to the peripheral stalk." (Maegawa, Morita et al. 2006).

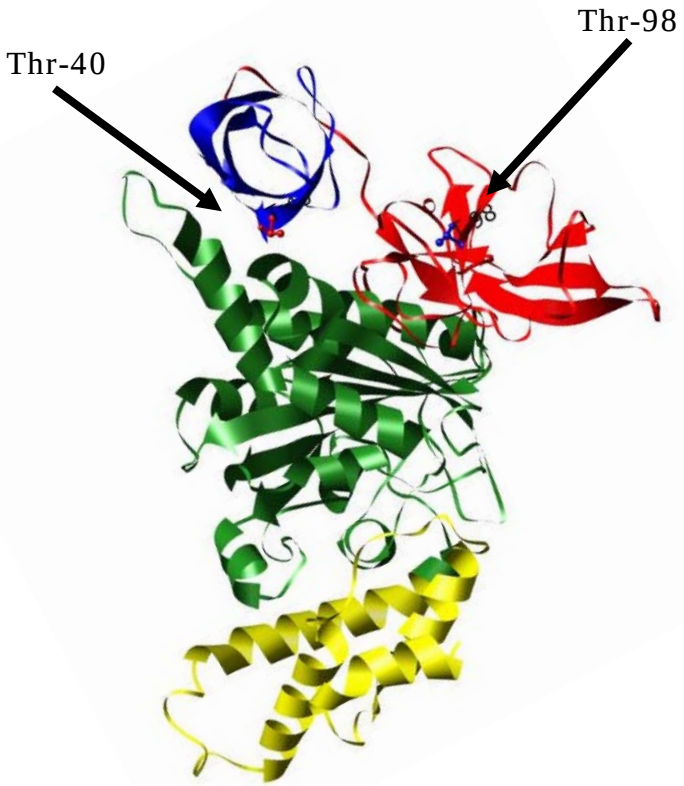

Figure 6-2. Model of *S. solfataricus* AtpA. The model was derived from homology alignments of known catalytic subunit structures from *Pyrococcus horikoshii*, (PDB: 1VdzA), *Thermotoga maritima* (PDB: 2r9vA) and *Thermophillic bacillus* P53 (PDB: 2r9vA). Arrows highlight the pThr identified via MS. The model was generated using Swiss Model Workspace.

Based on the model in Figure 6-2, both Thr-40 and Thr-98 residues appear to be on the surface, accessible to SsoPK4, particularly since SsoPK4 contains a transmembrane domain and would be located at the plasma membrane. Thr-98 near the NHR may also interact with other ATPase subunits (e.g. AtpE, AtpG) believed to bridge the catalytic and membrane domains. Therefore, phosphorylation of Thr-98 by SsoPK4 could be involved in affecting the coupling efficiency of the A_O sector.

Phosphorylation of V- and F-ATPase subunits

The decreased-activity mutations in the yeast NHR did not include potential protein serine/threonine-kinase target residues (Shao, Nishi et al. 2003) but phosphorylated subunits of F, V, and A-type ATPases have been reported. Chloroplasts and mitochondrial F_1F_O-ATPases isolated from barley were found to have phosphoserine-binding and phosphothreonine-binding regulatory proteins associated with the β-subunit, implying that the catalytic subunit was phosphorylated at serine and/or threonine residues (Bunney, van Walraven et al. 2001). Mitochondrial β-subunits from human skeletal muscle were phosphorylated *in vivo* at multiple locations though the identity of phosphoresidues was not determined (Højlund, Wrzesinski et al. 2003). Activation of an isoform of protein kinase C, PKCα, by chemical stress phosphorylated the β-subunit from renal cells with a resultant decrease in ATPase activity, oxidative phosphorylation, and a loss of mitochondrial repair (Liu, Godwin et al. 2004).

In 2006 the first report of V-ATPase phosphorylation was discovered in *Arabidopsis*. A recombinant serine/threonine protein kinase phosphorylated the C-

subunit of the V_1-sector on multiple serine and threonine residues *in vitro* (Hong-Hermesdorf, Brüx et al. 2006). The *Arabidopsis* kinase also phosphorylated several subunits from *Manduca sexta* (tobacco hornworm) including subunit A (AtpA homologue in *S. solfataricus*). Subunit C from the tobacco hornworm was later phosphorylated by protein kinase A (PKA) *in vitro* and was believed to play a role in V_1V_O holoenzyme assembly (Voss, Vitavska et al. 2007). Voss et al. do point out that subunit C is not highly conserved among V-ATPases. In fact, this subunit has not been discovered within *S. solfataricus* P2 though it is present in a number of other archaeal systems. Perhaps phosphorylation still plays a role in ATPase regulation in organisms lacking subunit C.

Future Directions

The scope of my research did not extend beyond the identification and functional characterization of *sso0563* (AtpA) and mutant variant associations with the kinase SsoPK4. However a case for SsoPK4 phosphoregulation of the *S. solfataricus* A_1A_O-ATPase can be conjectured. It was hypothesized that the Walker-threonine (Thr-240 of AtpA from *S. solfataricus*) may act allosterically by coupling nucleotide-binding with protein partner interactions (Nagy, Wu et al. 2009). Supporting evidence was obtained by means of mutational analysis of a member of the AAA+-ATPase (ATPases associated with various cellular activities) superfamily. Perhaps a similar allosteric regulation mechanism occurs at the plasma membrane via Thr-98 phosphorylation by SsoPK4.

The function of the *S. solfataricus* enzyme is to produce ATP *in vivo*. Phosphorylation of AtpA by SsoPK4 could regulate ATPase/ATP synthase activity in a manner accounting for the absence of the C-subunit found to be phosphorylated in V-

ATPase model systems. The phosphorylation of Thr-98 in the NHR could serve to inhibit or enhance the proton coupling efficiencies in the A_O sector through disturbances of protein-protein interactions. The coupling mechanism for ATP synthesis in A_1A_O-ATPases/ATP synthases remains largely unknown (Grüber and Marshansky 2008). We have seen that AtpA forms cross-links with AtpB, as expected, and also with AtpE. Isolation of an intact A_1A_O-ATPase from *S. solfataricus* membranes and incubation with SsoPK4 and radiolabeled ATP would provide more insight into the potential phosphorylation and regulation of this complex enzyme complex. Alternatively, cultures of *S. solfataricus* could be supplemented with radiolabeled ATP and the cells fractionated to determine if and where ^{32}P is incorporated in fractions containing ATPase activity. The identification of phosphorylated AtpA isolated from *S. solfataricus* cultures would lead the way to more involved *in vivo* studies.

Conclusion

The use of a genomic phage expression library has proved a useful tool in the identification of endogenous substrates for the *S. solfataricus* kinase SsoPK4. The ability to quickly screen a number of peptides derived from genomic DNA can help narrow the field of potential kinase substrates. Also, the library can be probed with other *S. solfataricus* protein kinases to elucidate other phosphoregulation pathways. Similar libraries can be constructed with other organisms of similar genome size with putative protein kinases. Even now, very few phosphorylated proteins with confirmed phosphoacceptor sites have been identified within the *Archaea* (Kirkland, Gil et al. 2008).

Of course, drawbacks do exist in using this method to identify protein kinase substrates. The potential for false-positive results due to frame-shift expression ruled out two of the potential ORFs identified from secondary library screening; the recombinant expression products of ORFs *sso1969* and *sso9378* were not radiolabeled after incubation with SsoPK4 and [γ-^{32}P]-ATP. Also the expression of library screen peptides lacks regulatory elements such as transcriptional or translational factors that would be present *in vivo*. However any hypothetical protein kinase substrates identified using other high-throughput techniques would need more thorough investigation to determine them as *bona fide* targets for phosphorylation.

So the caveat remains: any *in vitro* results need to be verified by *in vivo* studies. However, the results of my research show that 1) I was able to identify an endogenous substrate for SsoPK4 via library screening, 2) the substrate was an enzyme whose function could be characterized, and 3) the enzymatic activity of the potential substrate could be altered by substituting a negative charge at the threonine residue targeted by SsoPK4.

References

Abrahams, J. P., A. G. W. Leslie, et al. (1994). "Structure at 2.8 Â resolution of F1-ATPase from bovine heart mitochondria." Nature **370**: 621-628.

Arnold, K., L. Bordoli, et al. (2006). " The SWISS-MODEL Workspace: A web-based environment for protein structure homology modelling." Bioinformatics **22**: 195-201.

Ashman, K. and E. L. Villar (2009). "Phosphoproteomics and cancer research." Clinical & Translational Oncology **11**: 356-362.

Basu, A. and U. Sivaprasad (2007). "Protein kinase C[epsilon] makes the life and death decision." Cellular Signalling **19**(8): 1633-1642.

Berwick, D. C. and J. M. Tavare (2004). "Identifying protein kinase substrates: hunting for the organ-grinder's monkeys." Trends in Biochemical Sciences **29**(5): 227-232.

Bickel-Sandkötter, S., V. Wagner, et al. (1998). "ATP-synthesis in archaea: Structure-function relations of the halobacterial A-ATPase." Photosynthesis Research **57**(3): 335-345.

Biukovic, G., M. Rossle, et al. (2007). "Small-Angle X-ray Scattering Reveals the Solution Structure of the Peripheral Stalk Subunit H of the A1AO ATP Synthase from Methanocaldococcus jannaschii and Its Binding to the Catalytic A Subunit." Biochemistry **46**(8): 2070-2078.

Blenis, J. (1993). "Signal transduction via the MAP kinases: proceed at your own RSK." Proc Natl Acad Sci USA **90**: 5889-5892.

Boldyreff, B., F. Meggio, et al. (1994). "Efficient autophosphorylation and phosphorylation of the beta-subunit by casein kinase-2 require the integrity of an acidic cluster 50 residues downstream from the phosphoacceptor site." Journal of Biological Chemistry **269**(7): 4827-4831.

Bowman, E. J., K. Tenney, et al. (1988). "Isolation of genes encoding the Neurospora vacuolar ATPase. Analysis of vma-1 encoding the 67-kDa subunit reveals homology to other ATPases." Journal of Biological Chemistry **263**(28): 13994-14001.

Boyer, P. D., R. L. Cross, et al. (1973). "A New Concept for Energy Coupling in Oxidative Phosphorylation Based on a Molecular Explanation of the Oxygen Exchange Reactions." Proceedings of the National Academy of Sciences of the United States of America **70**(10): 2837-2839.

Bradford, M. M. (1976). "A rapid and sensitive method for the quantitation of microgram quantities of protein utilizing the principle of protein-dye binding." Analytical Biochemistry **72**: 248-254.

Bridges, A. J. (2005). "Therapeutic challenges of kinase and phosphatase inhibition and use in anti-diabetic strategy." Biochem. Soc. Trans. **33**(Pt 2): 343-345.

Bunney, T. D., H. S. van Walraven, et al. (2001). "14-3-3 protein is a regulator of the mitochondrial and chloroplast ATP synthase." Proceedings of the National Academy of Sciences of the United States of America **98**(7): 4249-4254.

Burgard, S., J. H. Nett, et al. (1994). "Effects of magnesium ions on the relative conformation of nucleotide binding sites of F1-ATPases as studied by electron spin resonance spectroscopy." Journal of Biological Chemistry **269**(27): 17815-17819.

Carnero, A. (2002). "Targeting the cell cycle for cancer therapy." Br J Cancer **87**(2): 129-133.

Chang, C., S. F. Kwok, et al. (1993). "Arabidopsis Ethylene-Response Gene ETR1: Similarity of Product to Two-Component Regulators." Science **262**(5133): 539-544.

Ciccarelli, F. D., T. Doerks, et al. (2006). "Toward Automatic Reconstruction of a Highly Resolved Tree of Life." Science **311**(5765): 1283-1287.

Cipriano, D. J., Y. Wang, et al. (2008). "Structure and regulation of the vacuolar ATPases." Biochimica et Biophysica Acta (BBA) - Bioenergetics **1777**(7-8): 599-604.

Cohen, P. (2002). "Protein kinases - the major drug targets of the twenty-first century?" Nat Rev Drug Discov **1**(4): 309-315.

Coskun, Ü., G. Grüber, et al. (2002). "Cross-talk in the A1-ATPase from Methanosarcina mazei Gö1 Due to Nucleotide Binding." Journal of Biological Chemistry **277**(19): 17327-17333.

Coskun, Ü., V. F. Rizzo, et al. (2004). "Ligand-Dependent Structural Changes in the V1 ATPase from Manduca sexta." Journal of Bioenergetics and Biomembranes **36**(3): 249-256.

Coulter-Mackie, M. B. and Q. Lian (2008). "Partial trypsin digestion as an indicator of mis-folding of mutant alanine:glyoxylate aminotransferase and chaperone effects of specific ligands. Study of a spectrum of missense mutants." Molecular Genetics and Metabolism **94**(3): 368-374.

Cozzone, A. J. (1998). "Post-translational modification of proteins by reversible phosphorylation in prokaryotes." Biochimie **80**(1): 43-48.

Davis, R. J. (1993). "The mitogen-activated protein kinase signal transduction pathway." J. Biol. Chem. **268**(20): 14553-14556.

Dixon, R., T. Eydmann, et al. (1991). "Substitutions at a single amino acid residue in the nitrogen-regulated activator protein NTRC differentially influence its activity in response to phosphorylation." Molecular Microbiology **5**(7): 1657-1667.

Du, M., R. L. S. Perry, et al. (2008). "Protein Kinase A Represses Skeletal Myogenesis by Targeting Myocyte Enhancer Factor 2D." Mol. Cell. Biol. **28**(9): 2952-2970.

Eckhart, W., M. A. Hutchinson, et al. (1979). "An activity phosphorylating tyrosine in polyoma T antigen immunoprecipitates." Cell **18**(4): 925-933.

Eichler, J. and M. W. W. Adams (2005). "Posttranslational Protein Modification in Archaea." Microbiol. Mol. Biol. Rev. **69**(3): 393-425.

Fairbanks, G., T. L. Steck, et al. (1971). "Electrophoretic transfer of the major polypeptides of the human erythrocyte membrane." Biochemistry **10**: 2606-2617.

Feilner, T., C. Hultschig, et al. (2005). "High Throughput Identification of Potential Arabidopsis Mitogen-activated Protein Kinases Substrates." Mol Cell Proteomics **4**(10): 1558-1568.

Fischer, E. H. and E. G. Krebs (1955). "Conversion of phosphorylase b to phosphorylase a in muscle extracts." Journal of Biological Chemistry **216**(1): 121-132.

Forgac, M. (1999). "Structure and Properties of the Vacuolar (H+)-ATPases." Journal of Biological Chemistry **274**(19): 12951-12954.

Fukunaga, R. and T. Hunter (1997). "MNK1, a new MAP kinase-activated protein kinase, isolated by a novel expression screening method for identifying protein kinase substrates." EMBO J **16**(8): 1921-1933.

Fukunaga, R., Hunter, T. (1997). " MNK1, a new MAP kinase-activated protein kinase, isolated by a novel expression screening method for identifying protein kinase substrates." The EMBO Journal **16**(8): 1921-1933.

Futai, M., G.-H. Sun-Wada, et al. (2004). Proton Translocating ATPases: Introducing Unique Enzymes Coupling Catalysis and Proton Translocation through Mechanical Rotation. Handbook of ATPases: biochemistry, cell biology, pathophysiology. Weinheim, Wiley-VCH**:** 235-260.

Garnak, M. and H. C. Reeves (1979). "Phosphorylation of Isocitrate Dehydrogenase of Escherichia coli." Science **203**(4385): 1111-1112.

Grüber, G. and V. Marshansky (2008). "New insights into structure-function relationships between archeal ATP synthase (A1A0) and vacuolar type ATPase (V1V0)." BioEssays **30**(11-12): 1096-1109.

Gruber, G., H. Wieczorek, et al. (2001). "Structure-function relationships of A-, F- and V-ATPases." J Exp Biol **204**(15): 2597-2605.

Hanks, S. (2003). "Genomic analysis of the eukaryotic protein kinase superfamily: a perspective." Genome Biology **4**(5): 111.

Hanks, S. K. and T. Hunter (1995). "Protein kinases 6. The eukaryotic protein kinase superfamily: kinase (catalytic) domain structure and classification." FASEB J. **9**(8): 576-596.

Hanks, S. K., A. M. Quinn, et al. (1988). "The Protein Kinase Family: Conserved Features and Deduced Phylogeny of the Catalytic Domains." Science **241**(4861): 42-52.

Häsler, K., S. Engelbrecht, et al. (1998). "Three-stepped rotation of subunits [gamma] and [epsilon] in single molecules of F-ATPase as revealed by polarized, confocal fluorometry." FEBS Letters **426**(3): 301-304.

Hicks, D. B. and T. A. Krulwich (1986). "The membrane ATPase of alkalophilic Bacillus firmus RAB is an F1-type ATPase." Journal of Biological Chemistry **261**(27): 12896-12902.

Hilario, E. and J. P. Gogarten (1998). "The Prokaryote-to-Eukaryote Transition Reflected in the Evolution of the V/F/A-ATPase Catalytic and Proteolipid Subunits." Journal of Molecular Evolution **46**(6): 703-715.

Højlund, K., K. Wrzesinski, et al. (2003). "Proteome Analysis Reveals Phosphorylation of ATP Synthase ¢E -Subunit in Human Skeletal Muscle and Proteins with Potential Roles in Type 2 Diabetes." Journal of Biological Chemistry **278**(12): 10436-10442.

Hong-Hermesdorf, A., A. Brüx, et al. (2006). "A WNK kinase binds and phosphorylates V-ATPase subunit C." FEBS Letters **580**(3): 932-939.

Huang, S. Y., M. L. Tsai, et al. (2007). "A Systematic MS-Based Approach for Identifying in vitro Substrates of PKA and PKG in Rat Uteri." J. Proteome Res. **6**(7): 2674-2684.

Hunter, T. (1995). "Protein kinases and phosphatases: The Yin and Yang of protein phosphorylation and signaling." Cell **80**(2): 225-236.

Jefferies, K. C., D. J. Cipriano, et al. (2008). "Function, structure and regulation of the vacuolar (H+)-ATPases." Archives of Biochemistry and Biophysics **476**(1): 33-42.

Johnson, S. A. and T. Hunter (2005). "Kinomics: methods for deciphering the kinome." Nat Meth **2**(1): 17-25.

Kannan, N., S. S. Taylor, et al. (2007). "Structural and Functional Diversity of the Microbial Kinome." PLoS Biol **5**(3): e17.

Kayalar, C., J. Rosing, et al. (1977). "An alternating site sequence for oxidative phosphorylation suggested by measurement of substrate binding patterns and exchange reaction inhibitions." Journal of Biological Chemistry **252**(8): 2486-2491.

Kennelly, P. and M. Potts (1996). "Fancy meeting you here! A fresh look at "prokaryotic" protein phosphorylation." J. Bacteriol. **178**(16): 4759-4764.

Kennelly, P., M. Starovasnik, et al. (1990). "Modulation of the stability of rabbit skeletal muscle myosin light chain kinase through the calmodulin-binding domain." J. Biol. Chem. **265**(3): 1742-1749.

Kennelly, P. J. (1999). Bits for an organic microprocessor. Introduction to Cellular Signal Transduction. A. Sitaramayya. Boston, Birkhauser 235-264.

Kennelly, P. J. (2003). "Archaeal protein kinases and protein phosphatases: insights from genomics and biochemistry." Biochem J **370**(Pt2): 373-389.

Kennelly, P. J. (2007). Sensing, Signal Transduction, and Posttranslational Modification. Archaea: Molecular and Cellular Biology. R. Caviccioli. Washington, D.C., ASM Press**:** 224-259.

Kiefer, F., K. Arnold, et al. (2009). "The SWISS-MODEL Repository and associated resources." Nucleic Acids Research **37**: D387-D392.

Kirkland, P. A., M. A. Gil, et al. (2008). "Genetic and Proteomic Analyses of a Proteasome-Activating Nucleotidase A Mutant of the Haloarchaeon Haloferax volcanii." J. Bacteriol. **190**(1): 193-205.

Kish-Trier, E., L.-A. K. Briere, et al. (2008). "The Stator Complex of the A1A0-ATP Synthase--Structural Characterization of the E and H Subunits." Journal of Molecular Biology **375**(3): 673-685.

Kish-Trier, E. and S. Wilkens (2009). "Domain Architecture of the Stator Complex of the A1A0-ATP Synthase from Thermoplasma acidophilum." J. Biol. Chem. **284**(18): 12031-12040.

Kostich, M., J. English, et al. (2002). "Human members of the eukaryotic protein kinase family." Genome Biology **3**(9): research0043.1 - research0043.12.

Kumar, A., M. S. S. Manimekalai, et al. (2010). "Nucleotide Binding States of Subunit A of the A-ATP Synthase and the Implication of P-Loop Switch in Evolution." Journal of Molecular Biology **396**(2): 301-320.

Kumar, A., M. S. S. Manimekalai, et al. (2008). "Structure of the nucleotide-binding subunit B of the energy producer A1A0 ATP synthase in complex with adenosine diphosphate." Acta Crystallographica Section D **64**(11): 1110-1115.

Kuo, J. F. and P. Greengard (1969). "An Adenosine 3',5'-Monophosphate-dependent Protein Kinase from Escherichia coli." Journal of Biological Chemistry **244**(12): 3417-3419.

Laemmli, U. K. (1970). "Cleavage of structural proteins during the assembly of the head of bacteriophage T4." Nature **227**(5259): 680-685.

Lanzetta, P. A., L. J. Alvarez, et al. (1979). "An improved assay for nanomole amounts of inorganic phosphate." Analytical Biochemistry **100**(1): 95-97.

Lee, C.-H., C.-Y. Lee, et al. (2008). "PKA-mediated phosphorylation is a novel mechanism for levetiracetam, an antiepileptic drug, activating ROMK1 channels." Biochemical Pharmacology **76**(2): 225-235.

Lemker, T., C. Ruppert, et al. (2001). "Overproduction of a functional A1 ATPase from the archaeon Methanosarcina mazei Gö1 in Escherichia coli." European Journal of Biochemistry **268**(13): 3744-3750.

Leonard, C. J., L. Aravind, et al. (1998). "Novel Families of Putative Protein Kinases in Bacteria and Archaea: Evolution of the ‚ÄúEukaryotic‚Äù Protein Kinase Superfamily." Genome Research **8**(10): 1038-1047.

Levitzki, A. (2003). "Protein Kinase Inhibitors as a Therapeutic Modality." Acc. Chem. Res. **36**(6): 462-469.

Lewalter, K. and V. Müller (2006). "Bioenergetics of archaea: Ancient energy conserving mechanisms developed in the early history of life." Biochimica et Biophysica Acta (BBA) - Bioenergetics **1757**(5-6): 437-445.

Liu, X., M. L. Godwin, et al. (2004). "Protein kinase C-{alpha} inhibits the repair of oxidative phosphorylation after S-(1,2-dichlorovinyl)-L-cysteine injury in renal cells." Am J Physiol Renal Physiol **287**(1): F64-73.

Lower, B. H. and P. J. Kennelly (2003). "Open Reading Frame sso2387 from the Archaeon Sulfolobus solfataricus Encodes a Polypeptide with Protein-Serine Kinase Activity." J. Bacteriol. **185**(11): 3436-3445.

Lower, B. H., M. B. Potters, et al. (2004). "A Phosphoprotein from the Archaeon Sulfolobus solfataricus with Protein-Serine/Threonine Kinase Activity." J. Bacteriol. **186**(2): 463-472.

Maeda, T., S. M. Wurgler-Murphy, et al. (1994). "A two-component system that regulates an osmosensing MAP kinase cascade in yeast." Nature **369**(6477): 242-245.

Maegawa, Y., H. Morita, et al. (2006). "Structure of the catalytic nucleotide-binding subunit A of A-type ATP synthase from Pyrococcus horikoshii reveals a novel

domain related to the peripheral stalk." Acta Crystallographica Section D **62**(5): 483-488.

Mahoney, C. W., N. Nakanishi, et al. (1996). "Phosphoamino Acid Analysis by Semidry Electrophoresis on Cellulose Thin-Layer Plates Using the Pharmacia/LKB Multiphor or Atto Flatbed Apparatus." Analytical Biochemistry **238**(1): 96-98.

Manning, G., D. B. Whyte, et al. (2002). "The Protein Kinase Complement of the Human Genome." Science **298**(5600): 1912-1934.

Martin, J. B. and D. M. Doty (1949). "Determination of Inorganic Phosphate." Analytical Chemistry **21**(8): 965-967.

McCarty, R. E. and E. Racker (1968). "Partial Resolution of the Enzymes Catalyzing Photophosphorylation." Journal of Biological Chemistry **243**(1): 129-137.

Mulkidjanian, A. Y., K. S. Makarova, et al. (2007). "Inventing the dynamo machine: the evolution of the F-type and V-type ATPases." Nat Rev Micro **5**(11): 892-899.

Müller, V., Grüber, G. (2003). "ATP synthases: structure, function and evolution of unique energy converters." CMLS **60**(3): 474-494.

Nagy, M., H.-C. Wu, et al. (2009). "Walker-A threonine couples nucleotide occupancy with the chaperone activity of the AAA+ ATPase ClpB." Protein Science **18**(2): 287-293.

Nelson, N. (1992). "Evolution of organellar proton-ATPases." Biochimica et Biophysica Acta (BBA) - Bioenergetics **1100**(2): 109-124.

Noji, H., R. Yasuda, et al. (1997). "Direct observation of the rotation of F1-ATPase." Nature **386**(6622): 299-302.

Olsen, G. J., Woese, C. R. (1997). "Archaeal Genomics: An Overview." Cell **89**(7): 991-994.

Ota, I. M. and A. Varshavsky (1993). "A Yeast Protein Similar to Bacterial Two-Component Regulators." Science **262**(5133): 566-569.

Pei, Y. and S. Shuman (2003). "Characterization of the Schizosaccharomyces pombe Cdk9/Pch1 Protein Kinase." Journal of Biological Chemistry **278**(44): 43346-43356.

Peitsch, M. C. (1995). "Protein modeling by E-mail Bio/Technology." **13**: 658-660.

Pertseva, M. and A. Shpakov (2009). "The Prokaryotic Origin and Evolution of Eukaryotic Chemosignaling Systems." Neuroscience and Behavioral Physiology **39**(8): 793-804.

Popov, K. M., Y. Zhao, et al. (1992). "Branched-chain alpha-ketoacid dehydrogenase kinase. Molecular cloning, expression, and sequence similarity with histidine protein kinases." Journal of Biological Chemistry **267**(19): 13127-13130.

Raman, M., W. Chen, et al. (2007). "Differential regulation and properties of MAPKs." Oncogene **26**(22): 3100-3112.

Ray, W. K., S. M. Keith, et al. (2005). "A Phosphohexomutase from the Archaeon Sulfolobus solfataricus Is Covalently Modified by Phosphorylation on Serine." J. Bacteriol. **187**(12): 4270-4275.

Roach, P. (1991). "Multisite and hierarchal protein phosphorylation." J Biol Chem **266**(22): 14139-14142.

Sambrook, J., E. F. Fritsch, et al. (1989). Molecular Cloning: A Laboratory Manual. Cold Spring Harbor, N.Y., Cold Spring Harbor Laboratory Press.

Schacter, E. (1984). "Organic extraction of Pi with isobutanol/toluene." Analytical Biochemistry **138**(2): 416-420.

Schäfer, G. (1996). "Bioenergetics of the archaebacterium Sulfolobus." Biochim Biophys Acta. **1277**(3): 163-200.

Schafer, G., M. Engelhard, et al. (1999). "Bioenergetics of the Archaea." Microbiol. Mol. Biol. Rev. **63**(3): 570-620.

Schäfer, I., M. Rössle, et al. (2006). "Structural and functional analysis of the coupling subunit F in solution and topological arrangement of the stalk domains of the methanogenic A1AO ATP synthase." Journal of Bioenergetics and Biomembranes **38**(2): 83-92.

Schoenhofen, I. C., G. Li, et al. (2005). "Purification and Characterization of the N-Terminal Domain of ExeA: a Novel ATPase Involved in the Type II Secretion Pathway of Aeromonas hydrophila." J. Bacteriol. **187**(18): 6370-6378.

Shao, E. and M. Forgac (2004). "Involvement of the Nonhomologous Region of Subunit A of the Yeast V-ATPase in Coupling and in Vivo Dissociation." Journal of Biological Chemistry **279**(47): 48663-48670.

Shao, E., T. Nishi, et al. (2003). "Mutational Analysis of the Non-homologous Region of Subunit A of the Yeast V-ATPase." Journal of Biological Chemistry **278**(15): 12985-12991.

She, Q., R. K. Singh, et al. (2001). "The complete genome of the crenarchaeon Sulfolobus solfataricus P2." Proceedings of the National Academy of Sciences of the United States of America **98**(14): 7835-7840.

Shevchenko, A., M. Wilm, et al. (1996). "Mass Spectrometric Sequencing of Proteins from Silver-Stained Polyacrylamide Gels." Analytical Chemistry **68**(5): 850-858.

Shi, L., M. Potts, et al. (1998). "The serine, threonine, and/or tyrosine-specific protein kinases and protein phosphatases of prokaryotic organisms: a family portrait." FEMS Microbiology Reviews **22**(4): 229-253.

Skorko, R. (1984). "Protein phosphorylation in the Archaebacterium *Sulfolobus acidocaldarius*." European Journal of Biochemistry **145**(3): 617-622.

Smith, R. F. and K. Y. King (1995). "Identification of a eukaryotic-like protein kinase gene in Archaeabacteria." Protein Science **4**(1): 126-129.

Smith, S., P. Kennelly, et al. (1997). "Protein-tyrosine phosphorylation in the Archaea." J. Bacteriol. **179**(7): 2418-2420.

Sopko, R. and B. Andrews (2008). "Linking the kinome and phosphorylome - a comprehensive review of approaches to find kinase targets." Molecular BioSystems **4**: 920-933.

Turk, B. E. (2008). "Understanding and exploiting substrate recognition by protein kinases." Current Opinion in Chemical Biology **12**(1): 4-10.

Voss, M., O. Vitavska, et al. (2007). "Stimulus-induced Phosphorylation of Vacuolar H+-ATPase by Protein Kinase A." Journal of Biological Chemistry **282**(46): 33735-33742.

Walsh, D. A., C. O. Brostrom, et al. (1972). "Cyclic AMP-dependent protein kinases from skeletal muscle and liver." Adv Cyclic Nucleotide Res **1**: 33-45.

Walsh, D. A., J. P. Perkins, et al. (1968). "An Adenosine 3',5'-Monophosphate-dependant Protein Kinase from Rabbit Skeletal Muscle." Journal of Biological Chemistry **243**(13): 3763-3765.

Wang, J.-Z., I. Grundke-Iqbal, et al. (2007). "Kinases and phosphatases and tau sites involved in Alzheimer neurofibrillary degeneration." European Journal of Neuroscience **25**(1): 59-68.

Wang, J. Y. and D. E. Koshland (1978). "Evidence for protein kinase activities in the prokaryote Salmonella typhimurium." Journal of Biological Chemistry **253**(21): 7605-7608.

Westheimer, F. H. (1987). "Why nature chose phosphates." Science **v235**: p1173(6).

Whitman, W. B. (2009). "The Modern Concept of the Procaryote." J. Bacteriol. **191**(7): 2000-2005.

Wieczorek, H., D. Brown, et al. (1999). "Animal plasma membrane energization by proton-motive V-ATPases." BioEssays **21**(8): 637-648.

Wilkens, S. (2001). "Structure of the Vacuolar Adenosine Triphosphates." Cell Biochemistry and Biophysics **34**(2): 191-208.

Woese, C. R. and G. E. Fox (1977). "Phylogenetic structure of the prokaryotic domain: the primary kingdoms." Proceedings of the National Academy of Sciences of the United States of America **74**(11): 5088-5090.

Woese, C. R., O. Kandler, et al. (1990). "Towards a natural system of organisms: proposal for the domains Archaea, Bacteria, and Eucarya." Proc Natl Acad Sci U S A **87**(12): 4576-4579.

Yaffe, M. B. and A. E. H. Elia (2001). "Phosphoserine/threonine-binding domains." Current Opinion in Cell Biology **13**(2): 131-138.

Yohda, M., S. Ohta, et al. (1988). "Site-directed mutagenesis of stable adenosine triphosphate synthase." Biochimica et Biophysica Acta (BBA) - Bioenergetics **933**(1): 156-164.

Zhang, H., X. Zha, et al. (2002). "Phosphoprotein Analysis Using Antibodies Broadly Reactive against Phosphorylated Motifs." J. Biol. Chem. **277**(42): 39379-39387.

Zhang, W., J. Munoz-Dorado, et al. (1992). "Identification of a putative eukaryotic-like protein kinase family in the developmental bacterium Myxococcus xanthus." J. Bacteriol. **174**(16): 5450-5453.

Zimniak, L., P. Dittrich, et al. (1988). "The cDNA sequence of the 69-kDa subunit of the carrot vacuolar H+-ATPase. Homology to the beta-chain of F0F1-ATPases." Journal of Biological Chemistry **263**(19): 9102-9112.

Appendix A:

Mass Spectrometry Methods and Data

Sample Preparation for MS Analysis

Recombinant protein samples submitted in SDS-/native-polyacrylamide gels, were prepared at the Virginia Tech Mass Spectrometry Incubator (http://www.mass.biochem.vt.edu/) according to the following standard protocol:

Coomassie-stained gel bands of interest were excised from the polyacrylamide gel and cut into approximately 1-mm^3 slices using a fresh razor blade. The gel slices were placed into sterile microfuge tubes and destained using 2 x 2hr washes in 25 mM 1:1 ammonium bicarbonate:acetonitrile. During each wash the microfuge tubes containing the gel pieces were vortexed vigorously. Following the second wash the gel slices were dehydrated in acetonitrile, the tube placed on ice, and the gel slices rehydrated with enough 10 ng/µl trypsin in 25 mM ammonium bicarbonate to cover the gel fragments. The digestion reaction was incubated 16-18 hours at 37°C.

Samples were then collected by centrifugation and the digestion solution was transferred to fresh microfuge tubes that had been rinsed with acetonitrile. To increase peptide recovery, 50% (v/v) acetonitrile supplemented with 0.2% (v/v) trifluoroacetic acid (TFA) was added to the gel pieces and then sonicated in a water bath for 15 minutes. This solution was then added to the first and mixed thoroughly. When necessary, digests were desalted and concentrated using Varian OMIX C18 microextraction pipette tips (Palo Alto, CA) following the manufacturer's protocol prior to MALDI analysis. Approximately 1 µl of each digest was spotted onto a MALDI target plate and allowed to air dry. The sample was then overlaid with approximately 1 µl

matrix consisting of 4 mg/ml α-cyano-4-hydroxy cinnamic acid in 50% (v/v) acetonitrile supplemented with 0.2% (v/v) TFA and 20 mM ammonium citrate.

Data Analysis

Dr. Keith Ray at the Mass Spectrometry Incubator performed all data analysis on peptides. For protein-protein interactions identified from SDS-polyacrylamide gels (Chapter IV, Figure 4-11) and native-polyacrylamide gels (Chapter V, Figure 5-12) the following technical specifications were employed. Protein identifications were obtained by searching the peak lists versus a protein database containing only the amino acid sequences for the recombinant proteins AtpA, AtpB, AtpE and AtpG using the Mascot search engine (Matrix Science Inc, Boston, MA). The searches were limited using the following parameters: trypsin protease specificity with up to two missed cleavages, peptide mass tolerance ±200 ppm with the possible modification of methionine by oxidation and when utilized, a peptide fragment mass tolerance of ±0.2 Da.

The digests were analyzed using a 4800 MALDI TOF/TOF mass spectrometry instrument from Applied Biosystems (Foster City, CA). First, an MS spectrum was collected for each digest in reflector positive operating mode for the mass to charge range of 800 to 4000. This was performed in order to accumulate approximately 1000 individual laser shots to yield one MS spectrum per digest. Then, where indicated, MSMS data was collected for the top 16 peaks from each digest above a set signal to noise threshold using the MSMS 1kV positive operating mode. Each MSMS spectrum was typically the sum of approximately 1500 individual laser shots. A peak list for each digest containing information from both the MS and MSMS spectra (if acquired) was generated using the 4000 Explorer software from Applied Biosystems.

As the polyacrylamide gel samples contained proteins of known identity, peptide mass fingerprint (PMF) results were sufficient for protein identifications. The peptides identified in EDC cross-link bands are displayed in Table A-1. Due to the small molecular weight of AtpG it was difficult to observe sufficient peptide fragments for a Mascot PMF score of significance. The presence of AtpG was therefore determined by MSMS on the peak corresponding to the tryptic peptide "YLQILR" which corresponds to amino acids 5-11 of the 52 amino acid sequence:

mdqdk**ylqilr**nsleekkseilkninmeye kllknrlsqldevkrkvlkels

The peptides identified from native-PAGE are shown in Table A-2. The MS spectrum for the band isolated from Lane 6 was carefully checked for any signs of peptides originating from subunit AtpB; however, none were observed. Protein and/or peptide identifications corresponding to $p<0.05$ were considered significant.

For the identification of phosphoresidue Thr-98 on AtpA-T, the small molecular weight components of the kinase reaction were first removed by methanol precipitation of the proteins followed by several methanol washes of the resulting pellet. The pellet was resuspended in 10 ng/µl trypsin in 25 mM ammonium bicarbonate at a protease to substrate ratio of 1:50 (w/w) and the digestion reaction was incubated 16-18 hours at 37°C. The digest was subsequently desalted and concentrated using a Varian OMIX C18 microextraction pipette tip (Palo Alto, CA) following the manufacturer's protocol prior to MALDI analysis. MALDI analysis was performed as described above. The MSMS spectrum and the observed peptide fragment ions verifying the site of phosphorylation are displayed in Figure A-1. The phosphopeptide containing pThr-98 had a Mascot score of 58.

Band	Protein(s) Detected	Mascot PMF Score	Number of Matching Peptides	Sequence Coverage (%)	Peptide Mass RMS Error (ppm)	AtpG "YLQILR" peptide detected by MSMS?
a	AtpA	115	24	46	62	No
b	AtpA	82	19	40	27	Yes
c	AtpA	97	25	45	58	No
	AtpB	58	15	41	65	"
e	AtpB	66	15	38	60	Yes
f	AtpE	16	4	21	82	Yes

Table A-1. MS-identification results for EDC cross-linked protein bands isolated from a SDS-polyacrylamide gel. The labels "a, b, c, e, f" in the first column refer to the corresponding Coomassie-stained protein products within the SDS-polyacrylamide gel in Figure 4-11.

Lane	Protein(s) Detected	Mascot PMF Score	Number of Matching Peptides	Sequence Coverage (%)	Peptide Mass RMS Error (ppm)
5: *A(s)-B*	AtpA	223	21	46	162
	AtpB	64	8	22	156
6: *T98D-B*	AtpA	228	22	46	171
7: *A-B*	AtpA	170	20	43	168
	AtpB	108	13	38	169

Table A-2. MS-identification results for AtpA and AtpB protein interactions. Lane numbers 5, 6, and 7 in first column correlate to native-PAGE lanes designated in Figure 5-12. It was determined that Lane 5 contained both AtpA (AtpA with S-tag variant) and AtpB. Lane 6 contained only AtpA (T98D), and Lane 7 contained AtpA (WT) and AtpB.

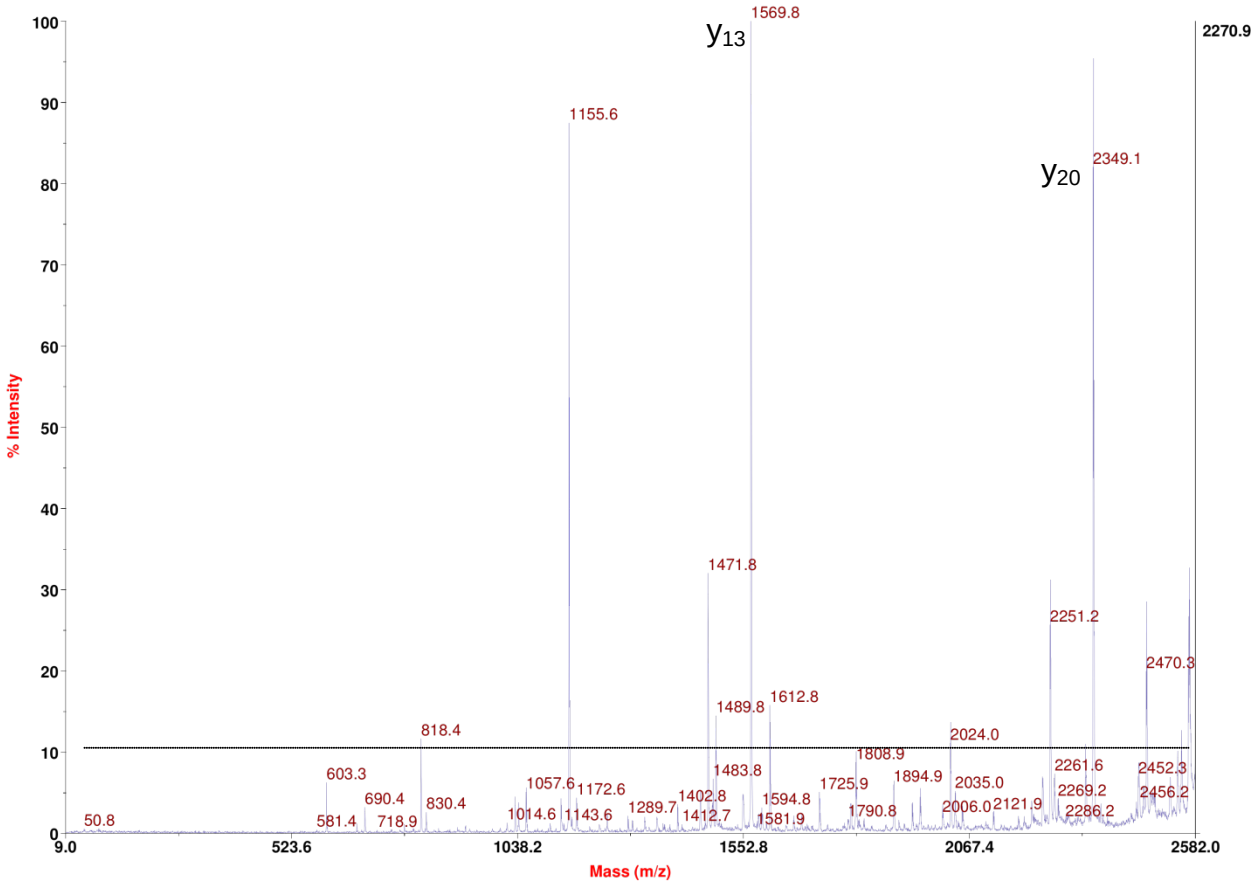

Figure A-1. Identification of phosphothreonine at residue 98 on AtpA from *Sulfolobus solfataricus* P2. Shown is the MS/MS fragmentation of the $[M+H^+]^+$ ion of the phosphopeptide IFDGLQRPLDSIKELpTKSPFIAR (2724.32). Observable –y and –b ion series fragments that validate the site of phosphorylation and peptide amino acid sequence are highlighted in red in Table A-3; these ion peaks appear above the dashed line, denoting a >10% identity match. Peaks y_{13} and y_{20} indicate retention of phosphate on Thr-98 (Δ m/z = 83).

#	b-H3PO4	b	Seq.	y-H3PO4	y	#
1	114.0913	114.0913	I			23
2	261.1598	261.1598	F	2513.3875	2611.3644	22
3	376.1867	376.1867	D	2366.319	2464.296	21
4	433.2082	433.2082	G	2251.2921	2349.269	20
5	546.2922	546.2922	L	2194.2706	2292.2475	19
6	674.3508	674.3508	Q	2081.1866	2179.1635	18
7	830.4519	830.4519	R	1953.128	2051.1049	17
8	927.5047	927.5047	P	1797.0269	1895.0038	16
9	1040.5887	1040.5887	L	1699.9741	1797.951	15
10	1155.6157	1155.6157	D	1586.8901	1684.867	14
11	1242.6477	1242.6477	S	1471.8631	1569.84	13
12	1355.7318	1355.7318	I	1384.8311	1482.808	12
13	1483.8267	1483.8267	K	1271.747	1369.7239	11
14	1612.8693	1612.8693	E	1143.6521	1241.629	10
15	1725.9534	1725.9534	L	1014.6095	1112.5864	9
16	1808.9905	1906.9674	pT	901.5254	999.5023	8
17	1937.0855	2035.0624	K	818.4883	818.4883	7
18	2024.1175	2122.0944	S	690.3933	690.3933	6
19	2121.1703	2219.1472	P	603.3613	603.3613	5
20	2268.2387	2366.2156	F	506.3085	506.3085	4
21	2381.3227	2479.2996	I	359.2401	359.2401	3
22	2452.3599	2550.3368	A	246.1561	246.1561	2
23			R	175.119	175.119	1

Table A-3. MS/MS ion fragments (–y and –b) generated from phosphopeptide: IFDGLQRPLDSIKELpTKSPFIAR. Columns b- and y-H3PO4 contain ions detected using the Mascot database where the modified threonine is reported as a neutral loss of phosphoric acid (Δ m/z = 98). Columns b and y list ions detected using the ProteinProspector web database (University of San Francisco, CA) where the phosphate is retained on the residue (Δ m/z = 83). Shown highlighted in red are ions with greater than 10% identity matches. "Seq." column refers to phosphopeptide sequence of AtpA.

Appendix B:

Oligonucleotide Primers for Site-directed Mutagenesis of AtpA

Site-directed mutagenesis procedures are outlined in Chapter II: Materials and Methods. The following table of primers was used to clone AtpA mutant variants in the pET-vector system for overexpression of recombinant proteins. Underlined segments refer to the new codon generated by PCR-amplification of the plasmid template with mutagenesic primers. Refer to Chapter III, Figure 3-5, for the nucleotide sequence of wild-type AtpA. SsoPK4 kinase activity assay and ATPase assay results using the mutant variants are discussed in Chapter V. In Table B-1 on the next two pages, "-x" refers to primer annealing direction: F, forward (5' - 3'), R, reverse (5' - 3', reverse complement).

Variant	Primer	Oligonucleotide Sequence (5'-3')	Template
T158A	T158A-F	CCTCCCTATGTTCACGGCGCCTTAAAGGAAGTC	AtpA
	T158A-R	GACTTCCTTTAAGGCGCCGTGAACATAGGGAGG	
T158D	T158D-R	CCTCCCTATGTTCACGGCGACTTAAAGGAAGTC	AtpA
	T158D-R	GACTTCCTTTAAGTCGCCGTGAACATAGGGAGG	
T169A	T169A-F	GCAGAGGGAGATTATGCAGTTGAAGATCCGATA	AtpA
	T169A-R	TATCGGATCTTCAACTGCATAATCTCCCTCTGC	
T169D	T169D-F	GCAGAGGGAGATTATGACGTTGAAGATCCGATA	AtpA
	T169D-R	TATCGGATCTTCAACGTCATAATCTCCCTCTGC	
T→Adm	T169A-F	GCAGAGGGAGATTATGCAGTTGAAGATCCGATA	T158A
	T169A-R	TATCGGATCTTCAACTGCATAATCTCCCTCTGC	
T→Ddm	T158D-F	CCTCCCTATGTTCACGGCGACTTAAAGGAAGTC	T169D
	T158D-R	GACTTCCTTTAAGTCGCCGTGAACATAGGGAGG	
T40A	T40A-F	GAGCCTAGATTAATCGGAGAGATTGCTAGAATAGAAGGAGAT	AtpA
	T40A-R	ATCTCCTTCTATTCTAGCAATCTCTCCGATTAATCTAGGCTC	
T40D	T40D-F	GAGCCTAGATTAATCGGAGAGATTGATAGAATAGAAGGAGAT	AtpA
	T40D-R	ATCTCCTTCTATTCTATCAATCTCTCCGATTAATCTAGGCTC	
T98A	T98A-F	CCACTAGACTCAATCAAAGAGCTCGCAAAATCTCCTTTTATAGCA	AtpA
	T98A-R	TGCTATAAAAGGAGATTTTGCGAGCTCTTTGATTGAGTCTAGTGG	
T98D	T98D-F	CCACTAGACTCAATCAAAGAGCTCGACAAATCTCCTTTTATAGCA	AtpA
	T98D-R	TGCTATAAAAGGAGATTTGTCGAGCTCTTTGATTGAGTCTAGTGG	
T4098D	T98D-F	CCACTAGACTCAATCAAAGAGCTCGACAAATCTCCTTTTATAGCA	T40D
	T98D-R	TGCTATAAAAGGAGATTTGTCGAGCTCTTTGATTGAGTCTAGTGG	
T240A	T240A-F	GGAAGTGGAAAAGCAGTCACATTGCAGAGTTTA	AtpA
	T240A-R	TAAACTCTGCAATGTGACTGCTTTTCCACTTCC	
D330A	D330A-F	ACATTACTAGTTGCAGCTTCAACTTCGAGATGGGCT	AtpA
	D330A-R	AGCCCATCTCGAAGTTGAAGCTGCAACTAGTAATGT	
R263G	R263G-F	TATGTGGGATGTGGTGAGGGAGGAAACGAGATG	AtpA
	R263G-R	CATCTCGTTTCCTCCCTCACCACATCCCACATA	
E266A	E266A-F	TGTGGTGAGAGAGGAAACGCGATGACAGATGAGTTA	AtpA
	E266A-R	TAACTCATCTGTCATCGCGTTTCCTCTCTCACCACA	
A-T dm	AtpA-F	TAAGTAACCATGGATAATGGAAGGATTGTCAGGATA	T40/98D
	T-AtpAR	AGCTATGTCGACTATCGTATCCAGTACTCTGGTTCC	
TripM	T240A-F	GGAAGTGGAAAAGCAGTCACATTGCAGAGTTTA	T40/98D
	T240A-R	TAAACTCTGCAATGTGACTGCTTTTCCACTTCC	

Table B-1. List of oligonucleotide primers used in site-directed mutagenesis of AtpA variants.

Appendix C:

Fair Use and Public Domain Figure Citations

Figure 1-1..... [used with permission]
File:Simplified tree.png. *Wikimedia Commons*. http://commons.wikimedia.org/wiki/File:Simplified_tree.pngkimedia.org/w/index.php?title=Main_Page&oldid=36978449 (accessed Feb. 10, 2010) Licensing attached.

Figure 1-2. ..... [used with permission]
Kannan, Taylor et al. (2007) "Structural and Functional Diversity of the Microbial Kinome." *PLoS Biol* 5(3):e17. http://dx.doi.org/10.1371%2Fjournal.pbio.0050017 (accessed Feb. 10, 2010) Licensing attached.

Figure 3-3..... [used with permission]
Lambda ZAP II Predigested EcoR I/CIAP-Treated Vector Kit Instruction Manual. Figure 2, page 4. Used with permission per email attached from Kevin White, Stratagene/Agilent.

Figure 4-1AB. .....[fair use]
Grüber, G. and V. Marshansky (2008). "New insights into structure-function relationships between archeal ATP synthase (A1A0) and vacuolar type ATPase (V1V0)." BioEssays **30**(11-12): 1096-1109. http://dx.doi.org/10.1002/bies.20827 (accessed Mar. 5, 2010) Fair use determination attached.

Figure 4-1C.....[fair use]
Kish-Trier, E., L.-A. K. Briere, et al. (2008). "The Stator Complex of the A1A0-ATP Synthase--Structural Characterization of the E and H Subunits." Journal of Molecular Biology **375**(3): 673-685. http://www.sciencedirect.com/science/article/B6WK7-4R1KVXS-5/2/830e95443ad38b016219992caa2047e9 (accessed Mar. 3, 2010) Fair use determination attached.

Figure 4-2.....[fair use]
Kumar, A., M. S. S. Manimekalai, et al. (2010). "Nucleotide Binding States of Subunit A of the A-ATP Synthase and the Implication of P-Loop Switch in Evolution." Journal of Molecular Biology

396(2): 301-320. http://www.sciencedirect.com/science/article/B6WK7-4XSTDC1-1/2/a4fef764476b10b00a82dcf268a19469 (accessed Mar. 3, 2010) Fair use determination attached.

Figure 6-1. .....[fair use]
Maegawa, Y., H. Morita, et al. (2006). "Structure of the catalytic nucleotide-binding subunit A of A-type ATP synthase from Pyrococcus horikoshii reveals a novel domain related to the peripheral stalk." Acta Crystallographica Section D **62**(5): 483-488. http://dx.doi.org/10.1107/S0907444906006329 (accessed Mar. 5, 2010) Fair use determination attached.

Figure 1-1. License:

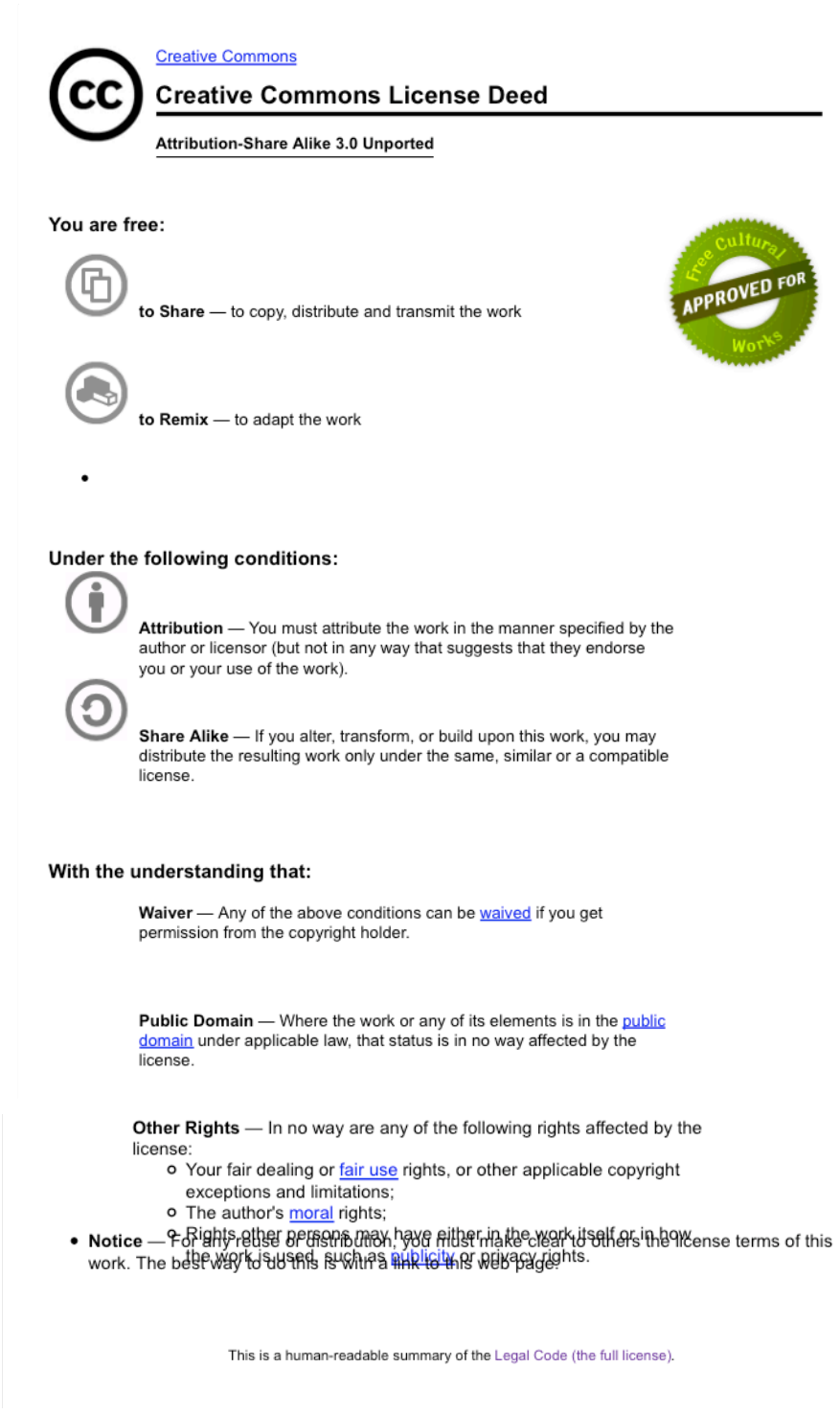

Creative Commons

Creative Commons License Deed

Attribution-Share Alike 3.0 Unported

You are free:

to Share — to copy, distribute and transmit the work

to Remix — to adapt the work

Under the following conditions:

Attribution — You must attribute the work in the manner specified by the author or licensor (but not in any way that suggests that they endorse you or your use of the work).

Share Alike — If you alter, transform, or build upon this work, you may distribute the resulting work only under the same, similar or a compatible license.

With the understanding that:

Waiver — Any of the above conditions can be waived if you get permission from the copyright holder.

Public Domain — Where the work or any of its elements is in the public domain under applicable law, that status is in no way affected by the license.

Other Rights — In no way are any of the following rights affected by the license:

- Your fair dealing or fair use rights, or other applicable copyright exceptions and limitations;
- The author's moral rights;
- Rights other persons may have either in the work itself or in how the work is used, such as publicity or privacy rights.

Notice — For any reuse or distribution, you must make clear to others the license terms of this work. The best way to do this is with a link to this web page.

This is a human-readable summary of the Legal Code (the full license).

Figure 1-2. License:

Open-Access License

No Permission Required

The Public Library of Science (PLoS) applies the Creative Commons Attribution License (CCAL) to all works we publish (read the human-readable summary or the full license legal code). Under the CCAL, authors retain ownership of the copyright for their article, but authors allow anyone to download, reuse, reprint, modify, distribute, and/or copy articles in PLoS journals, so long as the original authors and source are cited. **No permission is required from the authors or the publishers.**

In most cases, appropriate attribution can be provided by simply citing the original article (e.g., Kaltenbach LS et al. (2007) Huntingtin Interacting Proteins Are Genetic Modifiers of Neurodegeneration. *PLoS Genet* 3(5): e82. doi:10.1371/journal.pgen.0030082). If the item you plan to reuse is not part of a published article (e.g., a featured issue image), then please indicate the originator of the work, and the volume, issue, and date of the journal in which the item appeared. For any reuse or redistribution of a work, you must also make clear the license terms under which the work was published.

This broad license was developed to facilitate open access to, and free use of, original works of all types. Applying this standard license to your own work will ensure your right to make your work freely and openly available. Learn more about open access. For queries about the license, please contact us.

Figure 3-3: Permission letter.

Dear Ruth,

Thank you for your inquiry. All you would need to do is cite where you obtained the actual figure (i.e. if is from the manual, reference this). Good luck with your dissertation!

Sincerely,

Kevin White
Technical Support Scientist
Stratagene - An Agilent Technologies Company

Kevin.White@Agilent.com
(800) 894-1304 x5689 tel
858-777-5387 FAX

-----Original Message-----
From: techservices@agilent.com [mailto:techservices@agilent.com]
Sent: Saturday, February 27, 2010 12:10 AM
To: TECHSERVICES (A-LaJolla,ex1)
Subject: Contact Tech Services - Web Form

Name: Ruth Redbird
Position: Graduate Student
Department: Biochemistry
Institution: Virginia Polytechnic Institute and State University
Address: 1254 Sweeny Road
City: Blacksburg
State: VA
Zip/Postal Code: 24060
Country: United States of America
Email: redbird@vt.edu
Phone: 540-239-7246

Comments: Hello. I'm a grad student at VA Tech and wanted to use the pBluescript SK- MCS region from the Lambda Zap II Predigested kit as a figure in my dissertation. Would this be possible? What documentation would I need if required? Thanks! - ruth ann

Figure 4-1AB: Fair use determination.

Draft 09/01/2009

(Questions? Concerns? Contact Gail McMillan, Director of the Digital Library and Archives at Virginia Tech's University Libraries: gailmac@vt.edu)

(Please ensure that Javascript is enabled on your browser before using this tool.)

Virginia Tech ETD Fair Use Analysis Results

This is not a replacement for professional legal advice but an effort to assist you in making a sound decision.

Name: Ruth Ann Redbird

Description of item under review for fair use: Figure 4-1AB. Grüber, G. and V. Marshansky (2008). "New insights into structure-function relationships between archeal ATP synthase (A1A0) and vacuolar type ATPase (V1V0)." BioEssays 30(11-12): 1096-1109.

Report generated on: 04-10-2010 at : 18:25:51

Based on the information you provided:

Factor 1

Your consideration of the purpose and character of your use of the copyright work weighs: ***in favor of fair use***

Factor 2

Your consideration of the nature of the copyrighted work you used weighs: ***in favor of fair use***

Factor 3

Your consideration of the amount and substantiality of your use of the copyrighted work weighs: ***in favor of fair use***

Factor 4

Your consideration of the effect or potential effect on the market after your use of the copyrighted work weighs: ***in favor of fair use***

Based on the information you provided, your use of the copyrighted work weighs: *in favor of fair use*

Figure 4-1C: Fair Use determination.

Draft 09/01/2009

(Questions? Concerns? Contact Gail McMillan, Director of the Digital Library and Archives at Virginia Tech's University Libraries: gailmac@vt.edu)

(Please ensure that Javascript is enabled on your browser before using this tool.)

Virginia Tech ETD Fair Use Analysis Results

This is not a replacement for professional legal advice but an effort to assist you in making a sound decision.

Name: Ruth Ann Redbird

Description of item under review for fair use: Kish-Trier, E., L.-A. K. Briere, et al. (2008). "The Stator Complex of the A1A0-ATP Synthase--Structural Characterization of the E and H Subunits." Journal of Molecular Biology 375(3): 673-685.

Report generated on: 04-10-2010 at : 18:42:08

Based on the information you provided:

Factor 1

Your consideration of the purpose and character of your use of the copyright work weighs: ***in favor of fair use***

Factor 2

Your consideration of the nature of the copyrighted work you used weighs: ***in favor of fair use***

Factor 3

Your consideration of the amount and substantiality of your use of the copyrighted work weighs: ***in favor of fair use***

Factor 4

Your consideration of the effect or potential effect on the market after your use of the copyrighted work weighs: ***in favor of fair use***

Based on the information you provided, your use of the copyrighted work weighs: *in favor of fair use*

Figure 4-2: Fair Use determination.

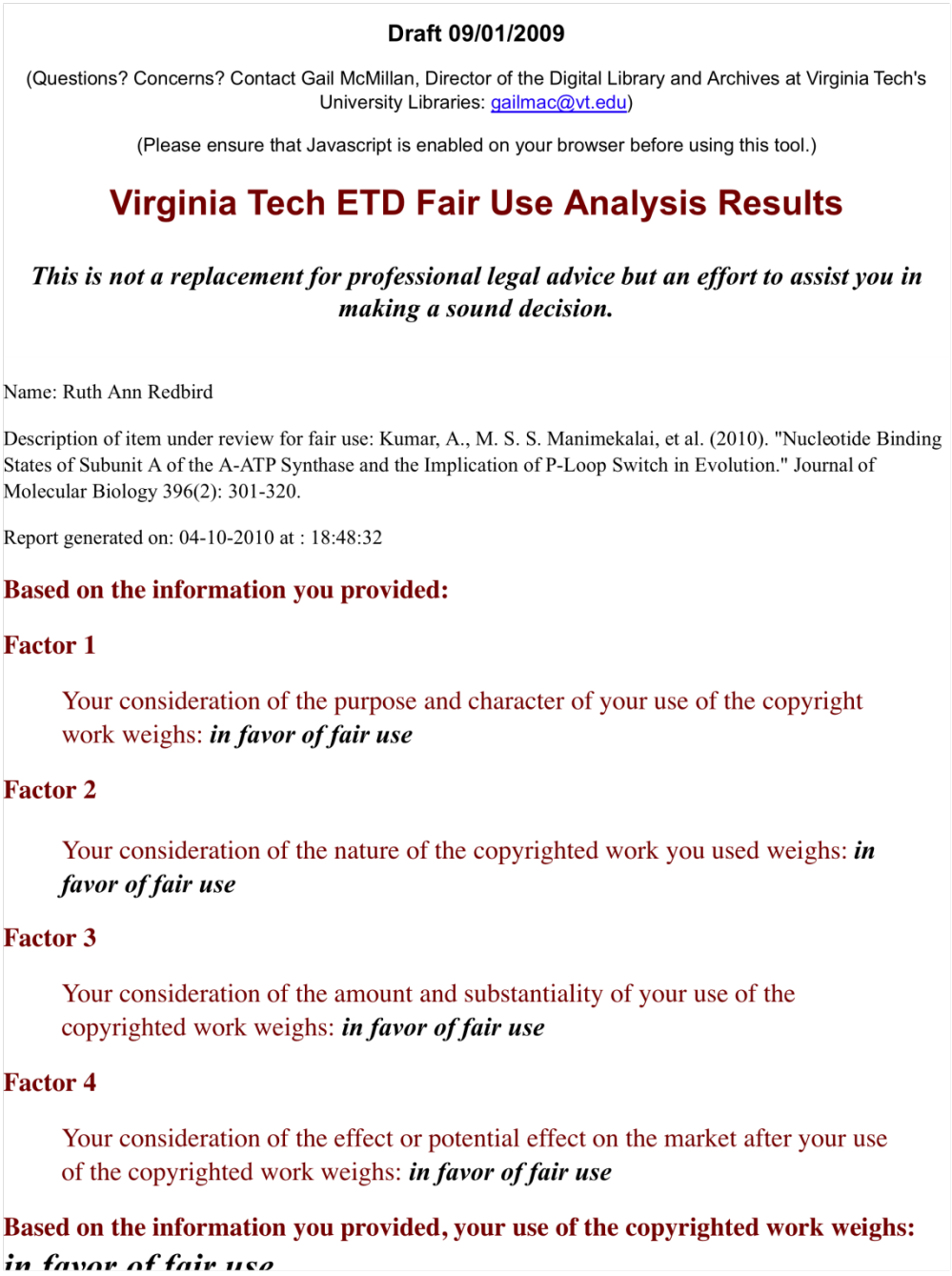

Draft 09/01/2009

(Questions? Concerns? Contact Gail McMillan, Director of the Digital Library and Archives at Virginia Tech's University Libraries: gailmac@vt.edu)

(Please ensure that Javascript is enabled on your browser before using this tool.)

Virginia Tech ETD Fair Use Analysis Results

This is not a replacement for professional legal advice but an effort to assist you in making a sound decision.

Name: Ruth Ann Redbird

Description of item under review for fair use: Kumar, A., M. S. S. Manimekalai, et al. (2010). "Nucleotide Binding States of Subunit A of the A-ATP Synthase and the Implication of P-Loop Switch in Evolution." Journal of Molecular Biology 396(2): 301-320.

Report generated on: 04-10-2010 at : 18:48:32

Based on the information you provided:

Factor 1

Your consideration of the purpose and character of your use of the copyright work weighs: ***in favor of fair use***

Factor 2

Your consideration of the nature of the copyrighted work you used weighs: ***in favor of fair use***

Factor 3

Your consideration of the amount and substantiality of your use of the copyrighted work weighs: ***in favor of fair use***

Factor 4

Your consideration of the effect or potential effect on the market after your use of the copyrighted work weighs: ***in favor of fair use***

Based on the information you provided, your use of the copyrighted work weighs: *in favor of fair use*

Figure 6-1: Fair Use determination.

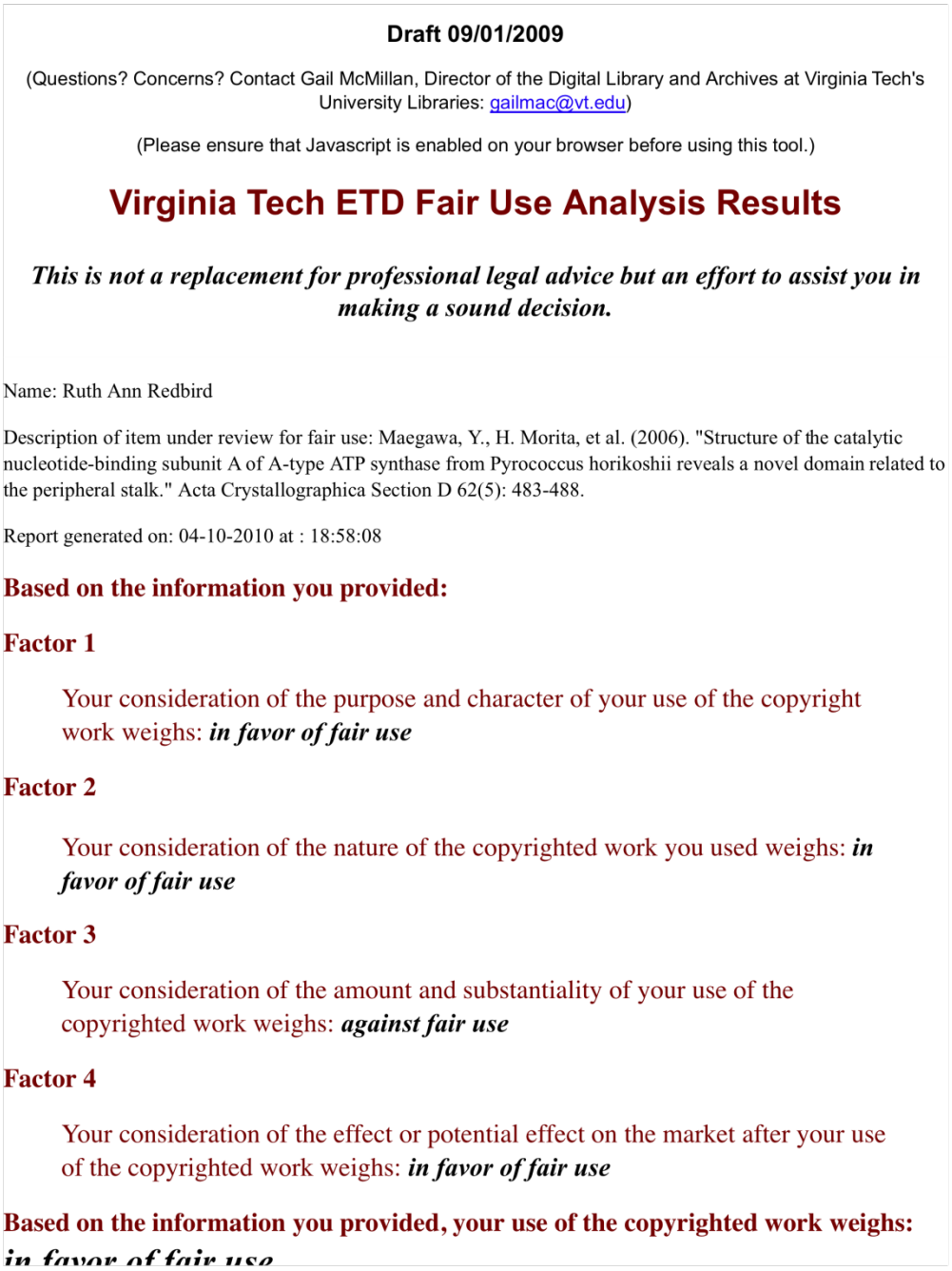

Draft 09/01/2009

(Questions? Concerns? Contact Gail McMillan, Director of the Digital Library and Archives at Virginia Tech's University Libraries: gailmac@vt.edu)

(Please ensure that Javascript is enabled on your browser before using this tool.)

Virginia Tech ETD Fair Use Analysis Results

This is not a replacement for professional legal advice but an effort to assist you in making a sound decision.

Name: Ruth Ann Redbird

Description of item under review for fair use: Maegawa, Y., H. Morita, et al. (2006). "Structure of the catalytic nucleotide-binding subunit A of A-type ATP synthase from Pyrococcus horikoshii reveals a novel domain related to the peripheral stalk." Acta Crystallographica Section D 62(5): 483-488.

Report generated on: 04-10-2010 at : 18:58:08

Based on the information you provided:

Factor 1

Your consideration of the purpose and character of your use of the copyright work weighs: ***in favor of fair use***

Factor 2

Your consideration of the nature of the copyrighted work you used weighs: ***in favor of fair use***

Factor 3

Your consideration of the amount and substantiality of your use of the copyrighted work weighs: ***against fair use***

Factor 4

Your consideration of the effect or potential effect on the market after your use of the copyrighted work weighs: ***in favor of fair use***

Based on the information you provided, your use of the copyrighted work weighs: *in favor of fair use*